

# B-Meson Properties from Modified Sum Rule Analyses

Tobias Kleinschmidt

Institut für Theoretische Physik  
Philosophenweg 16  
69120 Heidelberg  
Germany

## Abstract

We introduce two approaches to analyses of Borel sum rules. In the first method, we analyze the sum rules in the limit  $M^2 \rightarrow \infty$ . Here, the sum rules become very sensitive to the chosen threshold  $s_0$ . We fix the threshold by setting the daughter sum rule equal to the meson mass in this limit. The second method introduces a Borel mass dependent threshold  $s_0(M^2)$ . We choose functions  $s_0(M^2)$  such, that the corresponding sum rule is not dependent on  $M^2$  anymore. The relevant hadronic parameter is extracted at the most stable function  $s_0(M^2)$ . The two methods differ in the notion of quark-hadron duality. Whereas the first method emphasizes errors coming from the simple duality ansatz, the second method is constructed such as to extract hadronic properties from the region where the duality approximation is fulfilled best. We use these modifications of the sum rule approach to extract values for the B-meson decay constant  $f_B$ , the semi-leptonic form factor  $f^+(0)$  at zero momentum transfer and the strong coupling  $g_{B^*B\pi}$ . The results coincide with other sum rule analyses.

# Contents

<b>1</b>	<b>Introduction</b>	<b>1</b>
<b>2</b>	<b>Theoretical Foundations</b>	<b>4</b>
2.1	The SVZ sum rules . . . . .	5
2.1.1	The Hadronic Side of the Sum Rules . . . . .	5
2.1.2	The QCD-Side of the Sum Rules . . . . .	8
2.1.3	Equating the two Sides . . . . .	14
2.2	Quark-Hadron Duality . . . . .	15
2.3	Light-Cone Sum Rules . . . . .	16
<b>3</b>	<b>Decay Constant <math>f_B</math></b>	<b>21</b>
3.1	Discussion of Sum Rule Analyses from the Literature . . . . .	21
3.2	The Limit $M^2 \rightarrow \infty$ . . . . .	25
3.3	Borel Mass dependent Threshold $s_0(M^2)$ . . . . .	27
3.4	Summary of the Results and Relation to the Literature . . . . .	31
3.5	Weak Decay Constant $f_{B^*}$ . . . . .	32
<b>4</b>	<b>B-Form Factor <math>f^+(0)</math></b>	<b>34</b>
4.1	The Limit $M^2 \rightarrow \infty$ . . . . .	36
4.2	Borel Mass dependent Threshold $s_0(M^2)$ . . . . .	38
4.3	Summary of the Results and Relation to the Literature . . . . .	41
<b>5</b>	<b>Coupling <math>g_{B^*B\pi}</math></b>	<b>43</b>
5.1	Derivation of the Sum Rule . . . . .	43
5.2	The Limit $M^2 \rightarrow \infty$ . . . . .	46
5.3	Borel Mass dependent Threshold $s_0(M^2)$ . . . . .	47
5.4	Discussion and Relation to the Literature . . . . .	50
<b>6</b>	<b>Conclusion and Outlook</b>	<b>52</b>
<b>A</b>	<b>Renormalization Group Properties</b>	<b>54</b>
<b>B</b>	<b>Light-Cone Wave Functions</b>	<b>56</b>
B.1	Definitions of the Light-Cone Wave Functions . . . . .	56
B.2	Contributions to the semi-leptonic Form Factor . . . . .	57

# Chapter 1

## Introduction

In 1979 M. Shifman, A. Vainshtein and V. Zakharov proposed the so called QCD sum rules [1, 2] - a method to relate hadronic properties with QCD calculations, where non-perturbative effects are systematically included. With these sum rules, from now on referred to as SVZ sum rules, one is able to express static hadronic observables like masses and widths in terms of a few universal phenomenological parameters, the vacuum condensates of quark and gluon fields. Today, sum rules and their various derivatives are by no means the only approach to predict hadronic parameters. Other methods are calculations in heavy quark effective theories and chiral perturbation theory. Compared to sum rules they can only be applied to limited regions of hadronic physics - systems involving heavy quarks and only light quarks, respectively. Further methods are lattice calculations and various quark models. The advantages and disadvantages of lattice results are discussed below.

The basic idea of the SVZ sum rules is to represent hadrons by currents of quark fields, that have the same quantum numbers as the corresponding hadrons, and to construct the two-point correlator of a current and its hermitian conjugate. This structure is then evaluated in the euclidean region for large spacelike momenta, where the high virtualities of the quarks ensure that the main contribution to the two-point function can be extracted from perturbative calculations. Corrections are added by use of Wilson's operator product expansion (OPE), separating the hard and soft regime of the correlation function to take large distance dynamics into account. This gives rise to a truncated power series in  $\frac{\mu^2}{Q^2}$ , where  $\mu$  is the scale introduced in the OPE to separate short and long distance dynamics. By the use of *dispersion relations* the two-point function is then related to the hadronic spectral density. Finally, a so called *Borel transformation* is applied to improve the convergence of the power series on one side and suppress higher states and continuum contribution of the hadronic spectral density on the other side. The SVZ sum rules will be derived and discussed more intensively in section 2.1 of this thesis.

Over the last 25 years, the initial SVZ sum rules have further been developed and improved. They have been applied to three-point functions, baryonic currents and external fields and were used to determine the masses of the light quarks, decay constants, form factors, couplings and magnetic moments of mesons and baryons. They were extended to investigate properties of hadronic matter at high temperatures and densities and many more systems (see [3, 4] for some examples and applications of various sum rules). Besides the 2-point SVZ sum rules, we will make use of the so called light-cone sum rules (LCSR) in this thesis. Here, the relevant non-local matrix elements will be parameterized in form of wave functions instead of the expansion in local vacuum condensates. This method turned out to be quite useful to extract hadronic properties from reactions including three particles. We will derive the LCSR in section 2.3.

One of the major advantage of the sum rule approach is its flexibility. Sum rules can be applied to a variety of problems and give reliable predictions of hadronic parameters. Compared to lattice results, which became more and more important in the last years, sum rules do not give very accurate results - usual uncertainties lie in the range of 10% to 20%. Nowadays, lattice results have smaller errors and will certainly achieve higher accuracy in the near future, when unquenched calculations will be feasible within an acceptable period of time. But until now, lattice calculations still include relatively high masses for the light quarks, which are related to the length of the lattice. Thus, the results have to be extrapolated to the small masses of the light quarks to give physical predictions, which reduces the accuracy of lattice calculations. Furthermore, they only give *brute force* numerical results, where the fundamental physical dynamics are hidden beyond the extracted numbers and barely observable. On the other side, the simple analytical sum rule method allows physical insight into the systems they are applied to and an interpretation of the results - at the expense of accurate numerical results. Furthermore, the uncertainties of the results can be traced back to uncertainties of several ingredients of the sum rules, like the error coming from the truncation of the condensate expansion of the correlation function and the assumption of *quark-hadron duality*, which is necessary to compensate for the scarce knowledge of the hadronic spectral density. Another advantage of the sum rule approach is the fact, that it can be continued to Minkowski space in an analytical way, whereas this continuation of the numerical lattice results obtained in euclidean space sometimes is problematic. Thus, although they suffer from some inaccuracies, sum rules are still an important method of calculating hadronic properties.

In this thesis we will propose two modifications to the usual sum rule calculations of the decay constant  $f_B$ , the form factor  $f_B^+(0)$  at zero momentum transfer  $q^2 = 0$ , and the coupling  $g_{B^*B\pi}$  of the heavy-light B-meson. To have an precise measurement, or at least an accurate prediction of these parameters is of high importance. The weak decay constant  $f_B$  contributes to calculations of  $B - \bar{B}$ -mixing amplitudes and is needed in determinations of the CKM-matrix element  $V_{ub}$ , when it is extracted from leptonic decays of the B-meson. It contributes as well to the sum rule calculations of the form factor  $f_B^+(q^2)$  and the coupling  $g_{B^*B\pi}$ . The form factor can also be used in predictions of the CKM element. Knowledge of the fundamental parameter  $V_{ub}$  is of greatest importance in today's physics, since it contributes to the question of unitarity of the CKM-matrix and thus tests the standard model.

This thesis is structured as follows. In the next chapter, we will introduce the basic methods and theoretical tools. Different sum rules and their ingredients will be discussed. Furthermore, some of the crucial points of the sum rules will be stressed, like the dual relation of the hadronic spectral function to the perturbative QCD calculation.

In chapter 3, we will start with briefly reviewing the sum rule analysis for the weak decay constant  $f_B$ . We will basically follow an approach from Jamin and Lange[5], using the running b-quark mass in the  $\overline{MS}$ -scheme. Compared to analyses using the pole mass of the quark, this shows an improved convergence of the perturbative expansion in the strong coupling  $\alpha_s$ . In most sum rule approaches, the hadronic parameter is extracted at rather ambiguous values of the squared Borel mass  $M^2$  and the threshold  $s_0$ . In the sections 3.2 and 3.3, we will introduce two new methods to extract a distinct value of the hadronic parameter.

In section 3.2, we will evaluate the sum rule in the limit  $M^2 \rightarrow \infty$ . This is related to an approach proposed several times by Radyushkin[6, 7]. Hereby, uncertainties coming from the truncation of the expansion in the condensates essentially vanish and the threshold parameter  $s_0$  can be fixed to one distinct value, thus leading to a unique numerical result for  $f_B$ . The drawback of

this method lies in the emphasis of uncertainties coming from the simple duality ansatz.

Section 3.3 introduces another possible modification. Here, we will introduce a Borel mass dependent threshold  $s_0(M^2)$  instead of a constant  $s_0$ . With this at hand, one can find functions  $s_0(M^2)$ , for which the sum rule is constant in a given window of the Borel mass. In this case, also the ratio of the sum rule and its first derivative, which is often used to get a reading point  $(\hat{M}^2, \hat{s}_0)$ , is constant and equal to the squared mass of the ground state of the hadronic side. For each value of the sum rule, we find a corresponding function  $s_0(M^2)$ . We will give arguments to extract the value of the hadronic parameter, for which the function  $s_0(M^2)$  is most stable.

In the chapters 4 and 5 we will apply the two methods to the analyses of the B-meson form factor  $f_B^+(0)$  at zero momentum transfer  $q^2 = 0$  and the strong coupling  $g_{B^*B\pi}$ . The LCSR of these parameters are proportional to the weak decay constant  $f_B$  and, in the case of the coupling, also to the decay constant of the  $B^*$ -meson  $f_{B^*}$ . We expect some cancellations of the intrinsic errors of the two methods, when the ratio with the decay constants, analyzed within the same methods, is taken. Our extracted results are close to the values obtained in other sum rule approaches. Chapter 6 will conclude.

## Chapter 2

# Theoretical Foundations

Quantum Chromodynamics is described by the  $SU(3)$  Yang-Mills Lagrangian:

$$\mathcal{L}_{QCD} = -\frac{1}{4}(G_{\mu\nu})^2 + \sum_f \bar{\psi}_f(i\not{D} - m_f)\psi_f, \quad (2.1)$$

where  $G_{\mu\nu}$  is in the adjoint representation of the gauge group and  $\psi_f$  in the fundamental -  $f$  indicating the different quark-flavors. Although  $\mathcal{L}_{QCD}$  is made out of quarks, rather than hadrons, it is believed to incorporate all hadronic physics. However, due to confinement, individual quarks are never observed experimentally, and thus perturbative calculations, which start from this Lagrangian are limited. Calculations involving the free quark propagator are clearly only valid far off-shell, which is one of the features of the SVZ sum rules, where the perturbative coefficients of the operator product expansion are evaluated at large virtualities of the quarks.

To lower scales the running coupling  $\alpha_s(\mu)$  increases and the perturbative expansion breaks down. It even reaches a pole at a scale of order  $\Lambda_{QCD} \approx 200 \text{ MeV}$  and perturbative expressions are only valid down to energies of about  $1 \text{ GeV}$ . With increasing separation of two color charges, the interaction becomes so strong, that the potential between the charges cannot be described by the exchange of single gluons anymore. A whole cloud of gluons will develop between the charges and one has to describe physics at this scales with methods of (chromo-) electric and magnetic fields. A perturbative approach is not feasible in this region.

However, for the treatment of hadronic parameters perturbative QCD is still applicable, since the average separations of the color-charged partons in the hadrons are not too large. One can treat them perturbatively and add corrections to the expressions by considering interactions of the partons with the QCD-vacuum. The QCD-vacuum is described by slowly fluctuating fields and can be included in the calculations by introduction of the so called *condensates*. With the sum rules, a systematic treatment was introduced by Shifman, Vainshtein and Zakharov in 1979. The SVZ sum rules will be derived in the next section.

Throughout this thesis we will use the  $\overline{MS}$ -renormalization scheme with dimensional regularization in perturbative calculations. Adopted expressions from other authors are also obtained using this scheme. The coefficients of the corresponding Gell-Mann-Low function for the running coupling are listed in appendix A. Being a mass-independent scheme - the  $\beta$ -function is not a function of the quark masses - the application of this scheme leads to difficulties in treating the heavy quarks, since they do not decouple in non-physical quantities. If one tries to express the running coupling constant at a certain scale as a function of the coupling at another scale, one has to apply *matching conditions* if the mass-threshold of a heavy quark lies between the two scales. This is also described in appendix A.

## 2.1 The SVZ sum rules

The basic object of the SVZ sum rules is the two-point correlation function of a gauge invariant quark current and its hermitian conjugate:

$$\Pi_{AB}(q) = i \int d^4x e^{iqx} \langle 0 | T \{ j_A(x), j_B^\dagger(0) \} | 0 \rangle. \quad (2.2)$$

Here,  $j_A(x) = \bar{\psi}_f(x) \Gamma_A \psi_{f'}(x)$  is a quark field bilinear with Lorentz structure and flavor content chosen such, that it reflects the quantum numbers of the interpolated hadron. The currents are injected into the vacuum to avoid long distance dynamics, which would occur in case of an initial or final hadronic state. A typical process, which is relevant for investigation of properties of the  $\rho$ -meson, is shown in figure 2.1. Here, the T-product of two vector currents is considered. In this case, due to current conservation  $\partial_\mu j^\mu = 0$ , one can explicitly factor out the kinematical transverse Lorentz structure:

$$\Pi_{\mu\nu}(q) = (q_\mu q_\nu - q^2 g_{\mu\nu}) \Pi(q^2). \quad (2.3)$$

In general one can always decompose the initial n-point function into various terms, where the kinematical structure is factored out, and then proceed with the objects containing the dynamics.

The idea of the sum rules is to evaluate the correlation function in two different ways. On one side,  $\Pi(q^2)$  is calculated at large negative momentum transfer  $Q^2 \equiv -q^2 \gg \Lambda_{QCD}$ , where it can be shown to be dominated by short distance dynamics [4]. This will be done within the framework of Wilson's operator product expansion (OPE), which gives additional corrections to the pure perturbative part in form of an expansion in vacuum condensates. On the other side a complete set of hadronic states will be inserted in the correlator to obtain hadronic matrix elements. Usually, the sum rules are setup to extract values for these matrix elements or hadronic properties which they contain, like decay or coupling constants. The two sides are related to each other by the use of dispersion relations. A Borel transformation is applied to both sides to improve the stability. It suppresses higher states on the hadronic side and removes arbitrary subtraction terms that might appear in the dispersion relations. In the following we will derive the sum rules for the B-meson decay constant  $f_B$ .

### 2.1.1 The Hadronic Side of the Sum Rules

Starting point is the two-point function of two pseudoscalar currents of a bottom and a massless quark:

$$\Pi(q^2) = i \int d^4x e^{iqx} \langle 0 | T \{ \bar{q}(x) i\gamma_5 b(x), \bar{b}(0) i\gamma_5 q(0) \} | 0 \rangle. \quad (2.4)$$

It was shown by Källén and Lehmann that any two-point correlator  $\Pi(q^2)$  is an analytic function in the complex  $q^2$ -plane with possible singularities and a branch cut on the real positive  $q^2$ -axis. The singularities and the cut appear at momentum transfers  $q^2$ , where intermediate states go on-shell. For negative real  $q^2 < 0$ ,  $\Pi(q^2)$  is always real and fulfills Schwartz' reflection principle:

$$\Pi(z) = \Pi^*(z^*). \quad (2.5)$$

This identity can be analytically continued to the whole complex  $q^2$ -plane. With this at hand we can represent  $\Pi(Q^2)$ , where  $Q^2 = -q^2$ , by a dispersion integral, relating the two-point function at negative momentum transfer to its imaginary part at positive  $q^2$ . We consider the integral over the contour depicted in figure 2.2:

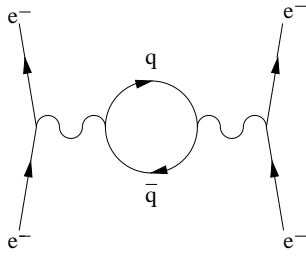


Figure 2.1: Appearance of the quark-loop in  $e^-e^- \rightarrow e^-e^-$ -scattering. At large negative values of the momentum  $q^2$  of the virtual photon, the quarks can be represented by their free propagator.

$$\Pi(Q^2) = \frac{1}{2\pi i} \int_C dz \frac{\Pi(z)}{z + Q^2}. \quad (2.6)$$

If  $\Pi(z)$  vanishes sufficiently fast at  $|z| \rightarrow \infty$ , the integration over the circle does not contribute and we are left with

$$\Pi(Q^2) = \frac{1}{2\pi i} \int_0^\infty \frac{\Pi(s + i\varepsilon) - \Pi(s - i\varepsilon)}{s + Q^2} ds. \quad (2.7)$$

With use of (2.5) the numerator can be replaced by the imaginary part of the correlation function and we get the dispersion relation:

$$\Pi(Q^2) = \frac{1}{\pi} \int_0^\infty \frac{Im\Pi(s + i\varepsilon)}{s + Q^2} ds = \int_0^\infty \frac{\frac{1}{\pi} Im\Pi(s)}{s + Q^2 - i\varepsilon} ds \quad (2.8)$$

In most cases the imaginary part does not vanish in the limit  $s \rightarrow \infty$  and one has to introduce subtraction terms to make the integral finite. In our case the two-point function has a mass dimension of two and an asymptotic behavior of  $\Pi(s) \propto s^2$  in the limit  $s \rightarrow \infty$ . We therefore setup the dispersion relation for  $\Pi(q^2)/q^4$  instead of  $\Pi(q^2)$ :

$$\Pi(Q^2) = Q^4 \int_0^\infty \frac{\frac{1}{\pi} Im\Pi(s)}{s^2(s + Q^2)} ds = \int_0^\infty \frac{\frac{1}{\pi} Im\Pi(s)}{s + Q^2} ds - \int_0^\infty \frac{\frac{1}{\pi} Im\Pi(s)}{s} ds + Q^2 \int_0^\infty \frac{\frac{1}{\pi} Im\Pi(s)}{s^2} ds \quad (2.9)$$

Instead of (2.8), we now have an additional polynomial in  $Q^2$  rendering the initial integral finite. The application of a Borel transformation (see section 2.1.3) will remove the subtraction terms and exponentially suppress higher contributions to the spectral function.

We can get an expression for the imaginary part of the correlator  $\Pi(q^2)$  by use of the optical theorem. It relates the imaginary part of a forward scattering amplitude with the sum over all intermediate states - and thus with the total cross section for particle production of these states. Inserting in (2.4) a complete set of states yields

$$2Im\Pi(q^2) = \sum_n \int d\tau_n (2\pi)^4 \delta^{(4)}(q - p_n) \langle 0 | \bar{q} i \gamma_5 b | n \rangle \langle n | \bar{b} i \gamma_5 q | 0 \rangle. \quad (2.10)$$

Here,  $|n\rangle$  is a single-/multiparticle state with quantum numbers of the quark current and  $d\tau_n$  indicates the integration over the corresponding phase space. In our case, the B-meson is



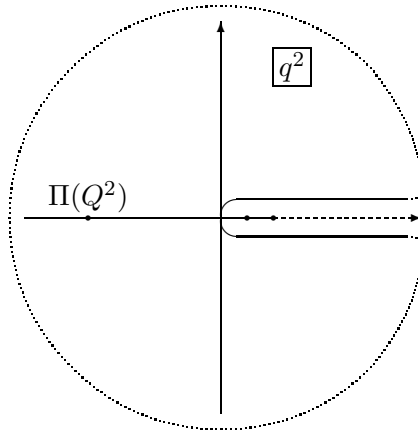


Figure 2.2: Contour of the integral relating  $\Pi(Q^2)$  at negative momentum transfers to its imaginary part at positive  $q^2$ . The circle is taken to infinity. The dots and the dashed line at the positive  $q^2$ -axis indicate bound states and multi-particle states.

the lowest lying state. The corresponding meson-to-vacuum matrix element defines the decay-constant  $f_B$ ,

$$\langle 0 | \bar{q} i \gamma_5 b | B \rangle = \frac{m_B^2 f_B}{m_b}, \quad (2.11)$$

where  $m_b$  is the b-quark mass and  $m_B$  the B-meson mass. Using this definition and integrating out the phase space, we get

$$\frac{1}{\pi} \text{Im} \Pi(q^2) = \frac{m_B^4 f_B^2}{m_b^2} \delta(q^2 - m_B^2) + \text{higher states}. \quad (2.12)$$

Here, *higher states* stands for the contribution of higher lying resonances (radial excitations) of the B-meson and the continuum contribution of multi-particle states. Very little is known of the spectral density, so for the time being, we write

$$\frac{1}{\pi} \text{Im} \Pi(q^2) = \frac{m_B^4 f_B^2}{m_b^2} \delta(q^2 - m_B^2) + \rho^h(q^2) \Theta(s_0^h - q^2), \quad (2.13)$$

where the step function is explicitly written out to emphasize that the onset of the contribution of the higher states and the continuum  $\rho^h(q^2)$  is at  $s_0^h > m_B^2$ . This ansatz, *first resonance plus continuum*, for the hadronic spectral density is typically used in most applications of sum rules. Only the lowest lying state enters explicitly the calculations, whereas the hadronic continuum will be approximated by the perturbative results (see section 2.2). Plugging (2.13) in the dispersion relation (2.8), we get

$$\Pi(Q^2) = \frac{m_B^4 f_B^2}{m_b^2 (m_B^2 + Q^2)} + \int_{s_0^h}^{\infty} \frac{\rho^h(s)}{s + Q^2} ds + \dots, \quad (2.14)$$

where the ellipses stand for subtraction terms necessary to make the integral finite.

Equation (2.14) is the hadronic side of the sum rules. On the other side, the correlation function  $\Pi(Q^2)$  will be derived by means of perturbative QCD. In the next section we will calculate the simple quark loop and introduce corrections to it, coming from an expansion in vacuum condensates.

### 2.1.2 The QCD-Side of the Sum Rules

We start with calculating the contribution of the simple quark-loop (figure 2.3 a). This means, we contract the quark fields in the correlator and replace them by the free quark propagators. In the chiral limit of massless  $u, d$ -quarks, we get

$$i\Pi(q^2) = -3 \int \frac{d^4k}{(2\pi)^4} \text{Tr} \left\{ (i\gamma_5) \frac{i(\not{q} - \not{k})}{(q-k)^2 + i\varepsilon} (i\gamma_5) \frac{i(\not{k} + m_b)}{k^2 - m_b^2 + i\varepsilon} \right\} \quad (2.15)$$

times an overall delta function. The '3' arises from summation over color indices. Instead of calculating this amplitude directly, we again setup a dispersion relation. By inspecting the poles in (2.15), it can be seen that the correlator  $\Pi(q^2)$  develops an imaginary part from  $q^2 \geq m_b^2$  on, and we can write:

$$\Pi(Q^2) = \int_{m_b^2}^{\infty} \frac{\frac{1}{\pi} \text{Im}\Pi(s)}{s + Q^2} ds \quad (2.16)$$

We calculate the imaginary part of (2.15) by applying the Cutcosky cutting rules to it. We get the discontinuity across the branch cut on the positive  $q^2$ -axis by replacement of the propagators with delta-functions<sup>1</sup>.

$$\text{Disc}\Pi(q^2) = \frac{-12}{i} \int \frac{d^4k}{(2\pi)^4} (k^2 - qk)(2\pi i)\delta((q-k)^2)(2\pi i)\delta(k^2 - m_b^2) \quad (2.17)$$

After integration and using  $\text{Disc}\Pi(q^2) = 2i\text{Im}\Pi(q^2)$  we get

$$\text{Im}\Pi(q^2) = \frac{3}{8\pi} \frac{(m_b^2 - q^2)^2}{q^2} \quad (2.18)$$

Inserting this expression in (2.16) the integral becomes divergent. Again, this will be cured later by application of the Borel transformation.

First order corrections in the strong coupling to the quark-loop (figure 2.3 b-d) are well known and we adopt the expressions from [8]:

$$\Delta\text{Im}\Pi(s) = \frac{\alpha_s}{2\pi^2} \frac{(m_b^2 - s)^2}{s} c^1(s), \quad (2.19)$$

with

$$\begin{aligned} c^1(s) = & \frac{9}{4} + 2Li_2\left(\frac{m_b^2}{s}\right) + \log\frac{s}{m_b^2} \log\frac{s}{s-m_b^2} + \frac{3}{2} \log\frac{m_b^2}{s-m_b^2} \\ & + \log\frac{s}{s-m_b^2} + \frac{m_b^2}{s} \log\frac{s-m_b^2}{m_b^2} + \frac{m_b^2}{s-m_b^2} \log\frac{s}{m_b^2} \end{aligned} \quad (2.20)$$

Here, the dilogarithmic function  $Li_2(x)$  satisfies

$$Li_2(x) = - \int_0^x \frac{\log(1-t)}{t} dt. \quad (2.21)$$

$O(\alpha_s^2)$ -corrections to the heavy-light system were calculated recently by Chetyrkin and Steinhauser[9] in a semi-analytic way. These three-loop corrections are available as a mathematica package.

---

<sup>1</sup>This is a purely mathematical treatment to calculate the imaginary part of  $\Pi(q^2)$  - putting the quarks on-shell is certainly not a physical procedure.

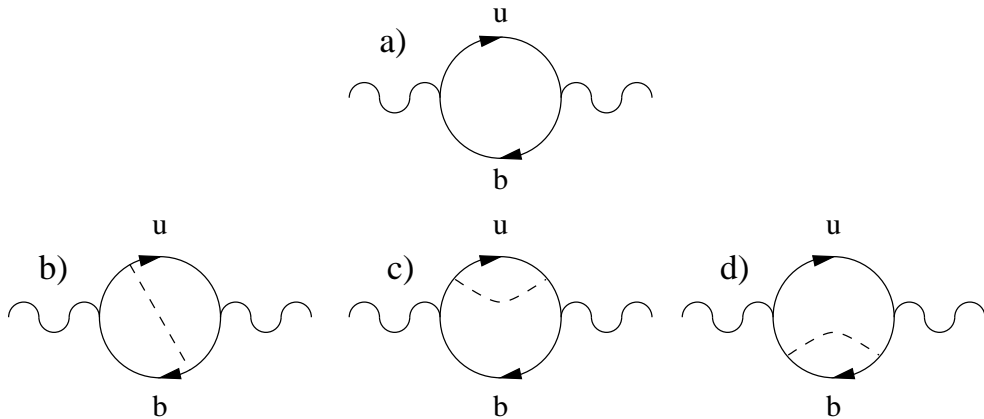


Figure 2.3: The free quark-loop (a) and  $O(\alpha_s)$ -corrections to it (b-d).

Up to now, the two-point correlator was calculated only within perturbation theory. One cannot expect to reproduce hadronic properties by only considering free quark propagators in the calculations. At some point perturbative QCD breaks down and non-perturbative objects have to be taken into account. This will be illustrated in the next section.

### Appearance of non-perturbative Contributions

If one considers higher order corrections to the quark loop, the appearance of non-perturbative corrections can be seen. We illustrate this by considering corrections to the simple loop of massless quarks appearing in figure 2.1, following Shifman[10]. The Adler function is defined as the first derivative of the two-point function:

$$D(Q^2) = -4\pi^2 Q^2 \frac{d\Pi(Q^2)}{dQ^2}. \quad (2.22)$$

With this definition the loop without  $\alpha_s$ -corrections is unity and the inclusion of a gluon-exchange gives:

$$\Delta D(Q^2) = \alpha_s(Q^2) \int_0^\infty dk^2 F(k^2, Q^2) = \frac{\alpha_s}{\pi}. \quad (2.23)$$

In higher orders one has to replace the coupling  $\alpha_s$  by the running coupling  $\alpha_s(k^2)$  in the integral. This replacement takes the increase of the strength of the coupling constant into account, if only small momenta  $k^2$  are exchanged by the gluon. It is equivalent to replace the free gluon propagator by the full one, carrying the effective charge (to one-loop accuracy):

$$\alpha_s(k^2) = \frac{\alpha_s(Q^2)}{1 + \frac{\alpha_s(Q^2)}{4\pi} b_0 \log \frac{k^2}{Q^2}}. \quad (2.24)$$

The resulting feynman diagrams are often referred to as bubble-chain graphs. The insertion of the effective charge leads to a resummation of graphs of this type (see figure 2.4). Inserting the running coupling, the integrand becomes infinite at the Landau pole  $k^2 = \Lambda^2$ :

$$\Lambda^2 = Q^2 e^{-\frac{4\pi}{b_0 \alpha_s}}. \quad (2.25)$$

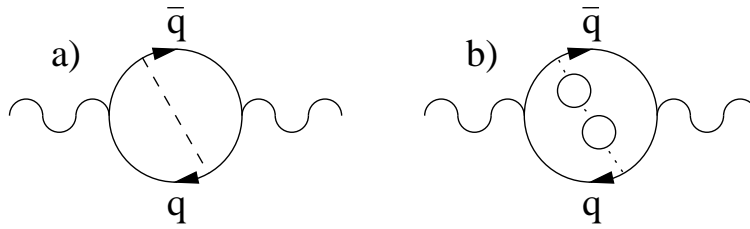


Figure 2.4: Replacement of the free gluon propagator by the effective *bubble chain*.

Dividing the integral in two parts at a scale  $\mu^2 \gg \Lambda^2$ , the IR-part can be separated:

$$\Delta D(Q^2)_{IR} = \alpha_s(Q^2) \int_0^{\mu^2} dk^2 \frac{1}{1 + \frac{\alpha_s(Q^2)}{4\pi} b_0 \log \frac{k^2}{Q^2}} F(k^2, Q^2). \quad (2.26)$$

There is no prescription for how to skip the pole, thus the integral cannot be solved in an unambiguous way. However, using the small  $k^2$ -behavior of  $F(k^2, Q^2) \rightarrow \frac{2}{\pi} \frac{k^2}{Q^4}$ , one can deduce the scaling-behavior

$$\Delta D(Q^2)_{IR} \propto \frac{\Lambda^4}{Q^4}. \quad (2.27)$$

Thus, the low momentum contribution to the Adler function scales like  $\frac{\Lambda^4}{Q^4}$  with an ambiguous numerical coefficient. However, since the Adler function is an observable, this term has to be cancelled by some non-perturbative object of mass-dimension four. In the operator product expansion, which will be introduced in the following, such non-perturbative effects are systematically taken into account by an expansion in vacuum condensates. The vacuum expectation value of the squared field strength,  $\langle 0 | \frac{\alpha_s}{\pi} G^{\mu\nu} G_{\mu\nu} | 0 \rangle$ , may be seen as the corresponding object incorporating the non-perturbative effects of the bubble chain.

## Wilson Operator Product Expansion

The idea of Wilson's operator product expansion[11] is to factor out the long-distance part below the scale  $\mu$  into the non-perturbative vacuum expectation values of gauge and Lorentz invariant local operators, the vacuum condensates. These are accompanied by  $\mu$ -dependent coefficients, which can be calculated perturbatively. This means that any correlation function will be split into a perturbative expansion, taking into account the coulomb interactions and an expansion in condensates, which bear the long distance interactions of the quark and gluon fields.

The effect of the product of two operators separated by a small distance  $x$  can be described as the effect of a local operator of the same quantum numbers. This local operator creates the same disturbance as the product and can be written in form of a linear combination in some basis:

$$O(x)O(0) = \sum_n C_n(x)O_n(0). \quad (2.28)$$

The resulting operators  $O_n$  are purely local ones, whereas the coefficients  $C_n(x)$ , which are c-numbers, now depend on the separation  $x$ .

In the case of the correlator of two quark currents, we have to expand the product of the currents into a series of local operators:

$$j^\mu(x)j^{\nu\dagger}(0) = \sum_n C_n^{\mu\nu}(x)O_n(0). \quad (2.29)$$

Since we are interested in the vacuum expectation value of the currents, only the local operators  $O_n$  which are Lorentz and gauge invariant, contribute to the expansion. Taking the Fourier transform we can write:

$$i \int d^4x e^{iqx} \langle 0|T\{j^\mu(x), j^{\nu\dagger}(0)\}|0\rangle = C_1^{\mu\nu}(q^2) \cdot 1 + C_{\bar{q}q}^{\mu\nu}(q^2) \langle \bar{q}q \rangle + C_{GG}^{\mu\nu}(q^2) \langle \frac{\alpha_s}{\pi} G_{\mu\nu} G^{\mu\nu} \rangle + \dots \quad (2.30)$$

Here, 1 stands for the unity operator, so the coefficient  $C_1^{\mu\nu}(q^2)$  is just the perturbative result of the quark loop. The condensates do not depend on the momentum transfer and also do not depend on quantum numbers or any other structure of the correlator. They are universal non-perturbative objects. The two condensates which are written explicitly in the expansion are the quark condensate of mass dimension three and the four dimensional gluon condensate. The quark condensate is the order parameter of chiral symmetry breaking. It is always accompanied by a quark mass and therefore effectively a dimension four object. The ellipses stand for higher dimensional condensates. The dimensions of the coefficients can be extracted directly from dimensional analysis. If the kinematical structure is factored out - in case of two conserved vector currents this is just the transverse Lorentz structure  $(q_\mu q_\nu - q^2 g_{\mu\nu})$  - it becomes clear that the condensates are suppressed by  $(Q^2)^{-d/2}$ , where  $d$  is the dimension of the relevant condensate. Thus the expansion in the dimensions of the condensates is suitable, if the correlator is evaluated at large negative momentum transfer.

The correlation function  $\Pi(q^2)$  does not depend on any renormalization scale  $\mu$ , so the expansion on the r.h.s has to obey the Callan-Symanzik equation. We introduce a normalization point  $\mu$  such, that it separates the hard and the soft regime of the correlator. The soft modes of the vacuum fluctuations are then described by the condensates, which become scale-dependent, whereas the hard modes are calculated perturbatively. One chooses a rather safe scale, where the coupling  $\alpha_s(\mu)$  is somewhat smaller than unity, so that the perturbative expansion and the calculation of the Wilson coefficients is valid.

The coefficients of the condensates are calculated by cutting the lines of the low momentum quark or gluon. Thereby, the momentum of this particle is set to zero and the fields are treated as external. In the case we are interested in, the heavy-light B-meson, the relevant diagrams up to dimension 6 are depicted in figure 2.5. The crosses indicate the insertion of the vacuum condensates.

In our case of a pseudoscalar current of one bottom and a massless quark we have to start with (2.4). To calculate the Wilson coefficient of the quark condensate  $\langle \bar{q}q \rangle$ ,  $C_{\bar{q}q}(q^2)$ , we contract the b-quarks in the T-product and replace it with the free quark propagator, whereas the light quarks are treated as external fields (see figure 2.5 a). We expand the quark-field  $q(x)$  around zero, to get an expression in the local condensates:

$$q(x) = q(0) + x^\mu \overrightarrow{D}_\mu q(0) + \dots \quad (2.31)$$

$$\bar{q}(x) = \bar{q}(0) + \bar{q}(0) \overleftarrow{D}_\mu x^\mu + \dots \quad (2.32)$$

The ellipses stand for higher derivatives which contribute to condensates of higher dimensions. The second term vanishes by the equations of motion for the dirac fields and we are left with:

$$\Pi(q^2) = \int \frac{d^4k}{(2\pi)^4} d^4x e^{i(q-k)x} \frac{m_b}{k^2 - m_b^2} \langle 0|\bar{q}q|0\rangle. \quad (2.33)$$

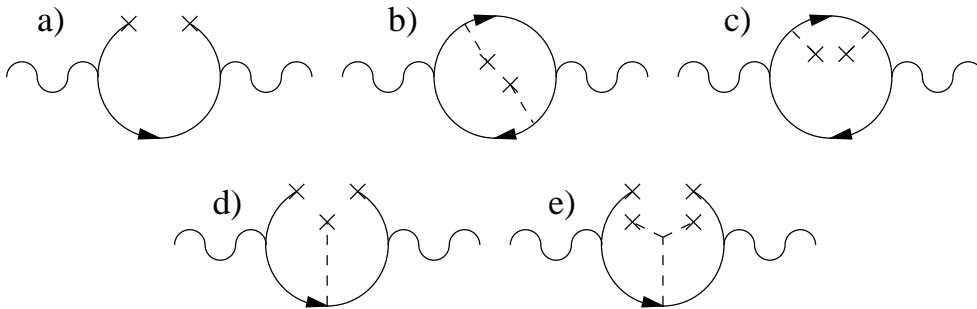


Figure 2.5: Relevant Feynman diagrams for calculation of the coefficients of the condensates up to dimension 6. Appearance of the quark condensate (a), the gluon condensate (b,c), the mixed quark-gluon condensate (d) and the four-quark condensate (e).

The term proportional to  $\langle 0|\bar{q}(x)\not{k}q(0)|0\rangle$  gives contributions of order  $O(m_q)$ , when the expansion (2.32) is inserted and we neglect its contribution. Evaluating the integral we get

$$C_{\bar{q}q}(q^2) = \frac{m_b}{q^2 - m_b^2}. \quad (2.34)$$

Besides the four-dimensional condensates in (2.30), there are further contributions to the sum rules from the condensates depicted in figure 2.5 d and 2.5 e. The dimension five mixed quark-gluon condensate is usually parameterized by:

$$\langle g_s \bar{q} \sigma^{\mu\nu} \frac{\lambda^a}{2} G_{\mu\nu}^a q \rangle = m_0^2 \langle \bar{q}q \rangle. \quad (2.35)$$

The quark-gluon condensate appears, if one expands the non-local quark condensate. Using Fock-Schwinger gauge,  $x_\mu A^\mu(x) = 0$ , to make the path ordered integral between the two quark fields unity, one gets an expansion of quark condensates with covariant derivatives between them. The condensate  $\langle \bar{q} D^2 q \rangle$  is directly related to the mixed quark-gluon condensate. Thus  $m_0^2$  stands for the ratio  $\langle \bar{q} D^2 q \rangle / \langle \bar{q}q \rangle$ , which can be interpreted as average virtuality of the quark fields.

The four quark condensates can be factorized into two two-quark condensates in the limit of large number of colors (corrections come with  $\frac{1}{N_c^2}$ ):

$$\langle O_{4q} \rangle = \alpha_s \langle \bar{q}q \rangle^2. \quad (2.36)$$

The calculation of the coefficients of the higher dimensional condensates for the heavy-light pseudoscalar currents can be found in [12]. In [13], Jamin and Münz calculated the coefficients to the condensates up to dimension 5 to all orders in the quark masses. It is found that long distance contributions in form of mass logarithms of the light quark mass  $m^n \log m^2/\mu^2$ , which appear in the calculations starting at order  $n = 3$ , can be absorbed in the condensates, if non-normal-ordered condensates are used in the operator product expansion. This fact was later used to obtain a first order correction in the strong coupling to the quark condensate [5].

Throughout this thesis, we neglect light quark masses, and we adopt the results from Aliev [14]

for the coefficients contributing to the heavy-light correlator:

$$C_{GG}(q^2) = -\frac{1}{12} \frac{1}{q^2 - m_b^2} \quad (2.37)$$

$$C_{\bar{q}Gq}(q^2) = -\frac{m_b}{2(q^2 - m_b^2)^2} \left( 1 + \frac{m_b^2}{2(q^2 - m_b^2)} \right) \quad (2.38)$$

$$C_{4q}(q^2) = -\frac{16\pi}{27} \frac{1}{(q^2 - m_b^2)^2} \left( 1 + \frac{m_b^2}{2(q^2 - m_b^2)} - \frac{m_b^4}{2(q^2 - m_b^2)^2} \right). \quad (2.39)$$

Gathering all the coefficients of the expansion we get for the QCD-part of the correlation function  $\Pi(Q^2)$  up to dimension 6 in the condensates:

$$\begin{aligned} \Pi(Q^2) = \int_{m_b^2}^{\infty} \frac{\rho^{QCD}(s)}{(s + Q^2)} ds - \frac{1}{(m_b^2 + Q^2)} \left[ m_b \langle \bar{q}q \rangle + \frac{m_b}{2(m_b^2 + Q^2)} \left( 1 - \frac{m_b}{2(m_b^2 + Q^2)} \right) m_0^2 \langle \bar{q}q \rangle + \right. \\ \left. \frac{16\pi}{27(m_b^2 + Q^2)} \left( 1 - \frac{m_b^2}{2(m_b^2 + Q^2)} - \frac{m_b^4}{2(m_b^2 + Q^2)^2} \right) \alpha_s \langle \bar{q}q \rangle^2 \right] \quad (2.40) \end{aligned}$$

where

$$\rho^{QCD}(s) = \frac{3}{8\pi^2} \frac{(m_b^2 - s)^2}{s} \left( 1 + \frac{4\alpha_s}{3\pi} c^1(s) \right), \quad (2.41)$$

and  $c^1(s)$  is given in (2.20).

The values of the condensates do not depend on the channel one is investigating. We take the following typical numerical values for the condensates.

The value of the quark condensate can be extracted from the Gell-Mann-Oakes-Renner relation obtained by current algebra:

$$(m_u + m_d) \langle \bar{u}u + \bar{d}d \rangle = -m_\pi^2 f_\pi^2, \quad (2.42)$$

and we take from [15]:

$$\langle \bar{q}q \rangle (2 \text{ GeV}) = -(267 \pm 16)^3 \text{ MeV}^3. \quad (2.43)$$

The gluon condensate is extracted from sum rules themselves, thus one channel is sacrificed. Instead of giving a prediction to a hadronic matrix element, this value is taken by experiment and the condensate adjusted such, that the sum rules reproduce it. From charmonium sum rules we get:

$$\langle 0 | \frac{\alpha_s}{\pi} G^{\mu\nu} G_{\mu\nu} | 0 \rangle = 0.012 \text{ GeV}^4 \quad (2.44)$$

This value and the next two parameters are taken from Belyaev[16]:

$$m_0^2(1 \text{ GeV}) = (0.8 \pm 0.2) \text{ GeV}^2 \quad (2.45)$$

$$\alpha_s \langle \bar{q}q \rangle^2 = 8 \cdot 10^{-5} \text{ GeV}^6. \quad (2.46)$$

We did not quote an error on the gluon and the four quark condensate. We will later take an uncertainty of 100% on these values, which will still be numerically negligible.

The operator product expansion is an expansion in the soft non-perturbative condensates. This power series is only valid up to a certain dimension, where contribution from *direct instantons* appear. These short distance vacuum fluctuations give rise to an additional exponential term and the expansion in the condensates breaks down. However, the instanton contribution is numerically negligible.

### 2.1.3 Equating the two Sides

#### The Borel Transformation

After evaluating the two-point correlator in two different ways, the phenomenological, hadronic part and the QCD-part are equaled. To improve the stability, Shifman, Vainshtein and Zakharov proposed a so called Borel transformation. Applying it to the two parts will remove the subtraction terms of the dispersion relations and improve the convergence of the power-series expansion at the same time. The algebraic operator is that of an inverse Laplace transform:

$$B \equiv \lim_{n \rightarrow \infty} \lim_{Q^2 \rightarrow \infty} \Big|_{\frac{Q^2}{n^2} = M^2} \frac{(Q^2)^{(n+1)}}{n!} \left( -\frac{d}{dQ^2} \right)^n \quad (2.47)$$

Applying this operator on any negative power of  $(s + Q^2)$ , we get

$$B(s + Q^2)^{-k} = \frac{1}{(k-1)!} \left( \frac{1}{M^2} \right)^{k-1} e^{-\frac{s}{M^2}}, \quad k \geq 1. \quad (2.48)$$

After the Borel transformation, for sufficiently low values of the squared Borel mass  $M^2$  the integral over the imaginary part of the correlator (2.16) becomes finite and also the contribution of higher states in (2.14) gets suppressed. The truncated power series of the contribution of the condensates becomes an expansion in negative powers of  $M^2$  times an exponential function, which breaks down for  $M^2 \rightarrow 0$ . This gives a lower bound on  $M^2$ . On the other hand, the higher the Borel mass is chosen, the more the uncertainties in the hadronic spectral density are emphasized. Thus, in the typical sum rule applications a *working window* of the squared Borel mass  $M^2$  is defined. The boundaries are taken such, that the contributions from higher states and from the condensate expansion, respectively, do not exceed a certain percentage value of the whole expression. One hopes that inside this window the corresponding hadronic parameter the sum rule is set up for, is close to reality. The issue of which value of the Borel parameter should be taken as reading point, will be discussed several times throughout this thesis.

#### The final Sum Rule for the B-meson Decay Constant

Borel transforming (2.14) and the expansion in local operators (2.40), we get after equating both sides:

$$\begin{aligned} \frac{m_B^4 f_B^2}{m_b^2} e^{-\frac{m_B^2}{M^2}} &= \int_{m_b^2}^{\infty} ds \rho^{QCD}(s) e^{-\frac{s}{M^2}} - \int_{s_0^h}^{\infty} ds \rho^h(s) e^{-\frac{s}{M^2}} + \\ &+ \left[ -m_b \langle \bar{q}q \rangle + \frac{1}{12} \langle \frac{\alpha_s}{\pi} GG \rangle - \frac{m_b^2}{2M^2} \left( 1 - \frac{m_b^2}{2M^2} \right) m_0^2 \langle \bar{q}q \rangle - \right. \\ &\left. - \frac{16\pi}{27} \frac{1}{M^2} \left( 1 - \frac{m_b^2}{4M^2} - \frac{m_b^4}{12M^4} \right) \alpha_s \langle \bar{q}q \rangle^2 \right] e^{-\frac{m_b^2}{M^2}}, \end{aligned} \quad (2.49)$$

where  $\rho^{QCD}(s)$  is given in (2.41). The hadronic spectral function  $\rho^h(s)$  is not known. By the assumption of quark-hadron duality, it is related to the perturbative part of the correlator. It is assumed that at large momentum transfer the two-point function can be described by the free quark and gluon fields and thus, the integral over the hadronic spectral density equals the integral over the perturbative result from a certain threshold on:

$$\rho^h(s) \Theta(s - s_0^h) = \rho^{QCD}(s) \Theta(s - s_0). \quad (2.50)$$



This ansatz will be discussed more intensively in the next section. Inserting (2.50) in (2.49), we get the final expression for the B-meson decay constant:

$$\begin{aligned}
m_B^4 f_B^2 e^{-\frac{m_B^2}{M^2}} &= \frac{3m_b^2}{8\pi^2} \int_{m_b^2}^{s_0} ds \frac{(m_b^2 - s)^2}{s} \left( 1 + \frac{4\alpha_s}{3\pi} c^1(s) \right) e^{-\frac{s}{M^2}} + m_b^2 \left[ -m_b \langle \bar{q}q \rangle + \frac{1}{12} \langle \frac{\alpha_s}{\pi} GG \rangle \right. \\
&\quad \left. - \frac{m_b^2}{2M^2} \left( 1 - \frac{m_b^2}{2M^2} \right) m_0^2 \langle \bar{q}q \rangle - \frac{16\pi}{27} \frac{1}{M^2} \left( 1 - \frac{m_b^2}{4M^2} - \frac{m_b^4}{12M^4} \right) \alpha_s \langle \bar{q}q \rangle^2 \right] e^{-\frac{m_b^2}{M^2}}.
\end{aligned} \tag{2.51}$$

This sum rule was the starting point of many analyses through the last twenty years - see [14, 17, 5] as examples. However, the results obtained differ significantly - the estimates range from  $f_B = 130 \text{ MeV}$  to  $f_B = 270 \text{ MeV}$ . The reason for this discrepancy lies mainly in the sensitivity of the sum rule (2.51) to the chosen quark mass  $m_b$ . If one takes the pole mass  $m_{b,pole}$  and varies it from  $m_{b,pole} = 4.6 \text{ GeV}$  to  $m_{b,pole} = 4.8 \text{ GeV}$ , the result changes from  $f_B = 210 \text{ MeV}$  to  $f_B = 150 \text{ MeV}$ . Therefore, an accurate determination of the heavy quark mass is necessary<sup>2</sup>. The value for the b-quark mass is usually taken from lattice calculations or bottomonium sum rules. In [5], Jamin and Lange use the  $\overline{MS}$  mass instead of the pole mass. This seems to improve the convergence of higher order corrections in the strong coupling  $\alpha_s$ . The difference of the two analyses of Khodjamirian [8] and Jamin [5] will be discussed in section 3.1. We will give arguments in favor of choosing the  $\overline{MS}$  mass and adopt the sum rule from Jamin and Lange as the starting point of our analysis.

## 2.2 Quark-Hadron Duality

The uncertainties in the parameters  $m_b, s_0, M^2$  and the appropriate scale, where the sum rules should be analyzed, are not the only limitations to the accuracy of the sum rule results. Sum rules have an intrinsic uncertainty. On one side, they are limited by the truncation of the operator product expansion. At higher dimensions of the expansion in  $1/Q^2$  *small size instantons* come into play and OPE cannot take these hard non-perturbative corrections into account. Furthermore, higher corrections in the strong coupling to the coefficients of the condensates and the perturbative calculation are scarcely known. On the other side, the hadronic spectral function, since it is not known experimentally to all energies, is approximated by the arguments of quark-hadron duality. While we do not refer to the former limitations further, we will discuss the duality approximation more intense and give arguments for two modifications of the usual sum rule analysis, related to duality.

At large negative momentum transfer, the two-point correlator is believed to be described by the free quark and gluon fields. We can safely neglect the power expansion on the QCD-side and again equate the hadronic side (2.14) with the perturbative side (2.40) at large  $Q^2$ . We get

$$Q^4 \int_{s_0^h}^{\infty} \frac{\rho^h(s)}{s^2(s+Q^2)} ds = Q^4 \int_{m_b^2}^{\infty} \frac{\frac{1}{\pi} \text{Im} \Pi^p(s)}{s^2(s+Q^2)} ds, \tag{2.52}$$

in the limit  $Q^2 \rightarrow \infty$ . We took account for the subtraction terms by using  $\Pi(Q^2)/Q^4$  rather than  $\Pi(Q^2)$  as the relevant correlator. Equation (2.52) is known as *global duality* relation. The integrals over the hadronic spectrum and the imaginary part of the perturbative calculation equal

---

<sup>2</sup>However, the definition of the pole mass suffers from an ambiguity of order  $\Lambda_{QCD}$  and one cannot give a more precise value. This will be explained in section 3.1

in the limit of  $Q^2 \rightarrow \infty$ . Furthermore, the two integrands should have the same asymptotics at  $s \rightarrow \infty$  to fulfill the equation (2.52):

$$\rho^h(s) = \frac{1}{\pi} \text{Im} \Pi^P(s), \quad \text{at } s \rightarrow \infty. \quad (2.53)$$

Setting the hadronic spectral function point-wise equal to the perturbative part is known as *local duality*. It is now argued that one can find a threshold  $s_0$ , where the integral over the hadronic function equals the integral over the perturbative one at finite  $Q^2$ , leading to the *semi-local* duality relation:

$$Q^4 \int_{s_0^h}^{\infty} \frac{\rho^h(s)}{s^2(s+Q^2)} ds \cong Q^4 \int_{s_0}^{\infty} \frac{\frac{1}{\pi} \text{Im} \Pi^P(s)}{s^2(s+Q^2)} ds. \quad (2.54)$$

Thus, the uncertainty of the hadronic spectral function is replaced by the introduction of one more parameter. This is certainly only approximative and one has to argue for the right choice of the threshold-parameter  $s_0$ . However, Borel transforming (2.54) introduces an exponential factor, which suppresses the contribution at higher momenta. After the transformation, (2.54) is set in (2.49) and leads to the final sum rule (2.51).

In section 3.3 we will introduce a Borel mass dependent threshold  $s_0$ . We can find functions  $s_0(M^2)$  that will make  $f_B$  constant over the Borel mass  $M^2$  in a certain window. Furthermore, the derivative  $M^2 \frac{d}{dM^2} \log \Sigma(M^2, s_0(M^2))$ , where  $\Sigma(M^2, s_0(M^2))$  is the right hand side of (2.51), can be set constant over  $M^2$  and equal to the squared meson mass  $m_B^2$ . The threshold  $s_0(M^2)$  is not a unique function - we can find a continuum of functions, leading to a continuum of results for  $f_B$ . However, we can give arguments for a preferred value of  $f_B$ .

We will also apply a second method of analyzing the sum rules, which is related to the *local duality* approach used several times by Radyushkin and collaborators [6, 7]. Taking the Borel parameter  $M^2$  to infinity justifies the truncation of the condensate expansion. However at the same time, the exponential suppression of the contribution of the hadronic spectral function vanishes. In these approaches, the threshold  $s_0$  is usually taken to be around the midpoint between the ground state and the first resonance of the corresponding hadron. In the limit  $M^2 \rightarrow \infty$ , the sum rule results show a rather high sensitivity on the chosen threshold  $s_0$ . In section 3.2, we suggest setting the daughter sum rule equal to the meson mass, for which a distinct value for  $s_0$  and therefore for the decay constant  $f_B$  can be found.

In the next section, we will introduce the light-cone sum rules, which will be used with the above modification in this thesis to get values for the weak form factor  $f_B^+(0)$  and the coupling  $g_{B^*B\pi}$ .

## 2.3 Light-Cone Sum Rules

Considering processes of the type  $A \rightarrow B + C$ , involving three hadrons or external currents, one needs to modify the original sum rules. A natural extension of the SVZ sum rules would be to sandwich three currents, interpolating hadrons by quark fields, between the physical vacuum,

$$T_{ABC}(p, q) = - \int d^4x d^4y \langle 0 | T \{ j_A(x) j_B(0) j_C(y) \} | 0 \rangle, \quad (2.55)$$

and apply a similar procedure as for the two-point sum rules. However, this method, known as three-point sum rules, leads to difficulties in several applications. In section 4, we analyze the

weak form factor  $f^+(0)$  for the semileptonic decay of the B-meson, at maximal recoil ( $q^2 = 0$ ). It is defined by the matrix element for the  $B \rightarrow \pi$  transition:

$$\begin{aligned} \langle \pi(p_\pi) | \bar{u} \gamma_\mu d | B(p_B) \rangle &= (p_B + p_\pi)_\mu f^+(q^2) + (p_B - p_\pi)_\mu f^-(q^2) \\ &= 2f^+(q^2) p_{\pi\mu} + (f^+(q^2) + f^-(q^2)) q_\mu, \end{aligned} \quad (2.56)$$

$q = p_B - p_\pi$  being the momentum transfer to the leptons. In the following, we concentrate only on the form factor  $f^+(q^2)$  in front of the pion-momentum. In the case of large recoil ( $q^2 = 0$ ), the b-quark of the meson decays into a u-quark bearing a large energy of about  $E_u = m_b/2$ . This process is shown in figure 2.6. The u-quark has to recombine with the d-quark to form the pion. This can be done by exchanging a hard gluon over a small separation of the Fock state partons (hard contribution). If such an exchange is not present, the end-point regions, where one of the partons carries almost all momentum of the pion are enhanced (soft contribution).

Expanding the corresponding three-point amplitude in terms of local condensates immediately leads to problems of convergence. Replacing the d-quark propagator by the quark-condensate gives contributions to the correlation function only at the end-point regions, since the condensates are made out of slowly varying vacuum fields and do not carry high momenta. This leads to the fact that the condensates in the OPE are accompanied by increasing powers of the heavy quark mass  $m_b$  [18]. One has to take into account a whole chain of condensates of increasing dimension to make the result numerically stable.

This is, where the light-cone wave functions come into play [19, 20]. Here, the expansion runs in the transverse distance of the partons instead of the short distance expansion of the OPE. This leads to a partial resummation of operators of any dimension into a single wave-function of given twist, where the twist of an expression is defined by the difference of its mass dimension and its Lorentz spin.

Starting point for the light-cone sum rules for the weak form factor  $f^+(q^2)$  is the T-product of a pseudoscalar current, interpolating the B-meson, and a vector current sandwiched between the vacuum and the pion state:

$$\Pi_\mu(q, p_\pi) = i \int d^4x e^{iqx} \langle \pi(p_\pi) | T \{ \bar{u}(x) \gamma_\mu b(x), \bar{b}(0) i \gamma_5 d(0) \} | 0 \rangle, \quad (2.57)$$

where  $q$  is the momentum carried away by the W-boson. To lowest order, we contract the b-quark fields and plug in the free propagator. This process is depicted in figure 2.6. We get the expression

$$\begin{aligned} \Pi_\mu(q, p_\pi) &= -i \int \frac{d^4k}{(2\pi)^4} d^4x e^{i(q-k)x} \frac{1}{k^2 - m_b^2} [m_b \langle \pi(p_\pi) | \bar{u}(x) \gamma_\mu \gamma_5 d(0) | 0 \rangle \\ &\quad + k^\nu \langle \pi(p_\pi) | \bar{u}(x) \gamma_\mu \gamma_\nu \gamma_5 d(0) | 0 \rangle]. \end{aligned} \quad (2.58)$$

The two matrix elements are now expanded around  $x^2 = 0$ . The first term of the first element defines the twist 2 pion light-cone wave function:

$$\langle \pi(p_\pi) | \bar{u}(x) \gamma_\mu \gamma_5 d(0) | 0 \rangle = -i p_{\pi\mu} f_\pi \int_0^1 du \varphi_\pi(u) e^{iup_\pi x} + \dots, \quad (2.59)$$

where the ellipses stand for higher terms in the expansion.  $\varphi_\pi(u)$  is the two-particle Fock wave-function of the pion - its argument  $u$  is the momentum fraction carried by one of the constituents.

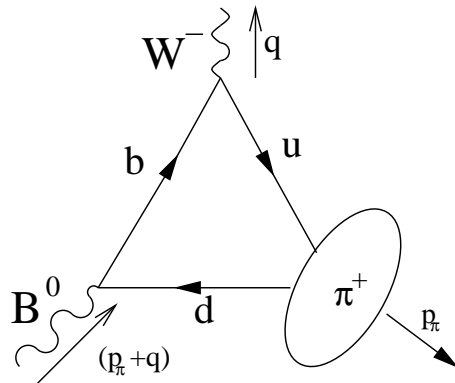


Figure 2.6: Leading order diagram to the  $B \rightarrow \pi$ -transition amplitude. The u- and d-quark combine to form the pion state, parametrized by its distribution amplitude in the light-cone sum rule approach.

Instead of the local condensates in the two-point sum rule approach, the correlation function is now expanded in non-local matrix elements, which are parametrized by the wave functions. Replacing in (2.58) the first matrix element by (2.59), we get after integration:

$$\Pi_\mu(q, p_\pi) = -p_{\pi\mu} m_b f_\pi \int_0^1 \frac{\varphi_\pi(u) du}{(u p_\pi + q)^2 - m_b^2} + \dots \quad (2.60)$$

Expanding the integrand around  $p_\pi = 0$  leads to a series in higher momenta of the wave function  $u^n \varphi_\pi(u)$ , which are directly related to higher derivatives of the matrix element in (2.59) and thus to higher dimensional condensates. The crucial point is that the coefficients of this series are given by (at  $q^2 = 0$ ):

$$c_n = \frac{(2q p_\pi)^n}{(m_b^2 - q^2)^{n+1}} = \frac{(p_\pi + q)^{2n}}{(m_b^2)^{n+1}} \simeq 1. \quad (2.61)$$

Thus, the expansion in local condensates as one would have obtained in the 3-point sum rule approach would be useless, since the coefficients are not suppressed and one had to take the infinite series of condensates into account. In the LCSR approach this series is replaced by a single wave function.

The shape of the pion wave function is not very well known. In the appendix B, we give a definition in terms of an expansion in Gegenbauer-polynomials. This gives corrections to the asymptotic form  $\varphi_\pi(u) = 6u(1-u)$ . The values of the scale-dependent coefficients are frequently discussed in the literature.

The hadronic side of the light-cone sum rules for the form factor is obtained following the same procedure as in the SVZ sum rules for the weak decay constant. Inserting in (2.57) a complete set of states, we get

$$\Pi_\mu(q, p_\pi) = \frac{\langle \pi(p_\pi) | \bar{u} \gamma_\mu b | B(p_\pi + q) \rangle \langle B(p_\pi + q) | \bar{b} i \gamma_5 d | 0 \rangle}{m_B^2 - (p_\pi + q)^2} + \sum_n \frac{\langle \pi(p_\pi) | \bar{u} \gamma_\mu b | n \rangle \langle n | \bar{b} i \gamma_5 d | 0 \rangle}{m_B^2 - (p_\pi + q)^2}, \quad (2.62)$$

where  $|n\rangle$  are the states of higher resonances and the continuum contribution. We rewrite these contribution in form of a dispersion integral over the hadronic spectral density as in (2.14) for

the decay constant. Defining the relevant correlator  $\Pi^+(q, p_\pi)$  by

$$\Pi_\mu(q, p_\pi) = \Pi^+(q^2, (p_\pi + q)^2) p_{\pi\mu} + \Pi^\pm(q^2, (p_\pi + q)^2) q_\mu, \quad (2.63)$$

and using the definitions for the decay constant (2.11) and the form factors (2.56), we get

$$\Pi^+(q^2, (p_\pi + q)^2) = \frac{2m_B^2 f_B f^+(q^2)}{m_b(m_B^2 - (p_\pi + q)^2)} + \int_{s_0^h}^{\infty} \frac{\rho^h(s) ds}{s - (p_\pi + q)^2}. \quad (2.64)$$

Applying the Borel transformation with respect to  $(p_\pi + q)^2$ , we finally get for the hadronic side

$$\Pi^+(q^2, M^2) = \frac{2m_B^2}{m_b} f_B f^+(q^2) e^{-\frac{m_B^2}{M^2}} + \int_{s_0^h}^{\infty} ds \rho^h(s) e^{-\frac{s}{M^2}}. \quad (2.65)$$

Again, the hadronic spectral function will be replaced by the perturbative result via the assumption of quark-hadron duality. Thus, we need to rewrite (2.60) in form of a dispersion relation<sup>3</sup> with respect to  $(p_\pi + q)^2$ . Taking the on-shell pion to be massless ( $p_\pi^2 = 0$ ), we write the denominator as:

$$(up_\pi + q)^2 - m_b^2 = u \left( (p_\pi + q)^2 + \frac{(1-u)q^2}{u} - \frac{m_b^2}{u} \right) \quad (2.66)$$

By making the substitution  $s = (m_b^2 - q^2)/u + q^2$ , we get

$$\Pi^+(q^2, (q + p_\pi)^2) = m_b f_\pi \int_0^1 \frac{du \varphi_\pi(u)}{u \left( \left( \frac{m_b^2 - q^2}{u} + q^2 \right) - (p_\pi + q)^2 \right)} = m_b f_\pi \int_{m_b^2}^{\infty} \frac{ds \tilde{\varphi}_\pi(s)}{(s - q^2)(s - (p_\pi + q)^2)}. \quad (2.67)$$

Thus, we identify  $\tilde{\varphi}_\pi(s)/(s - q^2)$  with the imaginary part of  $\Pi^+(q^2, (p_\pi + q)^2)$ :

$$\frac{1}{\pi} \text{Im} \Pi^+(q^2, (p_\pi + q)^2) = m_b f_\pi \frac{\tilde{\varphi}_\pi(s)}{(s - q^2)}. \quad (2.68)$$

Taking the simple duality ansatz,

$$\rho^h(s) \Theta(s - s_0^h) = \frac{1}{\pi} \text{Im} \Pi^+(q^2, (p_\pi + q)^2) \Theta(s - s_0), \quad (2.69)$$

and subtracting the integral over the hadronic spectral density on both sides, we effectively cut the integral on the right hand side at  $s_0$ . After Borel transformation with respect to  $(p_\pi + q)^2$  and taking back the substitution, the right hand side of the sum rule reads:

$$\Pi_{rhs}^+(q^2, M^2) = m_b f_\pi \int_{m_b^2}^{s_0} \frac{ds \tilde{\varphi}_\pi(s)}{s - q^2} e^{-\frac{s}{M^2}} = m_b f_\pi \int_{\Delta}^1 \frac{du}{u} \varphi_\pi(u) e^{-\frac{m_b^2 - (1-u)q^2}{uM^2}}, \quad (2.70)$$

where the lower limit in the integral is given by

$$\Delta = \frac{m_b^2 - q^2}{s_0 - q^2}. \quad (2.71)$$

---

<sup>3</sup>Here, only a single dispersion relation is necessary, which is another advantage of the LCSR approach compared to the ordinary three-point sum rules. In the case of the B-meson form factor, these make use of double dispersion relations [21], which leads to further uncertainties of the results.

Equating the hadronic and the perturbative side we get the LCSR to lowest order:

$$f_B f^+(q^2) e^{-\frac{m_B^2}{M^2}} = \frac{m_b^2 f_\pi}{2m_B^2} \int_{\Delta}^1 \frac{du}{u} \varphi_\pi(u) e^{-\frac{m_b^2 - (1-u)q^2}{uM^2}}. \quad (2.72)$$

Further contributions to the QCD-side come from higher terms in the expansion around the light-cone  $x^2 = 0$  of the matrix element (2.59):

$$\begin{aligned} \langle \pi(p_\pi) | \bar{u}(x) \gamma_\mu \gamma_5 d(0) | 0 \rangle &= -i p_{\pi\mu} f_\pi \int_0^1 du e^{iup_\pi x} (\varphi(u) + x^2 g_1(u)) \\ &+ f_\pi \left( x_\mu - \frac{x^2 p_{\pi\mu}}{p_\pi x} \right) \int_0^1 du e^{iup_\pi x} g_2(u) + \dots \end{aligned} \quad (2.73)$$

Here,  $g_1$  and  $g_2$  are two particle twist 4 wave functions. Their definition is given in the appendix B. The second matrix element in (2.58) can be split into a symmetric and an antisymmetric part. The corresponding elements define the two-particle wave functions of twist 3:

$$\langle \pi(p_\pi) | \bar{u}(x) \gamma_5 d(0) | 0 \rangle = f_\pi \mu_\pi \int_0^1 du e^{iup_\pi x} \varphi_p(u), \quad (2.74)$$

multiplied by the symmetric tensor  $g_{\mu\nu}$ . The antisymmetric matrix element is

$$\langle \pi(p_\pi) | \bar{u}(x) \sigma_{\mu\nu} \gamma_5 d(0) | 0 \rangle = i(p_{\pi\mu} x_\nu - p_{\pi\nu} x_\mu) \frac{f_\pi \mu_\pi}{6} \int_0^1 du e^{iup_\pi x} \varphi_\sigma(u), \quad (2.75)$$

where

$$\mu_\pi = \frac{m_\pi^2}{m_u + m_d}. \quad (2.76)$$

This normalization factor is directly related to the quark condensate via the Gell-Mann-Oakes-Renner relation, and leads to a further error source besides the coefficients in the definitions of the wave functions.

In appendix B we list further contributions to the LCSR, from taking into account higher orders of the contraction of the b-fields. This leads effectively to an additional gluon line going from the b-quark into the pion wave function. The relevant amplitudes are parametrized by three particle twist 3 and 4 wave functions. We also list  $O(\alpha_s)$ -corrections to the twist 2 pion wave function. Again, all these terms have to be integrated over  $x$  and  $k$  in (2.58) and then written in form of a dispersion relation. Here, terms proportional to higher powers of  $1/((up_\pi + q)^2 - m_b^2)$  than one have to be partially integrated, which leads to further contributions to the sum rule in form of surface terms.

Up to twist 4 we give the LCSR for the form factor at maximum recoil ( $q^2 = 0$ ) explicitly in chapter 4. The expression is taken from Khodjamirian and Rückl [8] with first order corrections to the twist 2 wave function  $\varphi_\pi(u)$  taken from Bagan, Ball and Braun [22].

# Chapter 3

## Decay Constant $f_B$

The leptonic decay constant  $f_B$  of the B-meson is a hadronic parameter of high interest in today's physics. It appears in most calculations concerning the B-meson. Its squared value enters in the calculation of the  $B - \bar{B}$ -mixing amplitude, which is an important tool to measure CKM elements and investigate CP-violation. Therefore, a precise knowledge of  $f_B$  is strongly desired. However, there are no experimental measurements of the decay constant and one has to rely on theoretical predictions. There exist numerous sum rule analyses of the decay constant. In the following section, we will reanalyze the SVZ- sum rules for the decay constant to NLO-accuracy in the perturbative expansion, following Jamin and Lange[5]. We compare the results with those of Khodjamirian and Rückl[8]. The two analyses mainly differ in the use of the heavy quark mass - the running mass and the pole mass, respectively.

We then proceed with our own analysis using the sum rule from [5] up to first order corrections in the strong coupling and neglecting the light quark masses.

### 3.1 Discussion of Sum Rule Analyses from the Literature

The Borel sum rules in the form of equation (2.51) are known for over twenty years. Unfortunately, the sum rule is very sensitive to the input parameters like the quark mass and the values of the threshold  $s_0$  and the Borel mass  $M^2$ . Therefore, the results of the various calculations vary in a rather wide range. In 1983, Aliev and Eletsii [14] used this sum rule to obtain  $f_B = 130 \text{ MeV}$ . This rather low value, compared to today's results, is due to the use of a quite high value of the pole mass ( $m_b = 4.8 \text{ GeV}$ ) and low value of the QCD-scale ( $\Lambda = 100 \text{ MeV}$ ). Using the same sum rule (2.51), Narison [17] extracted a typical value of about  $f_B = 185 \text{ MeV}$  with a very high threshold  $s_0 = 50 \text{ GeV}^2$  and a low Borel parameter  $M^2 \approx 2.8 \text{ GeV}^2$ .

In the late 90's analyses were applied using the running mass of the heavy quark in the  $\overline{MS}$ -scheme instead of the pole mass. Their definitions are given in appendix A. Although the pole mass is independent of the renormalization scheme, it is sensitive to long distance dynamics[23]. This can be observed by considering the self energy diagram. Replacing the gluon propagator by the full propagator with fermion loops, leads to a IR singularity of the integral. Therefore, an ambiguity, which is of order  $\Lambda_{QCD}$ , enters the definition of the pole mass and one cannot assign a value to it, which is more precise. In the case of the B-meson decay constant, using the pole mass in (2.51), the contributions from the first order and second order corrections are of the same size as the one loop perturbative results, whereas the expansion is under good control, if the running mass is used - see [5] and also table 3.1.

We will now briefly demonstrate the analysis of the sum rule for  $f_B$ , following Jamin and Lange [5]. Second order corrections to the perturbative result were found by Chetyrkin and Steinhauser [9] and are available as mathematica file *rvs.m*. Jamin and Lange also gave an expansion in the light quark mass up to  $O(m^4)$ . These corrections are numerically negligible, however, from terms of order  $O(m^3)$  on, mass logarithms of the form  $\log(\mu^2/m^2)$  appear. These can be cancelled by rewriting the normal ordered condensates into non-normal ordered [13]. With this at hand, Jamin and Lange found corrections to the quark-condensate to first order in the strong coupling  $\alpha_s$ :

$$c_{\bar{q}q}^{(1)}(M^2, s_0, \mu) = 2 \int_{\frac{m_b^2}{M^2}}^{\frac{s_0}{M^2}} dt e^{-t} t^{-1} - 2 \left[ 1 + \left( 1 - \frac{m_b^2}{M^2} \right) \left( \log \frac{\mu^2}{m_b^2} + \frac{4}{3} \right) \right] e^{-\frac{m_b^2}{M^2}}. \quad (3.1)$$

This expression is already Borel transformed. The dependence on the threshold  $s_0$  in the upper limit of the integral appears, when the initial expression is written as a dispersion relation and the continuum contribution from the hadronic side is subtracted.

The calculation of the simple quark loop involved the replacement of the quark propagators with delta functions, thus setting the quarks on-shell. It follows that the heavy quark mass  $m_b$ , appearing in the perturbative part of the sum rule (2.51), is per definition the pole mass. To express the decay constant  $f_B$  in terms of the running mass  $\bar{m}(\mu)$ , one has to apply equation (A.12). Effectively, this replacement only changes the size of the different loop-contributions - the total contribution should stay the same. However, the zero order perturbative contribution to the decay constant rises significantly after insertion of the running mass, while the first and second order show a convergent behavior. Thus, with the change to the running mass one can truncate the expansion even after the  $O(\alpha_s)$ -corrections. Keeping the pole mass leads to first- and second-order corrections of about the same size as the zeroth order. The truncation of the expansion in the strong coupling after the second order terms might lead to further errors, when contributions of higher order terms are not taken into account. The different contributions to the final results in the two schemes are shown in table (3.1).

The quark masses appearing in the leading order coefficients of the condensates are not defined to be the pole- or the running mass, either. We use the running mass without imposing  $O(\alpha_s)$ -corrections to the coefficients.

The final sum rule for the decay constant up to  $O(\alpha_s^2)$  and without corrections in the light quark mass reads:

$$m_B^4 f_B^2 e^{-\frac{m_B^2}{M^2}} = \Sigma(M^2, s_0), \quad (3.2)$$

where the right hand side is given by

$$\begin{aligned} \Sigma(M^2, s_0) = & \frac{3m_b^2}{8\pi^2} \int_{m_{b,pole}^2}^{s_0} ds \left[ \frac{(m_b^2 - s)^2}{s} \left( 1 + \frac{4\alpha_s}{3\pi} (c^1(s) + \Delta^{(1)}) \right) + \frac{\alpha_s^2}{3\pi^2} (c_{CS}^{(2)}(s) + \Delta^{(2)}) \right] e^{-\frac{s}{M^2}} \\ & + m_b^2 \left[ \left( -1 + \frac{\alpha_s}{\pi} c_{\bar{q}q}^{(1)} \right) m_b \langle \bar{q}q \rangle + \frac{1}{12} \langle \frac{\alpha_s}{\pi} GG \rangle - \frac{m_b^2}{2M^2} \left( 1 - \frac{m_b^2}{2M^2} \right) m_0^2 \langle \bar{q}q \rangle \right. \\ & \left. - \frac{16\pi}{27} \frac{1}{M^2} \left( 1 - \frac{m_b^2}{4M^2} - \frac{m_b^4}{12M^4} \right) \alpha_s \langle \bar{q}q \rangle^2 \right] e^{-\frac{m_b^2}{M^2}}. \end{aligned} \quad (3.3)$$

Here,  $\Delta^{(1)}$  and  $\Delta^{(2)}$  are the additional first and second order corrections coming from the replacement of the pole masses by use of equation (A.12). In the expression (3.3), the mass  $m_b$



is now understood as being the scale dependent running mass  $\overline{m}_b(\mu)$ . The quark mass in the lower limit of the integral is kept to the pole mass. It indicates the start of the branch cut on the positive  $q^2$ -axis. Replacing it by the running mass would lead to corrections starting at order  $O(\alpha_s^3)$ . The numerical results, if the running mass is used instead of the pole mass differ about 5%. A similar sum rule, except for the  $O(\alpha_s)$ - corrections to the coefficient of the quark condensate, was also used by Narison, who was further able to extract the running mass  $\overline{m}_b(\overline{m}_b)$  at the same time [24, 25]<sup>1</sup>.

Besides the QCD-parameters  $\alpha_s, \overline{m}_b(\mu)$  and the phenomenological condensates, the function  $\Sigma(M^2, s_0)$  also depends on the artificial parameters  $s_0$ , coming from the crude duality ansatz (2.50), and the Borel mass  $M^2$ . Ideally, if one knew the hadronic spectral density to all energies and the whole perturbative expansion and non-perturbative corrections to it on the right hand side of the sum rules, the resulting function for the decay constant would not depend on the momentum transfer  $q^2$  and thus not on the Borel mass. However, in the real world one has to give arguments for the values of these two parameters, where the decay constant is read off. After the Borel transformation, the contribution of the hadronic continuum is exponentially suppressed and the Borel parameter  $M^2$  should be small enough to ensure that errors coming from the approximation (2.50) do not contribute to a large extend. On the other side, the Borel mass should be high enough, such that the expansion in the condensates converges sufficiently fast and the truncation of the series is justified. In our analysis of the sum rule (3.2), we will take the window  $4 \text{ GeV}^2 < M^2 < 8 \text{ GeV}^2$ , where on the left boundary the contribution from the mixed quark gluon condensate contributes to less than 8% and the four quark contribution is negligible. The continuum contribution of the hadronic side is rather large in the whole window and rises to about the same size as the final sum rule on the right boundary. Therefore, the threshold parameter  $s_0$  has to be chosen carefully. It is considered to be roughly in the range of the first excited state of the hadron under investigation and taken such, that the decay constant does not vary strongly in the Borel window.

An often suggested procedure to get the reading point  $(\hat{M}_0^2, \hat{s}_0)$  of  $f_B$  is to look at the daughter sum rule of (3.3) [26], defined by

$$\Re(M^2, s_0) = M^4 \frac{d}{dM^2} \log \Sigma(M^2, s_0). \quad (3.4)$$

Applying the derivative on the left hand side of equation (3.2) it is then argued that the resulting function is independent of  $f_B$  and gives the squared pseudoscalar mass as a function of  $M^2$ . Setting this function equal to the experimental mass  $m_B^2$ , gives reading points for the threshold and the Borel mass. However, in our opinion this method sometimes is overrated in the literature. The crucial point is that the sum rule (3.2) leads to a rather complicated function for the decay constant  $f_B$ , which is by no means independent of  $M^2$ . The parameter that is constant in the sum rule (3.2) is the mass  $m_B$  of the pseudoscalar meson. Its input value in the final sum rule is the experimental mass, independent of  $M^2$ . Taking the derivative of the logarithm of both sides in (3.2) yields:

$$m_B^2 + \frac{M^4 f_B^{\prime 2}(M^2)}{f_B^2(M^2)} = \Re(M^2, s_0). \quad (3.5)$$

Thus, setting the ratio  $\Re(\hat{M}^2, \hat{s}_0)$  equal to the squared mass  $m_B^2$  at a point  $M_0^2$  is just a rather complicated procedure to find an extremum of the initial function  $f_B(M^2)$ . The argument for taking this distinct value for the Borel mass  $\hat{M}^2$  is then not the fact that it represents the *right*

---

<sup>1</sup>Narison adjusted the parameters  $s_0, M^2$  and the quark mass  $m_b$  such that the sum rule is in the most stable region. He extracted  $\overline{m}_b(\overline{m}_b) = (4.05 \pm 0.06) \text{ GeV}$ , which is rather small compared to typical values.

value for the meson mass (this is always the case), but rather that the function for the decay constant is in a stable region around this point. In figure 3.1, we plotted the decay constant  $f_B(M^2)$  for several values of the threshold  $s_0$  and the corresponding ratios  $\mathfrak{R}^{1/2}(M^2, s_0)$ , defined in (3.4) as functions of  $M^2$ . The intersections with the experimentally measured mass  $m_B = 5.279 \text{ GeV}$  give the values of the squared Borel parameter  $M^2$ , where  $f_B$  reaches an extremum.

There is a distinct pair of the threshold and the Borel parameter, where the ratio  $\mathfrak{R}^{1/2}(M^2, s_0)$  reaches a minimum at the meson mass. Taking one more derivative with respect to  $M^2$  in (3.5), gives

$$2 \frac{M^2 f_B^{\prime 2}(M^2)}{f_B^2(M^2)} - \frac{M^4 f_B^{\prime 2 2}(M^2)}{f_B^4(M^2)} + \frac{M^4 f_B^{\prime\prime 2}(M^2)}{f_B^2(M^2)} = \mathfrak{R}'(M^2, s_0). \quad (3.6)$$

Setting the minimum of  $\mathfrak{R}(M^2, s_0)$  equal to the mass  $m_B^2$  yields the condition

$$f_B''(\hat{M}^2, \hat{s}_0) = 0. \quad (3.7)$$

Therefore, the pair  $(\hat{M}^2, \hat{s}_0)$  found in this way gives a stable region, where the first two derivatives of the decay constant vanish, and one can extract a value for  $f_B$ . However, there is no physical argument except the stability of the sum rule around this point that this value resembles the true decay constant at best.

Using the sum rule (3.3) with additional corrections in the light quark mass up to order  $O(m_q^4)$ , Jamin and Lange extracted for the B-meson decay constant

$$f_B = (210 \pm 19) \text{ MeV}. \quad (3.8)$$

Here, the main uncertainties come from the value of the heavy quark mass  $m_b = 4.21 \pm 0.05$ , the scale  $\mu = (3-6) \text{ GeV}$  and the value of the quark condensate  $\langle \bar{q}q \rangle (2 \text{ GeV}) = -(267 \pm 17)^3 \text{ MeV}^3$ .

We repeated the analysis using the procedure described above, however, only including first order corrections. Replacing the pole mass by the running quark mass leads to corrections to the  $O(\alpha_s)$ -terms of:

$$\Delta^{(1)} = \frac{s - 3\bar{m}_b^2}{s - \bar{m}_b^2} \left( 2 + \frac{3}{2} \log \frac{\mu^2}{\bar{m}_b^2} \right). \quad (3.9)$$

For the running b-quark mass, we take the value from El-Khadra [27],  $m_b = 4.24 \pm 0.11 \text{ GeV}$ , which is obtained as an average from a large collection of different analyses, including lattice simulations and sum rule methods for several systems containing b-quarks. The corresponding pole mass is  $m_{b,pole} = 4.69 \text{ GeV}$ , using the two-loop relation (A.12). The values for the other input parameters we used in this analysis and the following ones are listed in table 3.2. Taking the mean values we obtained

$$f_B = 208 \text{ MeV} \quad s_0 = 34.1 \text{ GeV}^2 \quad M^2 = 5.5 \text{ GeV}^2. \quad (3.10)$$

$f_{B,JL}^2$	$f_1^{(0)}$	$f_1^{(1)}$	$f_{\langle \bar{q}q \rangle}^{(0)}$	$f_{\langle \bar{q}q \rangle}^{(1)}$	$f_{\langle - \rangle}$	$f_{B,KR}^2$	$f_1^{(0)}$	$f_1^{(1)}$	$f_{\langle \bar{q}q \rangle}^{(0)}$	$f_{\langle - \rangle}$
43468	33064	1855	13201	-4203	-449	32314	12045	11170	11388	-2290

Table 3.1: Contributions of the different terms to the squared decay constant  $f_B$  for the two analyses of Jamin and Lange (left table) and Khodjamirian and Ruckl (right table).  $f_{\langle - \rangle}$  indicates the contribution from condensates with mass dimension four or higher.

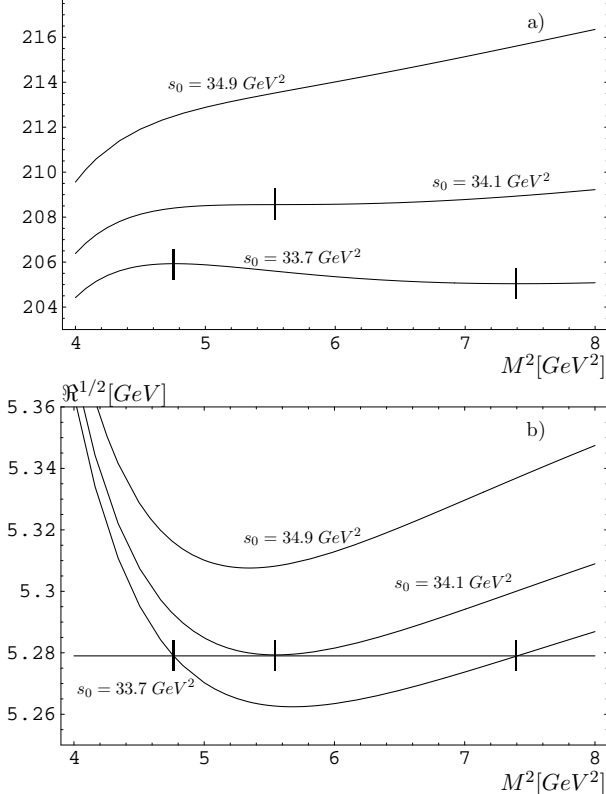


Figure 3.1: Decay constant  $f_B$  (graph a) and the Ratio  $\mathfrak{R}^{1/2}$  (b), defined in equation (3.5), as functions of the Borel parameter  $M^2$ , plotted for three different values of the threshold  $s_0$ . The intersections of  $\mathfrak{R}^{1/2}$  with the experimentally measured meson mass  $m_B = 5.279 \text{ GeV}$  correspond to extremal points of the decay constant. In the case of  $s_0 = 34.1 \text{ GeV}$ , also the second derivative of the corresponding function of the decay constant vanishes.

Although we only included first order corrections and used a different quark running mass and corresponding pole mass, this result is very close to (3.8). We do not give an estimate of the error, since we are only interested in the relative size of the different contributions to the decay constant.

The contributions to  $f_B^2$  from the several terms of the sum rule are shown in table 3.1. This table shows also our result for the sum rule analysis following Khodjamirian and Rückl [8]. By using the suggested values of  $m_{b,pole} = 4.7 \text{ GeV}$  for the b-quark pole mass and  $s_0 = 35 \text{ GeV}^2$  for the threshold, we could exactly reproduce the value  $f_B = 180 \text{ MeV}$ . Note that the first order corrections in the strong coupling are of about the same size than the zeroth order perturbative result and contribute to about 35% of the final result. By switching to the running mass the main contribution of the perturbative calculation is shifted to the zeroth-order term, whereas the  $O(\alpha_s)$ -corrections are about 4% of the final result. Including the second order corrections from Chetyrkin and Steinhauser [9] in the pole mass scheme, the contribution is again of the same size than the zeroth and first order corrections. In the analysis of Jamin and Lange the  $O(\alpha_s^2)$ -corrections are negligible.

Since the expansion in the strong coupling constant is under good control compared to the sum rule using the pole mass for the heavy quark, we will use the sum rule in the form of equation (3.2) up to  $O(\alpha_s)$  as the starting point of our own analysis.

### 3.2 The Limit $M^2 \rightarrow \infty$

As argued above, the method of setting the daughter sum rule (3.4) equal to the meson mass is equivalent to search for a threshold parameter  $s_0$ , for which the sum rule for the decay constant is in a stable region. Another method was suggested several times by Radyushkin [6, 7] in sum rule analyses of the pion form factor. By taking the limit  $M^2 \rightarrow \infty$ , one can get rid off

higher dimensional condensates and the sum rule is again in a stable region. In this limit, the uncertainties coming from the truncation of the power series vanish, whereas higher resonances and the continuum contribution are not suppressed exponentially anymore. Thus, the duality approximation is the crucial assumption in this approach and the source of the main error. In the limit  $M^2 \rightarrow \infty$ , the sum rule reads:

$$m_B^4 f_B^2 = \frac{3m_b^2}{8\pi^2} \int_{m_{b,pole}^2}^{s_0} ds \frac{(m_b^2 - s)^2}{s} \left( 1 + \frac{4\alpha_s}{3\pi} \left( c^1(s) + \Delta^{(1)} \right) \right) + m_b^2 \left[ \left( -1 - 2 \frac{\alpha_s(\mu)}{\pi} \left( \frac{7}{3} + \log \frac{\mu^2}{m_b^2} \right) \right) m_b \langle \bar{q}q \rangle + \frac{1}{12} \langle \frac{\alpha_s}{\pi} GG \rangle \right]. \quad (3.11)$$

Apart from the constant contributions of the two condensates, the decay constant is now described as the average of the transition of a free quark pair of invariant mass  $s$  in the duality interval  $m_{b,pole}^2 < s < s_0$ . In the analysis of the pion form factor [6], the threshold is estimated to be the midpoint between the first ( $\pi$ ) and second ( $A_1$ ) resonance. Applied to the B-meson sum rule, the threshold should then be around  $s_0 \simeq 31 \text{ GeV}^2$ , assuming that the mass of the first excited state  $B'$  is about  $0.5 \text{ GeV}$  higher than the ground state.

Instead of setting the threshold to the above value and varying it within a certain interval, we propose to take a distinct value of  $s_0$ . In the limit  $M^2 \rightarrow \infty$ , the sum rule for the decay constant is only a function of the threshold. Its first derivative scales like  $f_B^{2'} \propto 1/M^4$ . Although  $f_B$  is asymptotic for any value of the threshold, we suggest taking the value  $s_0^*$ , that satisfies

$$M^4 f_B^{2'}(M^2, s_0^*) \xrightarrow{M^2 \rightarrow \infty} 0, \quad (3.12)$$

for which the sum rule reaches its asymptotic value the fastest. Using (3.12) in equation (3.5),  $s_0^*$  can be found by setting the daughter sum rule of (3.3) to the meson mass in the limit  $M^2 \rightarrow \infty$ :

$$\Re(M^2, s_0^*) \xrightarrow{M^2 \rightarrow \infty} m_B^2. \quad (3.13)$$

In figure 3.2, we demonstrate the matching of  $\Re(M^2, s_0)$  to the meson mass for different values of the running quark mass and show the functions of the corresponding sum rules for the decay constant  $f_B$ . Using the values of table 3.2, we find a mean threshold of  $s_0^* = 31.7 \text{ GeV}$ . The corresponding decay constant is:

$$f_B = (178 \pm 18 \pm 20) \text{ MeV}. \quad (3.14)$$

Here, the first error is inflicted by the uncertainties in the quark mass. We separate this error from the remaining ones, since when the sum rule for the form factor in section 4.1 is divided

Parameter	Value	$\Delta f_B$	Taken from
$\bar{m}_b(\bar{m}_b)$	$(4.24 \pm 0.11) \text{ GeV}$	$\pm 18$	[27]
$\langle \bar{q}q \rangle$	$-(267 \pm 16)^3 \text{ MeV}$	$\pm 5$	[15]
$\mu$	$(3.5 - 6) \text{ GeV}$	$\pm 14$	-
$\langle \frac{\alpha_s}{\pi} GG \rangle$	$(0.012 \pm 0.012) \text{ GeV}^4$	$\pm 1$	[8]
$m_0^2$	$(0.8 \pm 0.2) \text{ GeV}^2$	$\pm 0$	[5]
$\alpha_s \langle \bar{q}q \rangle^2$	$(8 \pm 8)^{-5} \text{ GeV}^6$	$\pm 0$	[8]

Table 3.2: Values of the parameters used for the analysis  $M^2 \rightarrow \infty$  and the corresponding errors they inflict on the final value for the decay constant  $f_B = 178 \text{ MeV}$ .

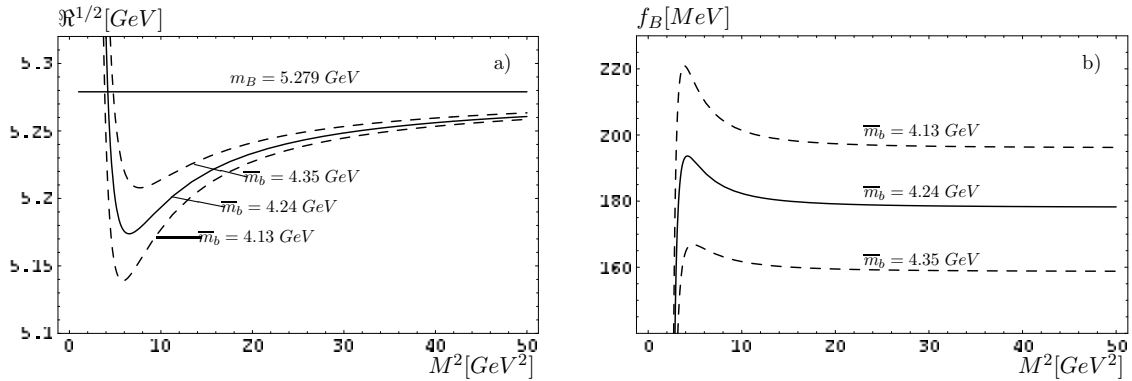


Figure 3.2: a: Matching of the daughter sum rule (3.4) to the meson mass  $m_B = 5.279 \text{ GeV}$  in the limit  $M^2 \rightarrow \infty$  for different values of the running quark mass  $\bar{m}_b$ . - b: The corresponding sum rules for the decay constant, using the threshold  $s_0^*$ , found by the matching procedure in the left figure.

by  $f_B$  and the quark mass is varied simultaneously, the uncertainties coming from the mass will almost cancel in the final result for  $f^+(0)$ .

The uncertainties of the parameters used and the corresponding errors to the final result are listed in table 3.2. The decay constant is very sensitive to the running quark mass and the scale. At lower values of  $\mu$ , the perturbative expansion becomes quite important. The inclusion of second order corrections in the strong coupling would give a better control of the scale dependence. However, we do not intend to give a too accurate result, for the accuracy of this method itself is limited intrinsically. Since the exponential damping of the higher excitations and the continuum contribution is taken away by the limiting procedure  $M^2 \rightarrow \infty$ , errors coming from the crude duality ansatz are rather emphasized. We therefore sum up linearly all errors inflicted by the several input parameters except the quark mass, leading to the relatively large overall error in (3.14).

Although the decay constant  $f_B$  is very sensitive to the values of the input parameters, the corresponding threshold  $s_0^*$  is not. Varying the parameters within the errors indicated in table 3.2 and adjusting the threshold such that the daughter sum rule matches the meson mass  $m_B$  in the limit  $M^2 \rightarrow \infty$  (3.13),  $s_0^*$  always stays in the rather small interval

$$31.5 \text{ GeV}^2 < s_0^* < 32.0 \text{ GeV}^2. \quad (3.15)$$

Vice versa, the value of the decay constant is quite sensitive to the threshold  $s_0$ . Thus, taking the limit  $M^2 \rightarrow \infty$  and guessing the threshold to be in a certain region, instead of fixing it by the method described above, leads to large uncertainties of the final result.

In section 3.4, we will relate the value (3.14) with the result of the analysis of the next section and compare our results with other analyses from the literature.

### 3.3 Borel Mass dependent Threshold $s_0(M^2)$

In this section, we propose a further approach to analyze the sum rule (2.51). As argued above and illustrated in figure 3.1, the method of setting the logarithmic derivative (3.4) equal to the meson mass is a rather sophisticated way to search for a value of the threshold  $s_0$ , for that the sum rule of the decay constant is in a stable region. This works nicely for the B-meson decay

constant - the resulting function of  $f_B$  is almost constant over the Borel window. However, there are sum rules, as will be seen later, in which the resulting function for the hadronic parameter has a strong dependence on  $M^2$ . Here, one cannot find a threshold  $s_0$  in a physical accessible region for which the first two derivatives of the sum rule vanish and sometimes not even the first one.

Ideally, the decay constant is not a function of the Borel parameter. From a certain value of  $M^2$  on, the expansion in the vacuum condensates in equation (3.3) is under good control and its truncation does not induce a significant error to the final result. Assuming that all errors to the sum rule come from the duality approximation (2.54), we introduce a Borel mass dependent threshold  $s_0(M^2)$  that compensates this error. This means, we search for functions  $s_0(M^2)$ , for which the decay constant  $f_B$  is not a function of the Borel mass.

At first sight, this modification is quite similar to the initial approach of adjusting the constant threshold such, that the sum rule is in stable region. Instead of having a decay constant that is dependent on  $M^2$ , this dependence is now shifted to the threshold  $s_0(M^2)$ . Furthermore one does not find a unique value of the decay constant. For each value of  $f_B$ , one should be able to find a function  $s_0(M^2)$ . However, this approach has an intuitive interpretation. It is rather clear that the hadronic spectral density can only be represented approximately by the perturbative free quark spectral function. Introducing in (2.54) a  $q^2$ -dependent threshold can compensate for this error. For each distinct value of the momentum transfer, one can then impose a value  $s(q^2)$  rendering the approximation exact. After Borel transformation, the resulting sum rule for the decay constant should then be independent of  $M^2$  provided that the errors induced from the truncation of the power series and the expansion in the strong coupling are negligible<sup>2</sup>.

It still remains the question of where to read off the value of the decay constant, since one can find a continuum of functions  $s_0(M^2)$ , for which the sum rule is constant over  $M^2$ . At this point, the duality assumption reenters the analysis. Assuming (2.54) is a good approximation in the sense that one can find a constant threshold for which the two sides equal, we suggest looking for the most stable function  $s_0(M^2)$  to reflect this duality ansatz. Thus, whereas in most other applications the threshold is a constant and its value enters by physical reasoning or is found by searching for the most stable function  $f(M^2)$ , the proposed modification features constant functions  $f_B$  in a given Borel window and we search for the most stable functions  $s_0(M^2)$ .

Since the sum rule for  $f_B(M^2)$ , which results from setting the minimum of the daughter sum rule equal to the meson mass is already quite constant in the window  $4 \text{ GeV} \leq M^2 \leq 8 \text{ GeV}$  (see figure 3.1), it is not surprising, that the following analysis will lead to the same result.

Taking the derivative  $M^4 d/dM^2$  of the logarithm of both sides of equation (3.2) yields:

$$m_B^2 + \frac{M^4 f_B^{\prime 2}(M^2)}{f_B^2(M^2)} = \frac{M^4 \frac{\partial}{\partial M^2} \Sigma(M^2, s_0(M^2)) + M^4 s_0'(M^2) \frac{\partial}{\partial s_0} \Sigma(M^2, s_0(M^2))}{\Sigma(M^2, s_0(M^2))}. \quad (3.16)$$

Setting the right hand side equal to the squared meson mass  $m_B^2$ , we get a differential equation for the function  $s_0(M^2)$ :

$$s_0'(M^2) = \frac{m_B^2 \Sigma(M^2, s_0(M^2)) - M^4 \frac{\partial}{\partial M^2} \Sigma(M^2, s_0(M^2))}{M^4 \frac{\partial}{\partial s_0} \Sigma(M^2, s_0(M^2))}. \quad (3.17)$$

---

<sup>2</sup>In the analysis below, we introduce the functional dependence of the threshold after the Borel transformation, since the limiting procedure of equation (2.47) would be non-trivial if one included the dependence on the momentum transfer  $q^2$  before the transformation. Nevertheless, the physical picture, that shifting the  $q^2(M^2)$ -dependence to the threshold is compensating errors coming from the duality approximation, stays the same

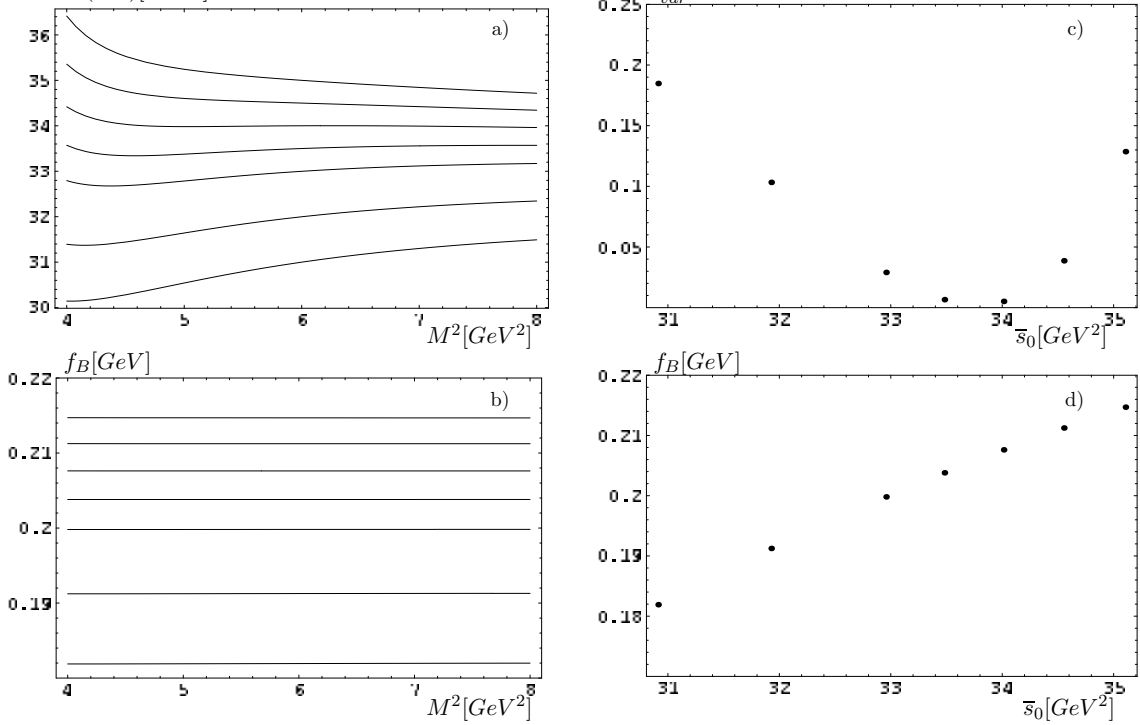


Figure 3.3: Sum rule analysis for Borel mass dependent thresholds. Graph a) shows various functions for  $s_0(M^2)$ , which are solutions to the differential equation (3.17). Below, the corresponding functions for the decay constant are plotted (b). Graph c) shows the variation of the threshold functions  $s_0(M^2)$  plotted in a), as a function of their average value in the given Borel window. Diagram d) shows the decay constant plotted over the average values of the thresholds.

We do not write the explicit form of the right hand side, since it is a rather complicated function of  $s_0(M^2)$  and its derivation is straightforward. Setting the solutions of equation (3.17) into the sum rule for the decay constant will yield constant functions of  $f_B$ .

This equation was solved numerically. We started at certain values for the threshold  $s_0$  at  $M^2 = 6 GeV^2$  and the functions were then evaluated with mathematica, using a numerical procedure with adaptive step size.

Figure 3.3a shows some solutions of  $s_0(M^2)$  we obtained for the mean values of the input parameters listed in table 3.3. The corresponding decay constants are given below (b). As argued above, we read off the decay constant at the most stable function of  $s_0(M^2)$ . This could be done by simply looking at the graphs of the threshold  $s_0(M^2)$ , since the method itself contains implicit errors and one should not seek for a too accurate result. However, to demonstrate the equivalence to the result (3.10) obtained by following the analysis of Jamin and Lange [5], we introduce a variation of the threshold functions:

$$s_{var}^n = \frac{1}{4} \int_4^8 (s_0^n(M^2) - \bar{s}_0^n)^2 dM^2. \quad (3.18)$$

In figure 3.3 c, we listed the variations of the functions  $s_0(M^2)$  over their average value. Graph 3.3 d shows the corresponding decay constants, again plotted as a function of the mean value of the threshold. Reading off the decay constant at the point with the least variation gives

$$f_B = 208 MeV. \quad (3.19)$$

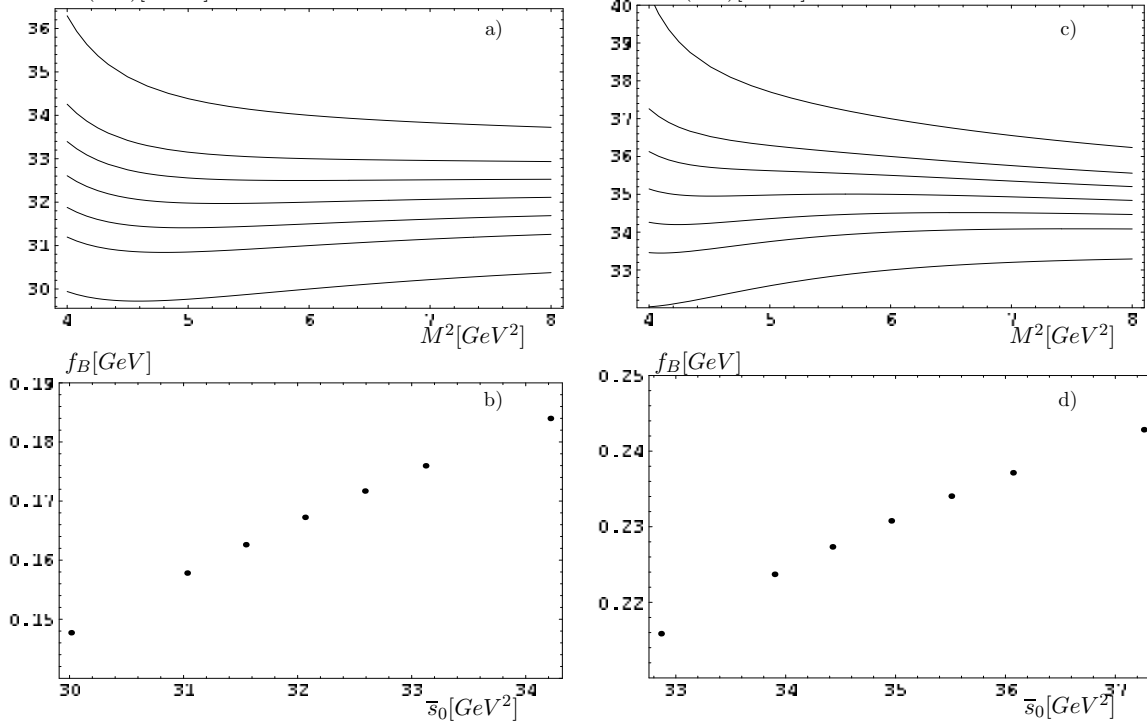


Figure 3.4: Borel mass dependent functions for the threshold  $s_0(M^2)$  and corresponding decay constants  $f_B$ , plotted over the average value of the thresholds. On the left side  $m_b = 4.35 \text{ GeV}$  was used as input value for the running quark mass - on the right side  $m_b = 4.13 \text{ GeV}$ .

Thus, we reproduced the result (3.10) from the analysis in section 3.1, following Jamin and Lange.

In table 3.3, we listed the value of the input parameter we used for this analysis and the corresponding errors they inflict on the final result. In figure 3.4 we plotted the results of our analysis for the b-quark masses  $m_b = 4.13 \text{ GeV}$  and  $m_b = 4.35 \text{ GeV}$ . Again,  $f_B$  is very sensitive to the running mass and the scale. We again separate the error coming from the quark mass from the remaining errors, added in quadrature:

$$f_B = (208_{-41}^{+23} \text{ }_{-14}^{+19}) \text{ MeV} \quad (3.20)$$

The total error of  $f_B$  is rather large. This is mainly due to the large uncertainties, which we assigned to the quark mass. In the following two chapters, we will analyze the sum rules for the B-meson semi-leptonic form factor  $f^+(0)$  and the coupling  $g_{B^*B\pi}$ . These sum rules are proportional to the decay constant. When the two sum rule results are divided by  $f_B$  and the quark

Parameter	Value	$-\Delta f_B$	$+\Delta f_B$	Taken from
$\overline{m}_b(\overline{m}_b)$	$(4.24 \pm 0.11) \text{ GeV}$	231	167	[27]
$\langle \overline{q}q \rangle$	$-(267 \pm 16)^3 \text{ MeV}$	200	212	[15]
$\mu$	$(3.5 - 6) \text{ GeV}$	192	221	-
$\langle \frac{\alpha_s}{\pi} GG \rangle$	$(0.012 \pm 0.012) \text{ GeV}^4$	207	208	[8]
$m_0^2$	$(0.8 \pm 0.2) \text{ GeV}^2$	208	203	[5]
$\alpha_s \langle \overline{q}q \rangle^2$	$(8 \pm 8)^{-5} \text{ GeV}^6$	208	208	[8]

Table 3.3: Input parameters used for the analysis with a Borel mass dependent threshold. The column  $-\Delta f_B(+\Delta f_B)$  shows the deviations from the central result  $f_B = 208 \text{ MeV}$ , when the lower(higher) limit of the input parameter is used.



masses are varied simultaneously, the final errors due to the uncertainties in the quark mass decrease drastically.

We also checked that changes in the boundaries of the Borel window have a minor effect on the corresponding variations of the functions  $s_0(M^2)$  and the point of extraction of the decay constant.

### 3.4 Summary of the Results and Relation to the Literature

The two results (3.14) and (3.20) differ about 15%. In the sum rules we analyze in this thesis, the method of taking the limit  $M^2 \rightarrow \infty$  will always lead to significantly lower results than the method of imposing a Borel mass dependent threshold  $s_0(M^2)$ . Considering only the LO-perturbative term of the daughter sum rule

$$\int_{m_b^2}^{s_0} ds s f(s) e^{-\frac{s}{M^2}}, \quad (3.21)$$

it is clear from the positivity of the integrand  $f(s)$  and the vanishing of the exponential damping in the limit  $M^2 \rightarrow \infty$ , that the relevant value of the integral needed in the fitting procedure is reached at a rather small threshold  $s_0$ . In the second method, we are looking for functions  $s_0(M^2)$  that do not depend strongly on the Borel mass. Thus, the contribution from the term proportional to  $s'_0(M^2)$  in (3.16) is small compared to (3.21) and therefore, the upper limit  $s_0(M^2)$  of the integral has to be higher than in the former case. The difference in the size of the two thresholds translates into the discrepancy of the final results for the decay constant. This can be inferred from the figures 3.2 and 3.1. Since the limit  $\Re(M^2, s_0^*) \rightarrow m_B^2$  is reached from below, the corresponding sum rule for the decay constant is monotonously decreasing and in the Borel window of figure 3.1 it would lie below the plotted curves.

In table 3.4, we listed our results for the decay constant and several results from the literature. The latest sum rule analyses [5] and [25], including three-loop corrections to the perturbative calculations and using the running quark mass, coincide with our result from using a Borel mass dependent threshold. The result from Wittig [30] is a global estimate of recent unquenched lattice calculations. It is about 10% lower than the sum rule results. Nevertheless, all the quoted values are in agreement, when the error bars are taken into account.

$f_B [MeV]$	Ref.	Method
$178 \pm 27$	This Thesis	SVZ-SR $O(\alpha_s)$ ; running mass; $\lim M^2 \rightarrow \infty$
$208^{+30}_{-43}$	This Thesis	SVZ-SR $O(\alpha_s)$ ; running mass; $s_0(M^2)$
$180 \pm 30$	Khodjamirian '98[8]	SVZ-SR $O(\alpha_s)$ ; pole mass
$190 \pm 9$	Narison '98[24]	SVZ-SR $O(\alpha_s)$ ; running mass
$210 \pm 19$	Jamin '01[5]	SVZ-SR $O(\alpha_s^2)$ ; running mass
$205 \pm 23$	Narison '01[25]	SVZ-SR $O(\alpha_s^2)$ ; running mass
$173 \pm 13^{+34}_{-1}$	Abada APE'99[28]	Lattice
$218 \pm 5^{+5}_{-41}$	Bowler UKQCD'00[29]	Lattice
$191 \pm 23^{+0}_{-19}$	Wittig '03[30]	Lattice-summary of unquenched results

Table 3.4: Comparison of our results with a collection of values from other analyses in the literature.

Before we proceed with the analysis of the B-meson weak form factor  $f^+(0)$  and the strong coupling  $g_{B^*B\pi}$ , we present briefly the analysis of the two point sum rule for the vector meson decay constant  $f_{B^*}$ .

### 3.5 Weak Decay Constant $f_{B^*}$

The decay constant  $f_{B^*}$  is needed in the analysis for the strong coupling  $g_{B^*B\pi}$ , since the sum rule we use to extract this coupling is proportional to the decay constants of the  $B$ - and the  $B^*$ -meson. We will analyze the light cone sum rule for the coupling by the use of the two new methods introduced in this chapter. To get a consistent value for  $g_{B^*B\pi}$ , we will divide the sum rule by the corresponding decay constants  $f_B$  and  $f_{B^*}$ , obtained within the same method. We therefore summarize in this section our analysis of the  $B^*$  decay constant.

We collected the sum rule for the heavy-light vector meson constant from Dominguez[31] and Reinders[12]. Neglecting the numerically insignificant contribution of the four quark condensate, we get up to mass dimension 5 in the condensates and first order in the perturbative expansion:

$$f_{B^*}^2 m_{B^*}^2 e^{-\frac{m_{B^*}^2}{M^2}} = \frac{1}{8\pi} \int_{m_b^2}^{s_0} ds \frac{(s - m_b^2)^2}{s} \left(2 + \frac{m_b^2}{s}\right) \left[1 + \frac{4\alpha_s}{3\pi} \left(f^{(1)}(s) + \Delta^{(1)}(s)\right)\right] e^{-\frac{s}{M^2}} + \left[-m_b \langle \bar{q}q \rangle \left(1 - \frac{m_0^2 m_b^2}{4M^4}\right) + \frac{1}{12} \langle \frac{\alpha_s}{\pi} GG \rangle\right] e^{-\frac{m_b^2}{M^2}}, \quad (3.22)$$

where the first order correction in the strong coupling is given by:

$$f^{(1)}(s) = \frac{13}{4} + 2Li_2\left(\frac{m_b^2}{s}\right) + \log\left(\frac{m_b^2}{s}\right) \log\left(1 - \frac{m_b^2}{s}\right) + \frac{3}{2} \frac{m_b^2}{2s + m_b^2} \log\left(\frac{m_b^2}{s - m_b^2}\right) - \log\left(1 - \frac{m_b^2}{s}\right) - \frac{(4s^2 - m_b^2 s - m_b^4)}{(s - m_b^2)^2 (2s + m_b^2)} m_b^2 \log\left(\frac{m_b^2}{s}\right) - \frac{5s^2 - m_b^2 s - 2m_b^4}{(s - m_b^2)(2s + m_b^2)}. \quad (3.23)$$

We again replaced the pole mass in the integrand by the running  $\overline{MS}$ -mass. This lead to the additional term:

$$\Delta^{(1)}(s) = \frac{6m_b^2(s + m_b^2)}{m_b^4 + m_b^2 s - 2s^2} \left(1 + \frac{3}{4} \log \frac{\mu^2}{m_b^2}\right) \quad (3.24)$$

As before, with the pole mass replaced by the running mass, the sum rule shows better convergence. The first order correction amounts to about 20% of the perturbative part, whereas before this contribution was about 60%. The use of the running mass increases the overall perturbative contribution about 30%.

Parameter	Value	$-\Delta f_{B^*}$	$+\Delta f_{B^*}$	Taken from
$\overline{m}_b(\overline{m}_b)$	$(4.24 \pm 0.11) GeV$	221	174	[27]
$\langle \bar{q}q \rangle$	$-(267 \pm 16)^3 MeV$	192	203	[15]
$\mu$	$(3.5 - 5) GeV$	182	208	-
$\langle \frac{\alpha_s}{\pi} GG \rangle$	$(0.012 \pm 0.012) GeV^4$	197	198	[8]
$m_0^2$	$(0.8 \pm 0.2) GeV^2$	197	197	[5]

Table 3.5: Values of the input parameters used in the sum rule analysis of  $f_{B^*}$  in the limit  $M^2 \rightarrow \infty$  and the corresponding errors they inflict on the final result. The central result is  $f_{B^*} = 197 MeV$ .

Parameter	Value	$-\Delta f_{B^*}$	$+\Delta f_{B^*}$	Taken from
$\overline{m}_b(\overline{m}_b)$	$(4.24 \pm 0.11) \text{ GeV}$	281	213	[27]
$\langle \bar{q}q \rangle$	$-(267 \pm 16)^3 \text{ MeV}$	233	257	[15]
$\mu$	$(3.5 - 5) \text{ GeV}$	226	258	-
$\langle \frac{\alpha_s}{\pi} GG \rangle$	$(0.012 \pm 0.012) \text{ GeV}^4$	245	246	[8]
$m_0^2$	$(0.8 \pm 0.2) \text{ GeV}^2$	252	243	[5]

Table 3.6: Values of the input parameters used in the sum rule analysis of  $f_{B^*}$  with a Borel mass dependent threshold  $s_0(M^2)$  and the corresponding errors they inflict on the final result. The central result of this analysis is  $f_{B^*} = 245 \text{ MeV}$ .

We analyzed this sum rule using the two methods introduced in the preceding sections. The values for the decay constant we extracted are:

$$f_{B^*} = (197 \pm 24 \pm 16) \text{ MeV}, \quad (3.25)$$

when the limit  $M^2 \rightarrow \infty$  is taken and

$$f_{B^*} = (245 \pm 35 \pm 23) \text{ MeV} \quad (3.26)$$

in the case of a Borel mass dependent threshold  $s_0(M^2)$ . Again, the first errors come from the uncertain running quark mass  $\overline{m}_b(\overline{m}_b) = (4.24 \pm 0.11) \text{ GeV}$ . The second error summarizes further uncertainties. The individual contributions of the uncertainties of the input parameters and the dependence on the scale  $\mu$  are collected in the tables 3.5 and 3.6.

The result (3.25) is close to a NLO-result from Khodjamirian[32],  $f_{B^*} = (195 \pm 35) \text{ MeV}$ , whereas (3.26) is far off that value. This can be traced back to the strong dependence of the sum rule on the Borel parameter if a constant threshold  $s_0$  is used. To stabilize the sum rule by introduction of a Borel mass dependent threshold will require rather high average values of  $s_0(M^2)$ . Nevertheless, we will use the two decay constants from this analysis in the extraction of the coupling  $g_{B^*B\pi}$ .

# Chapter 4

## B-Form Factor $f^+(0)$

In this chapter, we analyze the weak semileptonic form factor  $f_B^+(0)$  of the B-meson at maximal recoil. In section 2.3 we already gave the sum rule for the form factor of the twist two pion wave function. Up to twist 4 we adopt the sum rule from Khodjamirian [8]. For  $q^2 = 0$  this is:

$$f_B f^+(0) e^{-\frac{m_B^2}{M^2}} = \frac{m_b^2 f_\pi}{2m_B^2} \Phi(s_0, M^2), \quad (4.1)$$

where  $\Phi(s_0, M^2)$  is given by:

$$\begin{aligned} \Phi(s_0, M^2) = & \int_{\Delta}^1 \frac{du}{u} e^{-\frac{m_b^2}{uM^2}} \left[ \varphi_\pi(u) + \frac{\mu_\pi}{m_b} \left( u\varphi_p(u) + \frac{\varphi_\sigma(u)}{3} \left( 1 + \frac{m_b^2}{2uM^2} \right) \right) - \frac{4m_b^2}{u^2 M^4} g_1(u) \right. \\ & \left. - \frac{4m_b^2}{u^2 M^4} g_1(u) + \frac{2}{uM^2} \int_0^u dt g_2(t) \left( 1 + \frac{m_b^2}{uM^2} \right) \right] \\ & + A^+(s_0, M^2) + f_{3P}^+(s_0, M^2) - \frac{2\alpha_s}{3\pi} T^1(s_0, M^2). \end{aligned} \quad (4.2)$$

Here, the lower limit in the integral is now given by  $\Delta = m_b^2/s_0$ .  $A^+(s_0, M^2)$  is the surface term, coming from the partial integration necessary to build up a dispersion relation. The explicit form of the wave functions as well as the three particle contributions and the first order corrections to the twist 2 wave function is given in appendix B.

The right hand side of equation (4.2) is effectively an expansion in powers of  $1/uM^2$  rather than just  $M^2$ . Taking the Borel window of the sum rule for the decay constant  $f_B$ ,  $4 \text{ GeV}^2 < M^2 < 8 \text{ GeV}^2$ , and dividing the boundaries by an average value of the integration variable  $u$ , we obtain a new window that takes the change from the parameter  $M^2$  to  $uM^2$  into account. Evaluating the integral in (4.2) in the Borel window for the decay constant, we find an average value of  $\bar{u}$  varying between 0.5 and 0.7, for which the integrand is equal to the evaluated integral. Thus, we use for the analysis of the form factor a window with boundaries of about the doubled values as for the decay constant:

$$8 \text{ GeV}^2 < M^2 < 14 \text{ GeV}^2. \quad (4.3)$$

We checked that the hadronic contributions of higher states and the continuum, which are subtracted from the QCD side by the duality assumption are of about 25% of the final result on the right edge of the Borel window. Higher twist contributions are under good control and the contributions of the three particle wave functions are almost negligible. For central input parameters, we depicted the contributions from the single terms to the total sum rule in figure

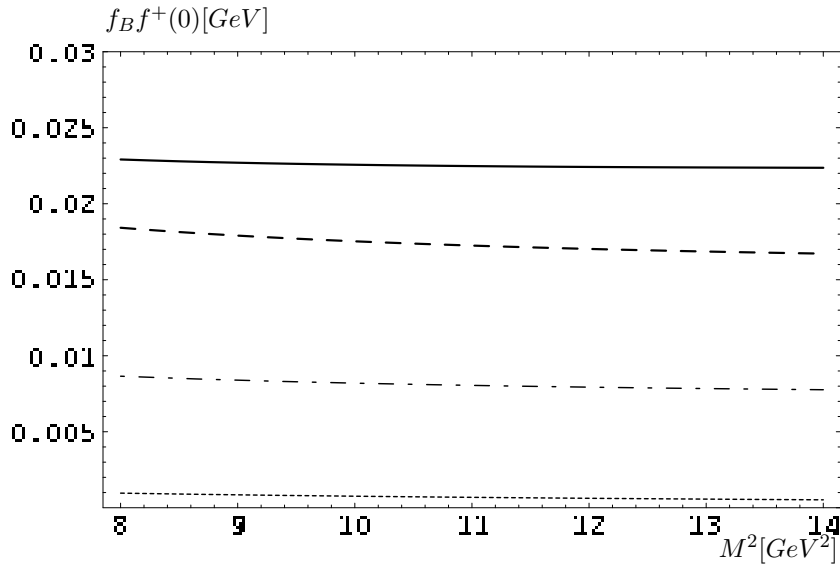


Figure 4.1: Contributions to the final sum rule for  $f_B f^+(0)$ : twist 2 (full line); 2P - twist 3 (dashed);  $O(\alpha_s)$ -twist 2 (dash-dotted); 3P - twist 3 and twist 4 (dotted). We used the central values  $m_b = 4.7 \text{ GeV}$  and  $s_0 = 35 \text{ GeV}^2$  as input parameters. The sum of all contributions is plotted in figure 4.2.

4.1. The dotted line collects the two particle twist 4 and all the three particle twist 3 and 4 contributions. The sum of these terms is only about 2%. Therefore, the truncation of the expansion after these terms is justified.

We will evaluate the sum rule at the scale

$$\mu_b = \sqrt{m_B^2 - m_b^2} = 2.4 \text{ GeV}. \quad (4.4)$$

This scale, which is often used in analyses of hadronic properties of the B-meson, reflects the average virtuality of the b-quark in the meson. A further ambiguity lies in the use of the quark mass. Nevertheless, taking the running mass  $\overline{m}_b(\overline{m}_b) = 4.24 \pm 0.11 \text{ GeV}$  and running it down to the scale (4.4), we get  $\overline{m}_b(\mu_b) = 4.69 \text{ GeV}$ , which is of about the same size as the pole mass obtained from the two-loop relation (A.12). Therefore, we will take the typically used value of the pole mass:

$$m_b = 4.7 \pm 0.1 \text{ GeV}. \quad (4.5)$$

The errors are also of the same size as for the running mass. In figure 4.2a, we plotted  $f_B f^+(0)$  for the three different masses  $m_b = \{4.6 \text{ GeV}, 4.7 \text{ GeV}, 4.8 \text{ GeV}\}$  and  $s_0 = 35 \text{ GeV}^2$ . Other input parameters and the values of the coefficients of the wave functions can be found in appendix B.

Taking the mean values  $M^2 = 11 \text{ GeV}^2$  and  $s_0 = 35 \text{ GeV}^2$ , we read off  $f_B f^+(0) = 0.049 \text{ GeV}$ , consistent with the analysis of Khodjamirian and Rückl, who extracted  $f^+(0) = 0.27$  with a rather low central value for the decay constant,  $f_B = 180 \text{ MeV}$ . However, the sum rule is quite unstable in the given Borel window as can be seen in figure 4.2. It decreases monotonously in  $M^2$  about 10%. In figure 4.2b, we plotted the corresponding daughter sum rules. They are clearly lower than the experimentally measured meson mass  $m_B = 5.279 \text{ GeV}$ . Intersections with the mass of the B-meson will only occur at higher values of the Borel parameter or the threshold  $s_0$ . A unique pair  $(\hat{M}^2, \hat{s}_0)$  that would correspond to a vanishing second derivative of  $f_B f^+(0)(M^2)$  is never reached within finite values of the Borel mass and the threshold. The

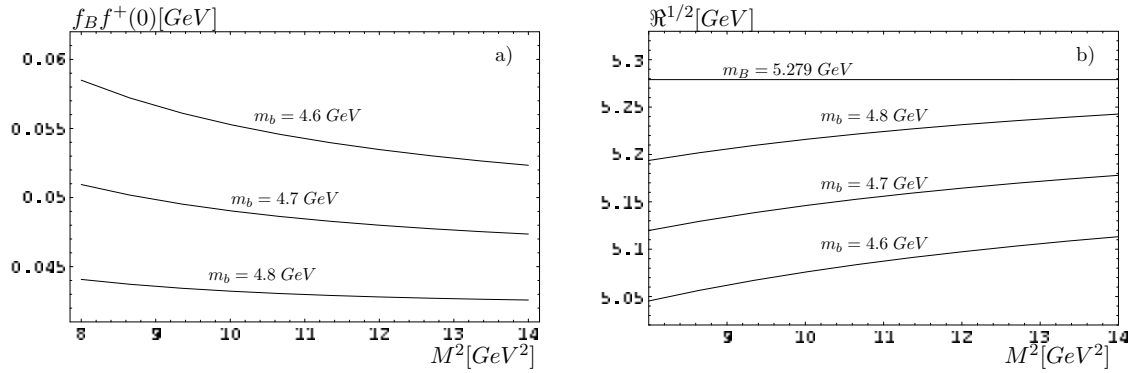


Figure 4.2: a: Sum rule for the product  $f_B f^+(0)$  for  $s_0 = 35$  GeV and quark masses  $m_b = (4.6, 4.7, 4.8)$  GeV. Graph b) shows the corresponding daughter sum rule. The curves do not intersect with the meson mass, and therefore  $f_B f^+(0)$  decreases monotonously and does not reach a minimum in the Borel window.

choice of the read off pair  $(\hat{M}^2, \hat{s}_0)$  is therefore rather ambiguous. This motivates the application of the two modified analyses introduced before.

## 4.1 The Limit $M^2 \rightarrow \infty$

In this section we will apply the method of local duality, introduced in section 3.2, to the sum rule for  $f_B f^+(0)$ . Taking the limit  $M^2 \rightarrow \infty$  justifies the truncation of the power expansion in  $1/M^2$  and minimizes uncertainties coming from higher twist wave functions. On the other side, uncertainties in the hadronic spectral function are emphasized, since they are not exponentially damped anymore.

We again take the derivative  $M^4 d/dM^2$  of the logarithm of the right hand side in equation (4.2). We then adjust the threshold  $s_0$  such, that the square root of this daughter sum rule takes on the value of the meson mass  $m_B = 5.279$  GeV in the limit  $M^2 \rightarrow \infty$ . Using the threshold obtained in this way in the sum rule (4.1), the product  $f_B f^+(M^2)$  reaches its asymptotic value very fast. In figure 4.3, we plotted the matching of the daughter sum rules for the center value of the quark mass and its largest errors  $m_b = (4.7 \pm 0.1)$  GeV, as well as the corresponding functions for  $f_B f^+(0)$  of  $M^2$ . The central value is

$$\lim_{M^2 \rightarrow \infty} f_B f^+(M^2) = 0.0463 \text{ GeV}, \quad (4.6)$$

and the error inflicted by the uncertainties of the quark mass is about 12%.

Since the decay constant obtained with this method was rather sensitive to the scale  $\mu$ , at which the sum rule was evaluated, we also calculated the values of  $f_B f^+(0)$  at the scales  $\mu = 2$  GeV and  $\mu = 3$  GeV. There are many  $\mu$ -dependent parameters in (4.2) and we will give their scaling laws in the following.

The scaling behavior of  $\mu_\pi$  can be obtained from the Gell-Mann-Oakes-Renner relation (2.42) and is therefore directly related to the running of quark masses. The scaling law of the coefficients of the twist two pion wave function  $\varphi_\pi(u)$  is given in (B.2). The scale dependence of the parameters

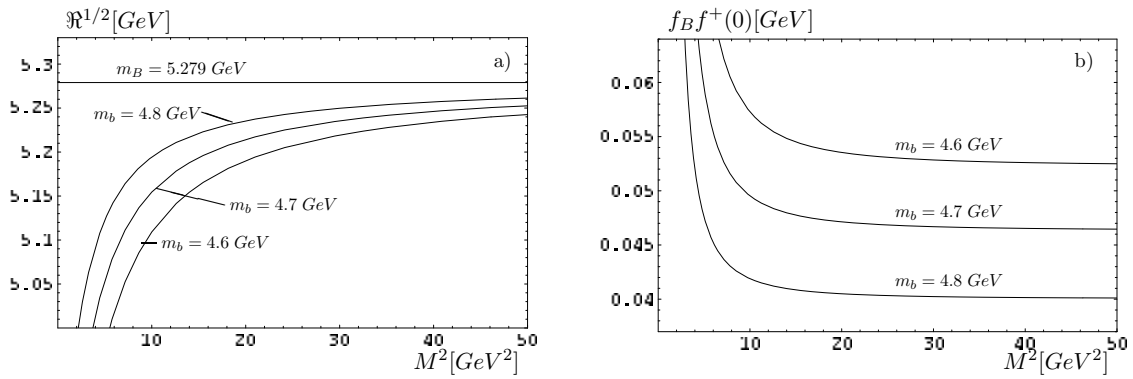


Figure 4.3: Matching of the daughter sum rule to the experimental meson mass  $m_B = 5.279 \text{ GeV}$  in the limit  $M^2 \rightarrow \infty$  (a). The values for the thresholds obtained by the matching are used to determine the values for the product  $f_B f^+(0)$  in the same limit (b).

appearing in the twist 3 and 4 wave functions are taken from Braun and Filianov[33]:

$$f_{3\pi}(\mu_2^2) = \left( \frac{\alpha_s(\mu_2^2)}{\alpha_s(\mu_1^2)} \right)^{\frac{11}{15}} f_{3\pi}(\mu_1^2) \quad (4.7)$$

$$f_{3\pi\omega_{1,0}}(\mu_2^2) = \left( \frac{\alpha_s(\mu_2^2)}{\alpha_s(\mu_1^2)} \right)^{\frac{104}{75}} f_{3\pi\omega_{1,0}}(\mu_1^2) \quad (4.8)$$

$$f_{3\pi} \begin{pmatrix} \omega_{1,1} \\ 4\omega_{2,0} \end{pmatrix} (\mu_2^2) = \left( 1 - \frac{\alpha_s}{4\pi} \log \frac{\mu_2^2}{\mu_1^2} \begin{pmatrix} \frac{122}{9} & \frac{5}{3} \\ \frac{21}{5} & \frac{511}{45} \end{pmatrix} \right) f_{3\pi} \begin{pmatrix} \omega_{1,1} \\ 4\omega_{2,0} \end{pmatrix}, \quad (4.9)$$

for the parameters of the two and three particle wave functions of twist 3 and

$$\delta^2(\mu_2^2) = \left( \frac{\alpha_s(\mu_2^2)}{\alpha_s(\mu_1^2)} \right)^{\frac{32}{75}} \delta^2(\mu_1^2) \quad (4.10)$$

$$\delta^2 \varepsilon(\mu_2^2) = \left( \frac{\alpha_s(\mu_2^2)}{\alpha_s(\mu_1^2)} \right)^{\frac{6}{5}} \delta^2 \varepsilon(\mu_1^2) \quad (4.11)$$

for the twist 4 wave functions. Using these scaling laws, we evaluated the sum rule (4.1) at the scales  $\mu = 2 \text{ GeV}$  and  $\mu = 3 \text{ GeV}$ . The two functions of the daughter sum rule are almost similar and the matching leads to two thresholds, which are also very close to each other:

$$s_0(2 \text{ GeV}) = 35.46 \text{ GeV}, \quad s_0(3 \text{ GeV}) = 35.45 \text{ GeV}. \quad (4.12)$$

Setting these two thresholds in the corresponding functions for  $f_B f^+(M^2)$ , we get a small scale dependence of about  $\pm 4\%$ , when varying the scale  $\mu = 2 \text{ GeV}$  to  $\mu = 3 \text{ GeV}$ . This is shown in figure 4.4 a. We finally obtain:

$$\lim_{M^2 \rightarrow \infty} f_B f^+(M^2) = (0.046 \pm 0.006 \pm 0.002) \text{ GeV}, \quad (4.13)$$

where the first error is due to uncertainties in the quark mass and the second comes from the scale at which the sum rule (4.2) is evaluated. There are further errors coming from the uncertainties of the input parameters  $\mu_\pi$  and  $f_{3\pi}$ , however, they are small compared to the values above and we do not take them into account in this analysis.

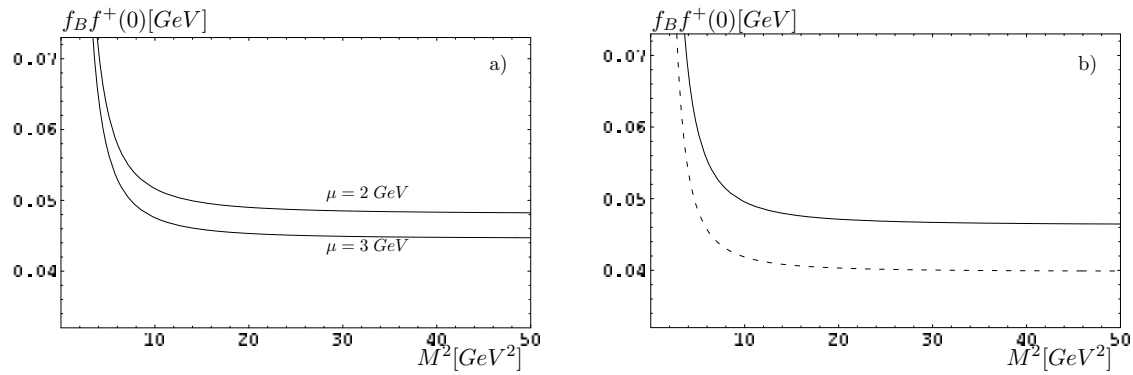


Figure 4.4: a: Sum rule for  $f_B f^+(0)$  evaluated at the scales  $\mu = 2 GeV$  and  $\mu = 3 GeV$ . b:  $f_B f^+(0)$ , when the asymptotic pion wave function is used (dashed line), compared to the central result (solid line).

A rather large error is inflicted by the uncertainties of the coefficients of the light cone wave functions, which are not known to a high accuracy. We therefore also analyzed the sum rule for the asymptotic twist 2 pion wave function. In figure 4.4b, we plotted the sum rule for the asymptotic wave function, compared to our central result. The value for the product  $f_B f^+(0)$  decreases about 13%. This number can be interpreted as a rather conservative error estimate on the result (4.13).

For consistency, we divide (4.13) by the decay constant (3.14), obtained with the same method in section 3.2. In the ratio, the two errors from the quark masses almost cancel, when they are varied simultaneously. Thus, although both sum rules show a high sensitivity to the chosen quark mass, this dependence becomes very weak if the two results are combined. We obtain:

$$f^+(0) = 0.26 \pm 0.05. \quad (4.14)$$

The error due to the unknown quark mass amounts to less than 4%. We included the error estimate of 13% from the uncertainties of the coefficients of the wave functions. Added to the other error sources, the final error estimate is about 20%. In section 4.3, we relate our results to values found in the literature.

The two individual analyses of the decay constant  $f_B$  in section 3.2 and the product  $f_B f^+(0)$  in this section show rather low values compared to other methods. However, since the ratio of the two values is taken, some errors cancel as shown above and the error of about 20% of the final result is reasonable. It is hoped that the intrinsic error coming from the method itself also shrinks when the ratio of the two results is taken. This will be highly supported in the next section.

## 4.2 Borel Mass dependent Threshold $s_0(M^2)$

The sum rule for the form factor (4.1) leads to functions that have a rather strong dependence on  $M^2$  for typical values of the input parameters, as can be seen from figure 4.2. With higher values of the thresholds the functions develop a minimum in the Borel window, however, the second derivative does not vanish as was the case in the analysis of the decay constant. Thus, one cannot find a unique pair  $(\hat{M}^2, \hat{s}_0)$  for which the daughter sum rule is equal to the meson mass at its extremal point.



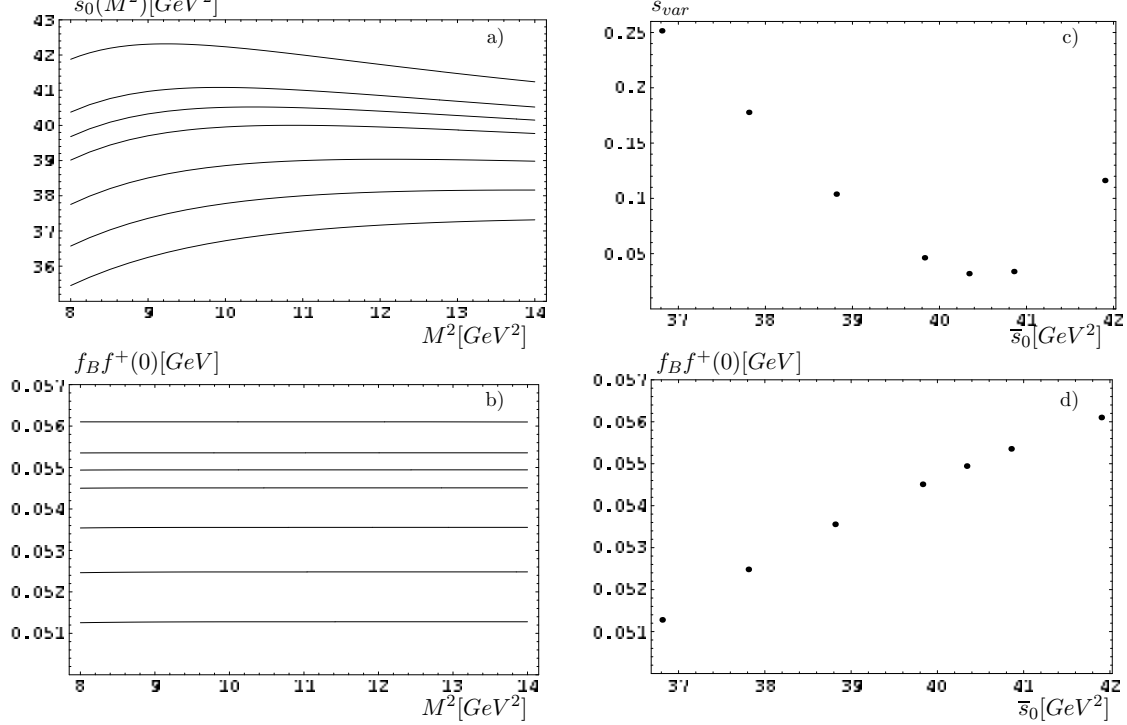


Figure 4.5: Sum rule analysis for  $f_B f^+(0)$  with a Borel mass dependent threshold  $s_0(M^2)$ . Diagram a) shows several solutions of the differential equation (4.15). Plot d) shows the corresponding values of  $f_B f^+(0)$  over the mean values of the thresholds. Graph c) shows the variations of the functions of the threshold to give the region where the value of  $f_B f^+(0)$  should be read off. Diagram b) shows the functions  $f_B f^+(0)$  when the solutions  $s_0(M^2)$  are inserted and gives a crosscheck of the numerical analysis.

In this section we apply the method outlined in section 3.3 to the sum rule of the form factor. Thus, we shift the functional dependence of the form factor to the threshold  $s_0$  by solving the differential equation

$$s'_0(M^2) = \frac{m_B^2 \Phi(M^2, s_0(M^2)) - M^4 \frac{\partial}{\partial M^2} \Phi(M^2, s_0(M^2))}{M^4 \frac{\partial}{\partial s_0} \Phi(M^2, s_0(M^2))}, \quad (4.15)$$

where  $\Phi(M^2, s_0(M^2))$  is given in (4.2). For central values of the input parameters, we plotted several solutions in figure 4.5. We again plotted the variations of the curves to read off the value for the product  $f_B f^+(0)$  at the most stable threshold. This threshold is rather high ( $\bar{s}_0 \approx 40.4 \text{ GeV}^2$ ) compared to the earlier analyses. As can be seen in figure 4.2, the dependence of the sum rule on the Borel parameter is rather strong for smaller values of the threshold. Thus, one needs to impose a function  $s_0(M^2)$  that is also strongly varying with the Borel mass. To higher thresholds, this dependence of the sum rules on  $M^2$  becomes weaker, which is then also the case for  $s_0(M^2)$ .

In figure 4.6, we plotted the results from using  $m_b = 4.6 \text{ GeV}$  and  $m_b = 4.8 \text{ GeV}$  as the values of the quark mass. As before, the error to the product  $f_B f^+(0)$  coming from the variation of the b-quark mass is large. It is about 15% of the final result.

We also examined the scale dependence of  $f_B f^+(0)$  extracted from this analysis. Like before, we evaluated the sum rule at  $\mu = 2 \text{ GeV}$  and  $\mu = 3 \text{ GeV}$ . The results are shown in figure 4.7. The values of  $f_B f^+(0)$  are quite stable to variations of the scale  $\mu$ . The error is less than 4%.

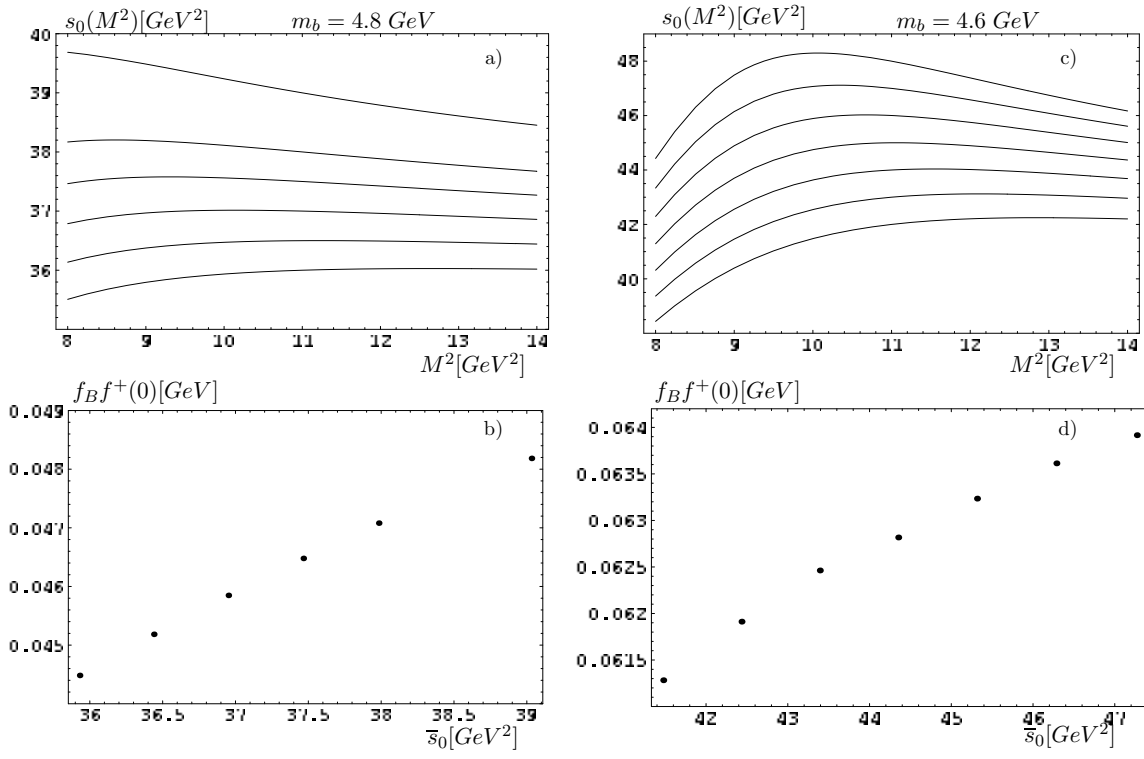


Figure 4.6: Analyses for the different values of the quark mass:  $m_b = 4.8 \text{ GeV}$  (left side) and  $m_b = 4.6 \text{ GeV}$  (right side). The upper diagrams show the solutions for the thresholds  $s_0(M^2)$  - the lower diagrams show the product  $f_B f^+(0)$ , plotted over the average values of the thresholds.

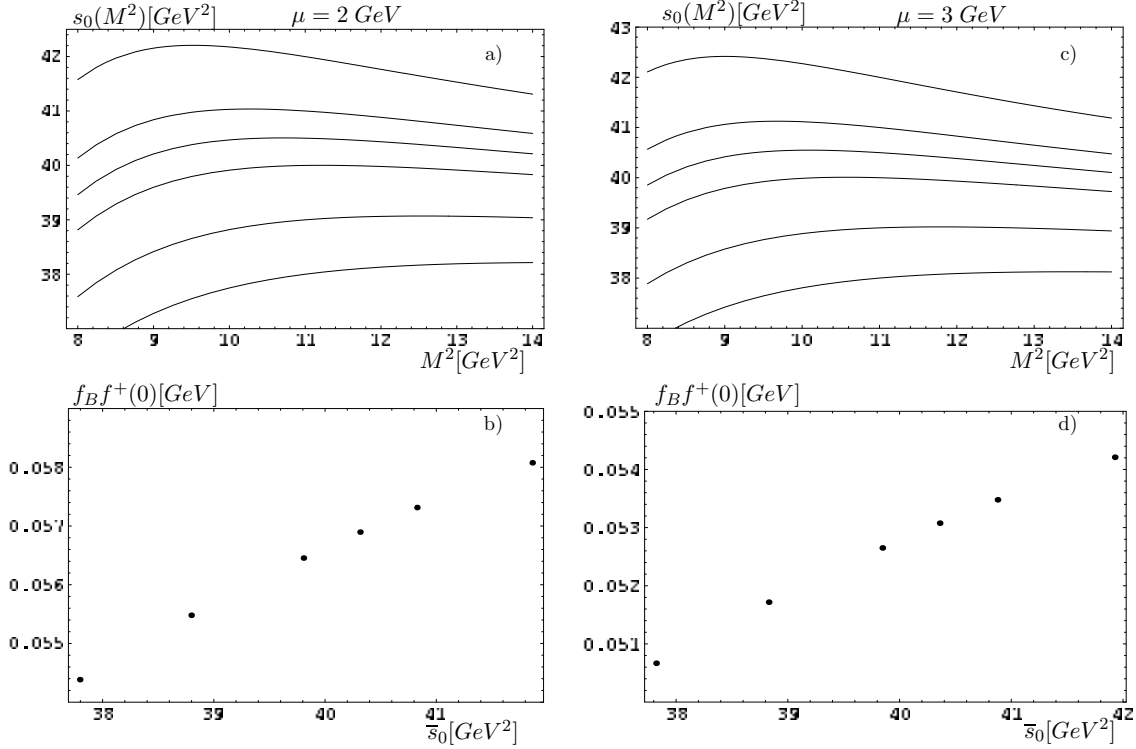


Figure 4.7: Scale dependence of the sum rule for  $f_B f^+(0)$ . On the left side, the results are shown for the scale  $\mu = 2 \text{ GeV}$  and on the right side, the scale  $\mu = 3 \text{ GeV}$  was used.

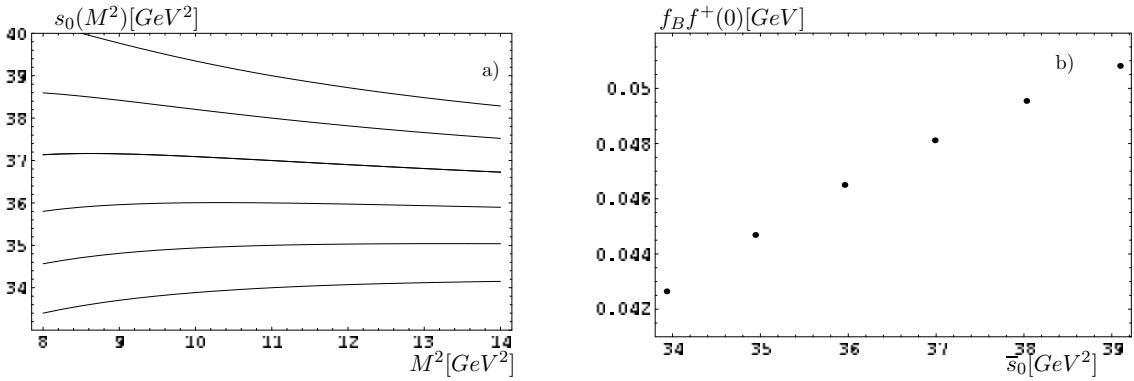


Figure 4.8: Sum rule analysis for the asymptotic pion wave function. The product  $f_B f^+(0)$  decreases significantly about 15%.

We again analyzed the sum rule using the asymptotic pion wave function to take the error from the uncertainties of the coefficients of the wave functions into account. The resulting thresholds  $s_0(M^2)$  and values for  $f_B f^+(0)$  can be seen in figure 4.8.

Neglecting further error sources, we extract for the product  $f_B f^+(0)$ :

$$f_B f^+(0) = (0.055 \pm 0.009 \pm 0.008) \text{ GeV}, \quad (4.16)$$

where the first error is the one coming from the variations of the quark mass and the second is due to the scale dependence and uncertainties of the coefficients of the wave functions. If we divide this result by the decay constant (3.20), that was analyzed using the same method, we obtain:

$$f^+(0) = 0.26 \pm 0.05. \quad (4.17)$$

The change of the quark mass to the extremal values in the two sum rule results (4.16) and (3.20) leads to slightly higher ratios (about 3%) than the central value in either case. Again, the main error comes from the conservative error estimate of the uncertainties in the coefficients of the wave functions.

### 4.3 Summary of the Results and Relation to the Literature

It is amazing that the two results (4.14) and (4.17) are so close to each other. The central results differ by less than 2%. The two methods have very different physical meanings. Whereas the first method of taking the limit  $M^2 \rightarrow \infty$  emphasizes errors coming from the duality approximation, the second method tries to suppress these uncertainties. Therefore, the discrepancy of the individual results for the decay constant and the product  $f_B f^+$  was rather natural. It was hoped that when the ratio of the two sum rule results was taken, the intrinsic errors from the methods would be lowered. However, we did not expect that the two results for the semi-leptonic form factor are that close to each other. In the next chapter we will analyze the sum rule for the strong coupling  $g_{B^* B \pi}$ . The sum rule is proportional to  $f_B$  and  $f_{B^*}$  and will be divided by these constants, analyzed within the same method. However, this time, the extracted couplings differ about 13%.

We did not take  $O(\alpha_s)$ -corrections to the two particle twist 3 wave functions into account. These were recently obtained in [35]. The  $O(\alpha_s)$ -corrections to the twist 2 wave function raised this contribution about 30%. Assuming that the new corrections are also about 30% of the twist 3

$f^+(0)$	Ref.	Method
$0.26 \pm 0.05$	This Thesis	LCSR; $O(\alpha_s)$ -twist 2 corrections; $\lim M^2 \rightarrow \infty$
$0.26 \pm 0.05$	This Thesis	LCSR; $O(\alpha_s)$ -twist 2 corrections; $s_0(M^2)$
$0.24 \pm 0.025$	Ball '91[21]	3-pt SR
$0.27 \pm 0.05$	Khodjamirian '97[34]	LCSR; $O(\alpha_s)$ -twist 2 corrections;
$0.28 \pm 0.05$	Bagan '97[22]	LCSR; $O(\alpha_s)$ -twist 2 corrections; average of full and asymptotic twist 2 pion wave function
$0.26 \pm 0.06 \pm 0.05$	Ball '01[35]	LCSR $O(\alpha_s)$ -twist 2 and 3 corrections
$0.28 \pm 0.04$	Abada APE'99[28]	Lattice

Table 4.1: Comparison of our results to a collection of values from the literature

wave functions, we expect the final result of  $f^+(0)$  to raise about 10%.

In table 4.1 we collected some values for the form factor  $f^+(0)$  from the literature. Our results seem to fit quite well in this table, especially when the large error bars are taken into account. Furthermore, the results from LCSR analyses and 3-point sum rules coincide with lattice calculations. This will be very different in case of the strong coupling  $g_{B^*B\pi}$  analyzed in the next section.

# Chapter 5

## Coupling $g_{B^*B\pi}$

In this chapter, we will apply our two methods on the sum rule for the strong coupling constant  $g_{B^*B\pi}$ . The process  $B^* \rightarrow B\pi$  is kinematically forbidden, thus one has to rely on theoretical predictions. This coupling is closely related to the  $B \rightarrow \pi$  form factor. It is assumed that the form factor is dominated by the vector meson at zero recoil. In the single pole model, the form factor at large  $q^2 \approx m_{B^*}^2$  is parametrized by

$$f^+(q^2) = \frac{f_{B^*} g_{B^*B\pi}}{2m_{B^*} \left(1 - \frac{q^2}{m_{B^*}^2}\right)}. \quad (5.1)$$

Thus, the coupling is part of the residue of the pole of the form factor. It was observed in the literature [21] that the vector meson dominance is also valid to smaller values of the transferred momentum. However, at  $q^2 = 0$ , the two approaches, the pole model and the LCSR for the form factor, differ in their scaling behavior in the heavy quark limit  $m_b \rightarrow \infty$  (see [36]). We therefore do not compare our results for the form factor at maximum recoil with the sum rule results for the coupling  $g_{B^*B\pi}$ .

In the next section, we will briefly sketch the derivation of the sum rule, following [36] and then apply the modified analyses to it.

### 5.1 Derivation of the Sum Rule

We take the following definition for the  $B^*B\pi$ -coupling:

$$\langle \bar{B}^{*0}(q) \pi^-(p_\pi) | B^-(p_\pi + q) \rangle = -g_{B^*B\pi} \varepsilon_\mu p_\pi^\mu, \quad (5.2)$$

where  $\varepsilon_\mu$  is the polarization vector of the  $B^*$ -meson. Matrix elements of states with different charges are related to the definition of the coupling by isospin symmetry.

Starting point is again the correlation function (2.57) of two pseudoscalar currents, sandwiched between a pion state and the vacuum. This function can be split in two parts

$$\Pi_\mu(p_\pi, q) = \Pi(q^2, (p_\pi + q)^2) p_{\pi\mu} + \tilde{\Pi}(q^2, (p_\pi + q)^2) q_\mu, \quad (5.3)$$

and again, we are only interested in the function in front of the pion momentum.

On the hadronic side, we first insert a set of intermediate states carrying B-meson quantum numbers. This leads to the product of two matrix elements:

$$\langle \pi | \bar{u} \gamma_\mu b | B \rangle \langle B | \bar{b} i \gamma_5 d | 0 \rangle \quad (5.4)$$

The second element is proportional to the B-meson decay constant. Using crossing symmetry and inserting another set of intermediate states, this time carrying  $B^*$ -meson quantum numbers, we obtain the matrix element of the upper definition (5.2) and a second element, which defines the vector-meson decay constant:

$$\langle 0 | \bar{q} \gamma_\mu b | B^* \rangle = m_{B^*} f_{B^*} \varepsilon_\mu. \quad (5.5)$$

Using this definition, we analyzed the sum rule for  $f_{B^*}$ . The results were summarized in section 3.5.

The hadronic side of the correlation function is:

$$\Pi(q^2, (p_\pi + q)^2) = \frac{m_B^2 m_{B^*} f_B f_{B^*} g_{B^* B \pi}}{m_b (q^2 - m_{B^*}^2) ((p_\pi + q)^2 - m_B^2)} + \int_{\Sigma_h} \frac{\rho^h(s_1, s_2) ds_1 ds_2}{(s_1 - q^2)(s_2 - (p_\pi + q)^2)} + \dots \quad (5.6)$$

The ellipses stand for subtraction terms, which will be removed when the Borel transformation is applied. The limit  $\Sigma_h$  of the double dispersion integral is now a region in the  $(s_1, s_2)$ -plane.

When the expressions (5.6) and the corresponding QCD-side are Borel transformed with respect to  $q^2$  and  $(p_\pi + q)^2$ , the two sides are equaled and the hadronic continuum is subtracted by the assumption of quark hadron duality:

$$f_B f_{B^*} g_{B^* B \pi} e^{-\frac{m_{B^*}^2}{M_1^2}} e^{-\frac{m_B^2}{M_2^2}} = \frac{m_b}{m_B^2 m_{B^*}} \int_{\Sigma_0} \rho^{QCD} e^{-\frac{s_1}{M_1^2}} e^{-\frac{s_2}{M_2^2}} ds_1 ds_2. \quad (5.7)$$

The derivation of the QCD spectral function is exactly the same as in section 2.3, since we used the same initial correlation function. The explicit subtraction procedure is rather complicated and we refer to the appendix in [36]. The two Borel parameters are believed to be of the same magnitude. The choice  $M_1^2 = M_2^2 \equiv 2M^2$  simplifies the derivation of the final expression for the sum rule:

$$f_B f_{B^*} g_{B^* B \pi} e^{-\frac{m_B^2 + m_{B^*}^2}{2M^2}} = \frac{m_b^2}{m_B^2 m_{B^*}} \Gamma(M^2, s_0), \quad (5.8)$$

with  $\Gamma(M^2, s_0)$  given by:

$$\begin{aligned} \Gamma(M^2, s_0) &= M^2 \left( e^{-\frac{m_b^2}{M^2}} - e^{-\frac{s_0}{M^2}} \right) \left[ \varphi_\pi(1/2) + \frac{\mu_\pi}{m_b} \left( \frac{1}{2} \varphi_\sigma(1/2) + \frac{1}{3} \varphi_\sigma(1/2) \right) + \frac{2f_{3\pi}}{m_b f_\pi} I_{3P}^{(3)} \right] \\ &+ e^{-\frac{m_b^2}{M^2}} \left[ \frac{\mu_\pi m_b}{3} \varphi_\sigma(1/2) + g_2(1/2) - \frac{4m_b^2}{M^2} \left( g_1(1/2) + \int_0^{1/2} g_2(v) dv \right) + I_{3P}^{(4)} \right] \\ &+ \frac{\alpha_s}{3\pi} \int_{2m_b^2}^{2s_0} f \left( \frac{t}{m_b^2} - 2 \right) e^{-\frac{t}{2M^2}} dt. \end{aligned} \quad (5.9)$$

Here, the three particle twist 3 and 4 contributions are given by:

$$I_{3P}^{(3)} = -\frac{3}{32} (20 + 5\omega_{1,0} + \omega_{1,1} - 4\omega_{2,0}) \quad (5.10)$$

$$I_{3P}^{(4)} = \frac{5}{3} \delta^2. \quad (5.11)$$

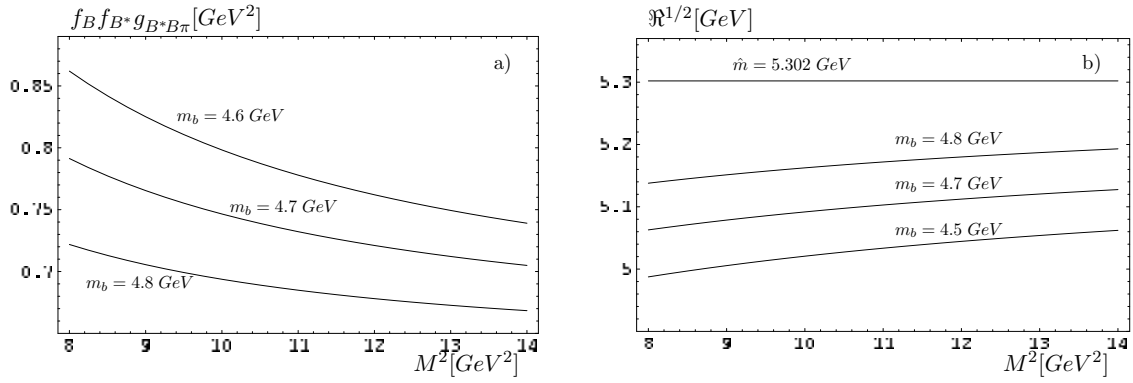


Figure 5.1: Sum rule for  $f_B f_{B^*} g_{B^* B \pi}$  and corresponding daughter sum rule. The threshold is set to  $s_0 = 35 \text{ GeV}$  and the graphs are plotted for  $m_b = (4.6, 4.7, 4.8) \text{ GeV}$ . The sum rule decreases about 10% in the Borel window.

The  $O(\alpha_s)$ -corrections to the two particle twist 2 wave function were obtained by Khodjamirian and collaborators, and we adopt the expression from [32]:

$$\begin{aligned}
f(x) = & \frac{\pi^2}{4} + 3 \log\left(\frac{x}{2}\right) \log\left(1 + \frac{x}{2}\right) - \frac{3(3x^3 + 22x^2 + 40x + 24)}{2(2+x)^3} \log\left(\frac{x}{2}\right) \\
& + 6Li_2\left(\frac{x}{2}\right) - 3Li_2(-x) - 3Li_2(-x-1) - 3 \log(1+x) \log(2+x) \\
& - \frac{3(3x^2 + 20x + 20)}{4(2+x)^2} + \frac{6x(1+x) \log(1+x)}{(2+x)^3}.
\end{aligned} \tag{5.12}$$

For the following analyses, we took the same window for the Borel parameter as for the form factor in chapter 4:

$$8 \text{ GeV} \leq M^2 \leq 14 \text{ GeV}^2. \tag{5.13}$$

The contribution of the twist 2 wave function at the left boundary is about 60% and of the twist 3 terms about 40% of the total. The twist 4 contribution is numerically negligible. The contribution from the hadronic continuum grows from 20% to about 30% at the right edge of the window. Thus, the use of this window is reasonable.

For typical values of the input parameters -  $s_0 = 35 \text{ GeV}$ ,  $m_b = (4.7 \pm 0.1) \text{ GeV}$  - we plotted in figure 5.1 the sum rule for the product  $f_B f_{B^*} g_{B^* B \pi}$  and the corresponding daughter sum rule, defined by:

$$\Re(M^2, s_0) = M^4 \frac{d}{dM^2} \log \Gamma(M^2, s_0). \tag{5.14}$$

Applying the same derivative on the left hand side of equation (5.8), we see that the sum rule reaches a minimum, when the daughter sum rule is equal to

$$\hat{m}^2 = \frac{m_{B^*}^2 + m_B^2}{2} = 28.11 \text{ GeV}^2, \tag{5.15}$$

if the experimental values for the meson masses  $m_B = 5.279 \text{ GeV}$  and  $m_{B^*} = 5.325 \text{ GeV}$  are taken. The daughter sum rule is rather far apart from  $\hat{m}$  and the sum rule for the product  $f_B f_{B^*} g_{B^* B \pi}$  is quite unstable in the chosen window.

In the following two sections, we will apply the methods introduced in the preceding two chapters on the sum rule (5.8).

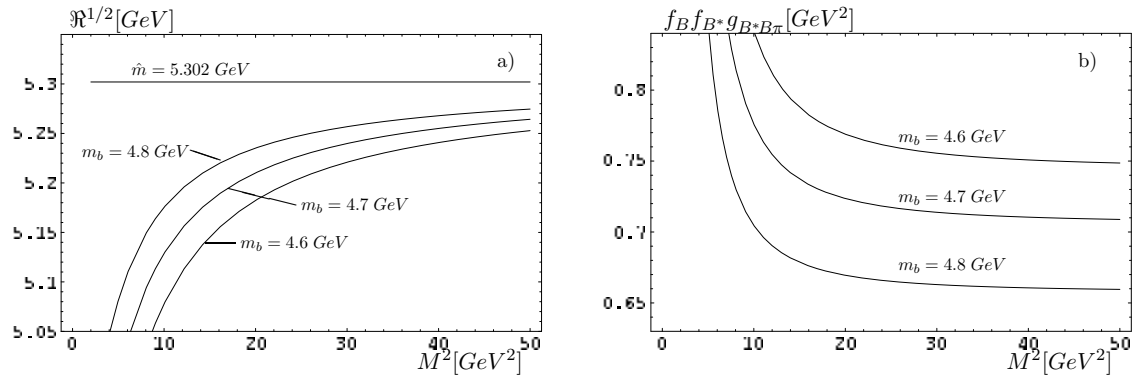


Figure 5.2: Matching procedure for the sum rule of  $f_B f_{B^*} g_{B^* B \pi}$ . Diagram a) shows the matching of the daughter sum rule in the limit  $M^2 \rightarrow \infty$  for three different values of the quark mass  $m_b$ . The values of the threshold obtained by this procedure are used to extract the value for  $f_B f_{B^*} g_{B^* B \pi}$  in same limit (b).

## 5.2 The Limit $M^2 \rightarrow \infty$

In this section, we will analyze the sum rule (5.8) by imposing *local duality*. We take the limit  $M^2 \rightarrow \infty$  and match the daughter sum rule (5.14) to the mass  $\hat{m}$ , defined in equation (5.15). From this matching, we can extract a unique value for the threshold  $s_0$  and therefore a unique value for  $f_B f_{B^*} g_{B^* B \pi}$ .

In figure 5.2, we plotted the graphs of the sum rule and its daughter sum rule for the central value of the quark mass  $m_b = 4.7 GeV$  and the two extremal values  $m_b = 4.6 GeV$  and  $m_b = 4.8 GeV$ . The error due to the uncertainties in the quark mass are about 7%. Besides this error source, we also analyzed the scale dependence of the sum rule. In figure 5.3 a, we plotted the resulting graphs for  $\mu = 2 GeV$  and  $\mu = 3 GeV$ . Again, we took account for the uncertainties of the coefficients of the wave functions by analyzing the sum rule for the asymptotic twist 2 wave function (figure 5.3b). The resulting deviation from the central result (9%) was assigned as additional error to the final result. Neglecting further error sources, we extract:

$$f_B f_{B^*} g_{B^* B \pi} = (0.71 \pm 0.05 \pm 0.07) GeV^2, \quad (5.16)$$

where the first error comes from the uncertain quark mass and the second summarizes the error from the scale dependence and the uncertainties of the coefficients of the wave functions. The value (5.16) is about 10% higher than the result obtained in [36], which did not include  $O(\alpha_s)$ -corrections, and again about 10% smaller than the result from [32], which was the first analysis using the  $O(\alpha_s)$ -corrections to the twist 2 wave function.

If we divide (5.16) by the corresponding value of the decay constant (3.14), extracted using the same method, we can get the residue of the form factor in the simple pole model:

$$c = \frac{f_{B^*} g_{B^* B \pi}}{2m_{B^*}} = (0.37 \pm 0.06) GeV. \quad (5.17)$$

Here, we simultaneously varied the quark mass, leading to a rather small contribution to the overall error (about 4%). This value is compatible with the result from the NLO-analysis [32] -  $(0.42 \pm 0.09) GeV$ .

Dividing (5.16) by the pseudoscalar decay constant (3.14) and the vector-meson decay constant



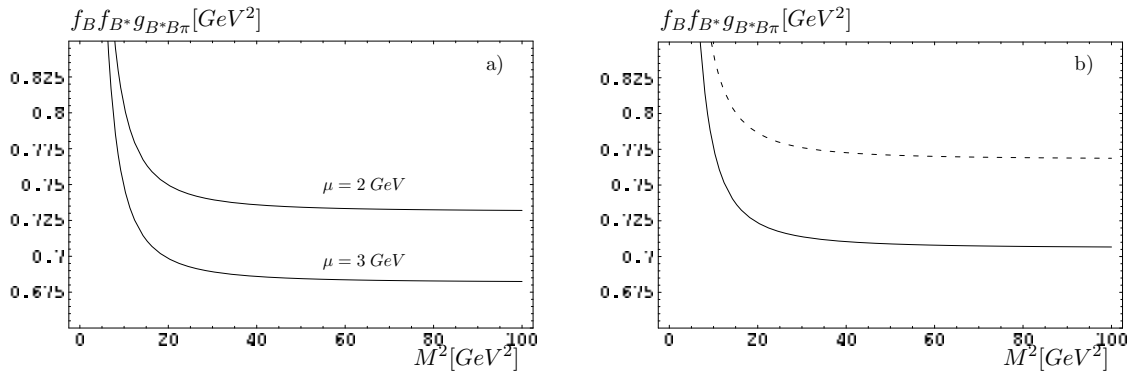


Figure 5.3: a: Scale dependence of the sum rule for the product  $f_B f_{B^*} g_{B^* B \pi}$  in the limit  $M^2 \rightarrow \infty$ . When the scale is varied from  $\mu = 2 \text{ GeV}$  to  $\mu = 3 \text{ GeV}$ , the resulting value of the sum rule decreases about 7%. - b: Comparison of the sum rule result using the asymptotic pion wave function (dashed line) with the central result. The coupling  $g_{B^* B \pi}$  increases about 9%, when the asymptotic function is used.

(3.25), we get for the  $B^* B \pi$ -coupling:

$$g_{B^* B \pi} = 20 \pm 5. \quad (5.18)$$

This time, the uncertainty of the quark mass inflicts an error of about the same size as the further error sources to the final result, which is about 17%. The result (5.18) is noticeably lower than the result of the LO-analysis [36] ( $g_{B^* B \pi} = 29 \pm 3$ ) and of about the same size as the NLO-result [32] -  $g_{B^* B \pi} = 22 \pm 7$ .

In section 5.4, we will discuss the results for the coupling  $g_{B^* B \pi}$  and relate them to the literature.

### 5.3 Borel Mass dependent Threshold $s_0(M^2)$

In this section we analyze the sum rule (5.8) with the method introduced in section 3.3. We take the threshold as a function of the Borel mass  $s_0(M^2)$  and solve the differential equation

$$s'_0(M^2) = \frac{\hat{m}^2 \Gamma(M^2, s_0(M^2)) - M^4 \frac{\partial}{\partial M^2} \Gamma(M^2, s_0(M^2))}{M^4 \frac{\partial}{\partial s_0} \Gamma(M^2, s_0(M^2))}, \quad (5.19)$$

to get constant functions for the product  $f_B f_{B^*} g_{B^* B \pi}$ . Since the initial sum rule was rather dependent on the Borel mass (see figure 5.1), we expect the resulting functions  $s_0(M^2)$  to have quite high average values.

For central values of the input parameters, the solutions  $s_0(M^2)$  and the corresponding sum rules are shown in figure 5.4. The average values of the threshold are quite high compared to the values in the last section. This is equivalent to the behavior of the initial sum rule, which gets more stable with higher values of the constant threshold  $s_0$ .

In figure 5.5, we plotted the functions  $s_0(M^2)$  for the two extremal input values for the quark mass  $m_b = 4.6 \text{ GeV}$  and  $m_b = 4.8 \text{ GeV}$ . Whereas we could find a minimum of the variation of the threshold functions in the case of  $m_b = 4.8 \text{ GeV}$ , we could not do so for  $m_b = 4.6 \text{ GeV}$ . Solving the differential equation (5.19) leads to functions  $s_0(M^2)$ , which are strongly dependent on the Borel mass (see figure 5.5 c). Their variations are rather high compared to the former analyses and do not show a minimum. Nevertheless, we could find a region where the variations

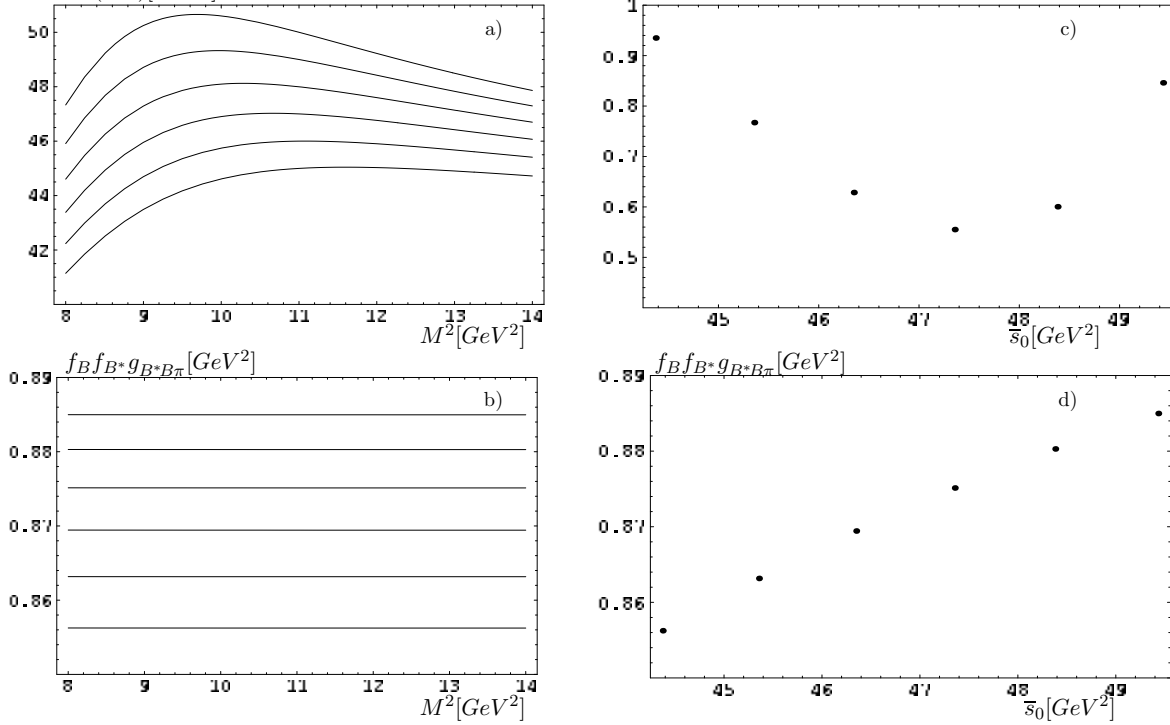


Figure 5.4: Sum rule analysis of the product  $f_B f_{B^*} g_{B^* B \pi}$ . Graph a) shows solutions to the differential equation (5.19), b) the corresponding functions for  $f_B f_{B^*} g_{B^* B \pi}$ , d) shows these values plotted as functions of the average threshold  $\bar{s}_0$ . Graph c) shows the variations of the thresholds  $s(M^2)$ . The product  $f_B f_{B^*} g_{B^* B \pi}$  is extracted at the minimum.

are changing very slowly. We plotted the corresponding values  $f_B f_{B^*} g_{B^* B \pi}$  in this region in figure 5.5d. However, to be on the safe side we added the difference of the central value and the lower bound from  $m_b = 4.8 \text{ GeV}$  to the mean result to obtain an upper bound.

The scale dependence of this sum rule analysis is shown in figure 5.6 and is less than 4% of the final result, if the scales  $\mu = 2 \text{ GeV}$  and  $\mu = 3 \text{ GeV}$  are used to extract  $f_B f_{B^*} g_{B^* B \pi}$ .

We also analyzed the sum rule for the asymptotic twist 2 wave function. The results are shown in figure 5.7. As in the last section, the central result increases about 9%.

The final result for the product  $f_B f_{B^*} g_{B^* B \pi}$  we extract, is:

$$f_B f_{B^*} g_{B^* B \pi} = (0.88 \pm 0.08 \pm 0.09) \text{ GeV}^2. \quad (5.20)$$

This is about 10% higher than the result obtained by Khodjamirian and collaborators using the same sum rule [32].

Using this result to again extract a value for the residue  $c$  in the single pole model, we get after dividing by (3.20):

$$c = (0.40_{-5}^{+7}) \text{ GeV}, \quad (5.21)$$

which is close to the result (5.17) obtained in the preceding section.

Dividing (5.20) by the two decay constants (3.20) and (3.26), we get:

$$g_{B^* B \pi} = 17_{-3}^{+6}. \quad (5.22)$$

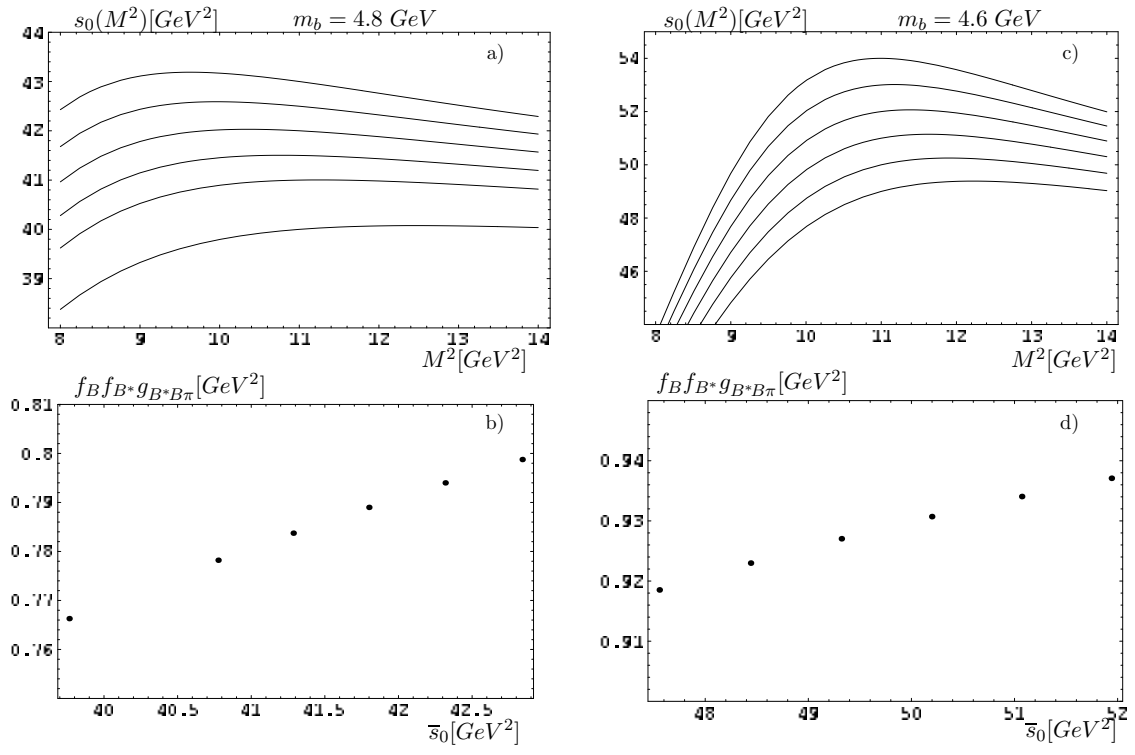


Figure 5.5: Sum rule analyses for different values of the quark mass. The left side shows the thresholds  $s_0(M^2)$  and corresponding values  $f_B f_{B^*} g_{B^* B \pi}$  plotted over  $\bar{s}_0(M^2)$  for the case  $m_b = 4.8 \text{ GeV}$ . The right side summarize the analysis for  $m_b = 4.6 \text{ GeV}$ .

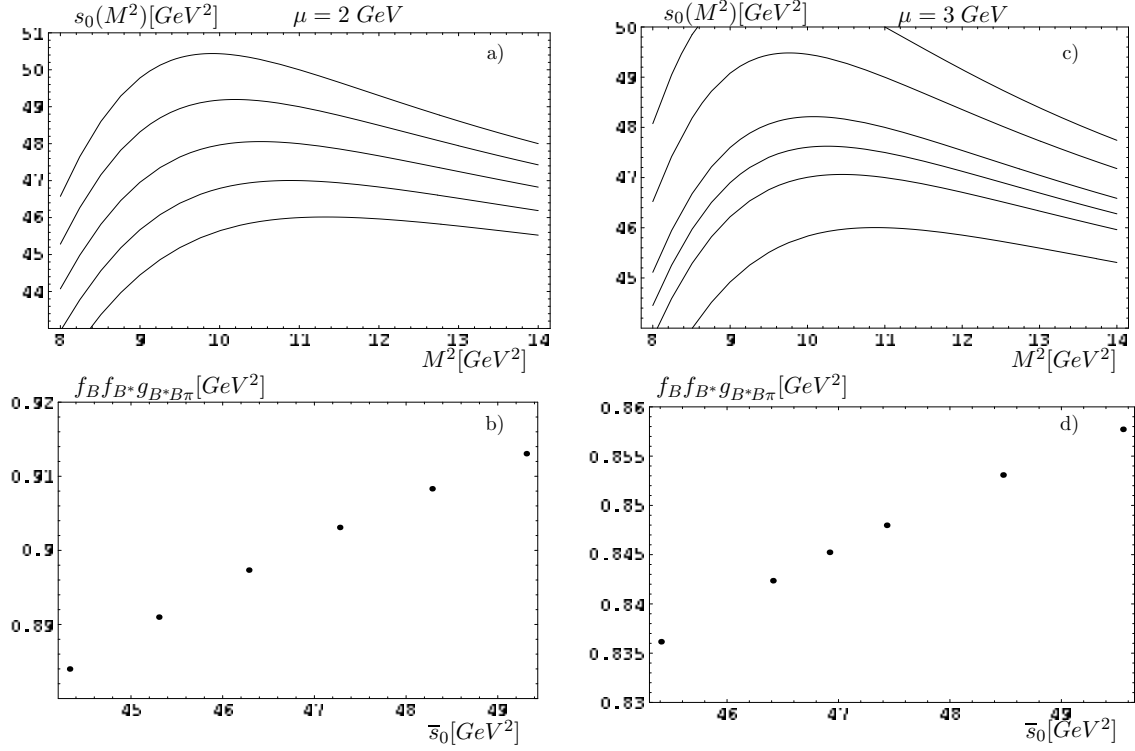


Figure 5.6:  $f_B f_{B^*} g_{B^* B \pi}$  evaluated at the scales  $\mu = 2 \text{ GeV}$  (left side) and  $\mu = 3 \text{ GeV}$  (right side).

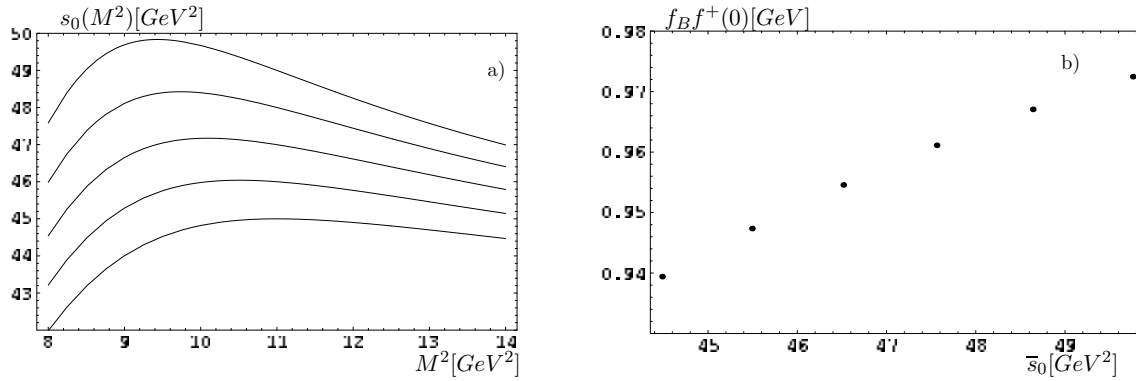


Figure 5.7: Sum rule analysis for the asymptotic twist 2 pion wave function. The extracted value is about 9% higher than the central result.

The difference between the positive and negative error assigned to the results (5.22) and (5.21) is due to the different effect of a higher and lower quark mass on the decay constant (3.20). The error inflicted on the final results by the different masses is about 18%.

## 5.4 Discussion and Relation to the Literature

In the last two sections, we analyzed the sum rule for the product  $f_B f_{B^*} g_{B^* B \pi}$ . As in chapter 4, it was hoped that when this sum rule is divided by the corresponding sum rule results for the decay constants, the intrinsic errors of the two methods would be reduced. The results (5.17) and (5.21) for the residue  $c$  of the pole in the simple pole model (5.1) are within 6% of each other, which is a quite satisfying, considering the significant difference of the two initial sum rule results (5.16) and (5.20). However, the extracted values for the coupling  $g_{B^* B \pi}$  (5.18) and (5.22) differ about 15%. The reason for this deviation might be the unusual large value for the vector meson decay constant, found in section 3.5.

We did not take further perturbative corrections into account. Assuming that the first order corrections to the twist 3 contribution is about the same relative size as the  $O(\alpha_s)$ -twist 2 corrections ( $\sim 40\%$ ), we get another uncertainty of 20%.

Furthermore, the hadronic continuum contribution was only subtracted from the leading terms in the expansion (5.9). The inflicted error to the final result is negligible as well as variations

$g_{B^* B \pi}$	Ref.	Method
$20 \pm 5$	This Thesis	LCSR; $O(\alpha_s)$ -twist 2; $\lim M^2 \rightarrow \infty$
$17_{-3}^{+6}$	This Thesis	LCSR; $O(\alpha_s)$ -twist 2; $s_0(M^2)$
$15 \pm 4$	Colangelo '94[37]	NLO-soft pion limit
$28 \pm 6$	Belyaev '95[36]	LCSR-LO
$14 \pm 4$	Dosch '96[38]	Double Moment SR
$22 \pm 7$	Khodjamirian '99[32]	LCSR; $O(\alpha_s)$ -twist 2;
$14.5 \pm 3.9$	Navarra '00[39]	3-pt SR
$32 \pm 5$	Melikhov '01[40]	Dispersion Approach
$47 \pm 5 \pm 8$	Abada '03[41]	Lattice, quenched

Table 5.1: Comparison of our results to a collection from the literature.

from the boundary  $\Sigma_0$  in the plane  $(s_1, s_2)$  [32].

In table 5.1, we listed our results for the coupling and a collection from the literature. It should be noted that the values obtained in sum rule approaches are significantly lower than results from quark models and lattice calculations. In the case of the D-meson coupling  $g_{D^*D\pi}$ , the situation is quite similar. Here, a first measurement of the coupling gave a value almost twice as large as the sum rule results[42]. Several ideas were proposed to cure this problem of the sum rules[43, 44]. We will discuss this issue in the conclusion of this thesis.

# Chapter 6

## Conclusion and Outlook

In this thesis we introduced two modifications of the analysis of SVZ sum rules and light-cone sum rules. These were aimed to extract the relevant hadronic property in a stable region of the sum rule. However, the two methods differ significantly in their physical meaning. In the first method, we took the limit  $M^2 \rightarrow \infty$ . In this limit, the exponential suppression of the higher states and the continuum vanishes. Therefore, this method rather emphasizes uncertainties from the duality ansatz. The result becomes quite sensitive to the chosen threshold  $s_0$ . We fixed this threshold by setting the daughter sum rule equal to the meson mass in the limit  $M^2 \rightarrow \infty$ . In the second method, we imposed a Borel mass dependence of the threshold and we chose it such, that the sum rules became constant in a given Borel window. With this procedure, we tried to damp the uncertainties of the duality approximation. The sum rule result was extracted from a stable region of the threshold functions  $s_0(M^2)$ , arguing that the duality assumption is still a good approximation and the corresponding thresholds  $s_0(M^2)$  should not vary strongly.

The individual sum rule results of the two methods gave rather different values of the hadronic properties. The values extracted from the limiting procedure  $M^2 \rightarrow \infty$  were always significantly lower than the values from the second method. However, when the ratio of two sum rule results was taken, as was the case for the B-meson form factor and the strong coupling, the intrinsic errors seemed to compensate partially. The final results of the form factor were almost identical. The results for the coupling came closer to each other, compared to the initial sum rule results for the product  $f_B f_{B^*} g_{B^* B \pi}$ .

In table 6, we listed the results from all analyses in this thesis. We also gave the average value for each hadronic property. Since one of the methods is emphasizing errors from the duality approximation and the other is trying to suppress them, it seems reasonable to give the mean value of the results obtained with the two methods, since the *true* value might lie in between these two extremal points of view.

We already related our results to values from the literature. Whereas the extracted values for the decay constants and the form factor seem to fit quite well to other results, the value for the coupling  $g_{B^* B \pi}$  is close to other sum rule results and far off from values obtained within other models and lattice calculations. In the case of the D-meson coupling, an experimental measurement[42] confirmed the values from quark models and lattice calculations. However, the experimental value was about 40% higher than the sum rule results<sup>1</sup>.

---

<sup>1</sup>The value (5.20) extracted from imposing a Borel mass dependent threshold  $s_0(M^2)$  is about 20% higher than the value one would extract from figure 5.1 and the inclusion of  $O(\alpha_s)$ -corrections to the twist 3 wave functions could raise the result by another 20%. However, when the result (5.20) is divided by the decay constants extracted from the same sum rule analysis, we get a rather low value for the coupling.

	$\lim M^2 \rightarrow \infty$	$s_0(M^2)$	average result
$f_B[MeV]$	$178 \pm 27$	$208^{+30}_{-43}$	$193^{+20}_{-25}$
$f_{B^*}[MeV]$	$197 \pm 29$	$245 \pm 42$	$221 \pm 26$
$f^+(0)$	$0.26 \pm 0.05$	$26 \pm 0.05$	$26 \pm 4$
$g_{B^*B\pi}$	$20 \pm 5$	$17^{+6}_{-3}$	$19^{+4}_{-3}$

Table 6.1: Summary of the hadronic properties extracted from the two different sum rule methods. In the last column, we gave the corresponding value when the average of the two sum rule results is taken.

One of the main uncertainties of sum rules is the scarcely known hadronic spectral function. Nevertheless, the crude ansatz of taking the first resonance and relating the remaining continuum to the QCD-side of the sum rules gave many results in agreement with experiment. In the case of the strong coupling the initial sum rule is very unstable in the Borel window (see figure 5.1). In [43], Becirevic et al. suggested to take the first radial excitations of the  $D$ - and the  $D^*$ -meson explicitly into the calculations. This introduces several further parameters. However, they were able to show that the inclusion of a negative radial excitation improves the stability of the sum rule. Furthermore, the region of best stability of the sum rule coincides with the experimentally measured value. It would therefore be interesting to incorporate the radial excitation in the analyses of this thesis. Ideally, one would expect a significant raise in the extracted coupling  $g_{B^*B\pi}$  and minor changes to the decay constants and the form factor.

In this thesis, we analyzed hadronic properties of the B-meson. These analyses can easily be applied to the  $D$ -meson. However, evaluating the sum rules at scales of about  $\mu = 1 \sim 2 \text{ GeV}$  demands a very careful treatment of perturbative corrections. The inclusion of higher order corrections should improve the stability with respect to variations of the scale  $\mu$ . In the light of the coming experimental data at CLEO [45], we try to give predictions in the near future.

## Acknowledgements

I am very grateful to my supervisor Dmitri Melikhov for many fruitful discussions and life beyond. I also want to thank Matthias Jamin for making available a sophisticated mathematica package.

# Appendix A

## Renormalization Group Properties

Any Green's function in QCD has to obey the Callan-Symanzik equation to make it independent of the artificial scale-parameter that comes in the calculations during the renormalization procedure. The solution of the Callan-Symanzik equation implies a scale-dependence of the strong coupling constant  $\alpha_s(\mu)$ . The running of the coupling is described by the Gell-Mann-Low  $\beta$ -function, which can be written as a power series of the coupling:

$$\beta(\alpha_s) \equiv \frac{\partial \alpha_s}{\partial \log \frac{\mu^2}{\mu_0^2}} = -b_0 \frac{\alpha_s^2}{4\pi} - b_1 \frac{\alpha_s^3}{(4\pi)^2} - b_2 \frac{\alpha_s^4}{(4\pi)^3} + \dots \quad (\text{A.1})$$

The leading coefficients of this series are:

$$\begin{aligned} b_0 &= 11 - \frac{2}{3}n_f \\ b_1 &= 102 - \frac{38}{3}n_f \\ b_2 &= \frac{1}{2} \left( 2857 - \frac{5033}{9}n_f + \frac{325}{27}n_f^2 \right) \end{aligned} \quad (\text{A.2})$$

The third coefficient is scheme dependent and we have given it in the  $\overline{MS}$ -scheme.  $n_f$  is the number of quark flavors below the scale  $\mu$ . Solving for the strong coupling up to two loop order yields:

$$\alpha_s(\mu) = \frac{\alpha_s(\mu_0)}{1 + \frac{\alpha_s(\mu_0)}{4\pi} b_0 \log \frac{\mu^2}{\mu_0^2}} \left( 1 - \frac{b_1 \alpha_s(\mu_0)}{4\pi b_0 + \alpha_s(\mu_0) b_0^2 \log \frac{\mu^2}{\mu_0^2}} \log \left( 1 + \frac{\alpha_s(\mu_0)}{4\pi} b_0 \log \frac{\mu^2}{\mu_0^2} \right) \right) \quad (\text{A.3})$$

This equation can be parametrized by introduction of a mass scale  $\Lambda$

$$\alpha_s(\mu) = \frac{4\pi}{b_0 \log \frac{\mu^2}{\Lambda^2}} \left[ 1 - \frac{2b_1}{b_0^2} \frac{\log \log \frac{\mu^2}{\Lambda^2}}{\log \frac{\mu^2}{\Lambda^2}} \dots \right] \quad (\text{A.4})$$

To one-loop order, the scale  $\Lambda$  is defined by:

$$b_0 \frac{\alpha_s(\mu_0)}{4\pi} \log \frac{\mu_0^2}{\Lambda^2} = 1. \quad (\text{A.5})$$

The scale  $\Lambda$  depends on the number of flavors used in the calculations. In the numerical analyses we will use the experimental value of the strong coupling at the Z-Boson mass, taken from the Particle Data Group:

$$\alpha_s(M_Z) = 0.1172(20); \quad M_Z = 91.1876(21) \text{ GeV} \quad (\text{A.6})$$



We will then run the coupling down to the scale at which we are evaluating the sum rules. At the threshold of the b-quark mass, one has to apply matching conditions [46, 47]. These are obtained by constructing an effective theory with  $n_f = 4$  light quarks and one heavy quark and matching it with the full theory at the b-quark threshold. The matching is done by considering several Green's functions and require consistency up to a certain order in  $(1/m_b)$  at the thresholds. Taking only continuous matching conditions of the strong coupling  $\alpha_s$  results in a rather strong dependence on the actual scale of the matching. In these cases, one usually accounts for the uncertainties by introducing errors via matching of the two effective couplings at  $2m_h$  and  $m_h/2$ . We are very grateful to M. Jamin for making available a sophisticated mathematica package for running of the strong coupling and the quark masses. It implements the matching conditions from Chetyrkin[47] up to four-loop accuracy.

Treating the quark masses like coupling constants in perturbative QCD, we get from the solution of the Callan-Symanzik equation a prescription for the running of the masses:

$$\frac{\partial \overline{m}^2(\mu)}{\partial \log \frac{\mu^2}{\mu_0^2}} = -\overline{m}^2(\mu_0) \left( \gamma_0 \frac{\alpha_s(\mu_0)}{\pi} + \gamma_1 \frac{\alpha_s^2(\mu_0)}{\pi^2} \dots \right). \quad (\text{A.7})$$

The  $\gamma$ 's are the anomalous dimensions of the scalar  $\bar{q}q$ -operator. They are given by

$$\begin{aligned} \gamma_0 &= 2 \\ \gamma_1 &= \frac{101}{12} - \frac{5}{18} n_f. \end{aligned} \quad (\text{A.8})$$

To one-loop accuracy we get

$$\overline{m}^2(\mu^2) = \overline{m}^2(\mu_0^2) \left( 1 + \frac{\alpha_s(\mu_0^2)}{4\pi} b_0 \log \frac{\mu^2}{\mu_0^2} \right)^{\frac{4\gamma_0}{b_0}}, \quad (\text{A.9})$$

which can be rewritten as:

$$\overline{m}(\mu^2) = \overline{m}(\mu_0^2) \left( \frac{\log \frac{\mu_0^2}{\Lambda^2}}{\log \frac{\mu^2}{\Lambda^2}} \right)^{\frac{4}{b_0}} = \overline{m}(\mu_0^2) \left( \frac{\alpha_s(\mu^2)}{\alpha_s(\mu_0^2)} \right)^{\frac{4}{b_0}}. \quad (\text{A.10})$$

The running quark-mass is defined during the renormalization of the quark mass. It is introduced to cancel the divergent part of the propagator. Up to first order in the running coupling it is in the  $\overline{MS}$ -scheme[48]:

$$\overline{m}(\mu) = m_0 \left( 1 + \frac{\alpha_s(\mu)}{\pi \omega} \right), \quad (\text{A.11})$$

where  $m_0$  is the bare quark mass and  $\omega$  is the deviation from four dimensions,  $D = 4 - 2\omega$ . Being defined in this way, the running mass is different from the pole mass, the location of the pole of the full renormalized quark propagator[49]. Unlike in the leptonic case, where the pole mass of the fermions can be identified with their physical mass, quarks are never observed on-shell due to confinement. Defined in this way, the two quark masses can be related to each other:

$$m_{pole} = \overline{m}(\mu^2) \left( 1 + \frac{\alpha_s(\mu)}{\pi} \left( \frac{4}{3} + \log \frac{\mu^2}{m_{pole}^2} \right) + O(\alpha_s^2) \right). \quad (\text{A.12})$$

Higher loop contributions can be found in [50], however the analyses in this thesis will not extend to this accuracy.

# Appendix B

## Light-Cone Wave Functions

In this appendix we give the definitions of the two- and three-particle light-cone wave functions up to twist four, and list terms, contributing to the form factor (4.2) in section 4.

### B.1 Definitions of the Light-Cone Wave Functions

The twist 2 pion wave function can be expressed as a sum of orthogonal polynomials, by using partial wave decomposition. The derivation can be found in [51]:

$$\varphi_\pi(u, \mu) = 6u(1-u) \left( 1 + a_2(\mu)C_2^{3/2}(2u-1) + a_4(\mu)C_4^{3/2}(2u-1) + \dots \right). \quad (\text{B.1})$$

$C_n^{3/2}$  are Gegenbauer polynomials. The coefficients  $a_n$  are not known very well. Efforts were made to extract them from several sources, like two-point sum rules, lattice and instanton physics. They are multiplicative renormalizable:

$$a_n(\mu) = a_n(\mu_0) \left( \frac{\alpha_s(\mu)}{\alpha_s(\mu_0)} \right)^{\frac{\gamma_n}{b_0}}, \quad (\text{B.2})$$

with

$$\gamma_n = -4 - \frac{8}{3(n+1)(n+2)} + \frac{16}{3} \sum_{k=1}^{n+1} k^{-1}. \quad (\text{B.3})$$

In our analysis, we will take the values from [34]:

$$a_2(\mu_b) = 0.218, \quad a_4(\mu_b) = 0.084, \quad (\text{B.4})$$

at the scale  $\mu_b = 2.4 \text{ GeV}$ .

Further definitions of two- and three-particle wave functions are taken from Khodjamirian [8]. The relevant references where they are collected from, can also be found in this review. For convenience, we list them in the following, where we did not write explicitly the scale dependence of the wave functions.

The three particle twist 3 wave function  $\varphi_{3\pi}$  and the corresponding two particle twist 3 wave

functions  $\varphi_p$  and  $\varphi_\sigma$ , which follow from  $\varphi_{3\pi}$  by equations of motion are given by:

$$\begin{aligned} \varphi_{3\pi}(\alpha_i) = & 180\alpha_1\alpha_2\alpha_3^2 (2 + \omega_{1,0}(7\alpha_3 - 3) + 2\omega_{2,0}(2 - 4\alpha_1\alpha_2 - 8\alpha_3 + 8\alpha_3^2) \\ & + 2\omega_{1,1}(3\alpha_1\alpha_2 - 2\alpha_3 + 3\alpha_3^2)) \end{aligned} \quad (\text{B.5})$$

$$\begin{aligned} \varphi_p(u) = & 1 + \frac{15f_{3\pi}}{\mu_\pi f_\pi} (3(2u - 1)^2 - 1) \\ & + \frac{3f_{3\pi}}{16\mu_\pi f_\pi} (4\omega_{2,0} - \omega_{1,1} - 2\omega_{1,0})(35(2u - 1)^4 - 30(2u - 1)^2 + 3) \end{aligned} \quad (\text{B.6})$$

$$\begin{aligned} \varphi_\sigma(u) = & 6u(1 - u) \left( 1 + \frac{3f_{3\pi}}{2\mu_\pi f_\pi} \left( 5 - \frac{1}{2}\omega_{1,0} \right) (5(2u - 1)^2 - 1) \right. \\ & \left. + \frac{3f_{3\pi}}{16\mu_\pi f_\pi} (4\omega_{2,0} - \omega_{1,1})(21(2u - 1)^4 - 14(2u - 1)^2 + 1) \right). \end{aligned} \quad (\text{B.7})$$

Here,  $\mu_\pi = 2.02 \text{ GeV}$  is given in (2.76). The other parameters at the scale  $\mu_b$  are given by:

$$\omega_{1,0} = -2.18, \quad \omega_{2,0} = 8.12, \quad \omega_{1,1} = -2.59, \quad f_{3\pi} = 0.0026 \text{ GeV}^2. \quad (\text{B.8})$$

The twist 4 three particle wave functions and the corresponding two-particle wave functions are defined as:

$$\varphi_\perp(\alpha_i) = 30\delta^2(\alpha_1 - \alpha_2)\alpha_3^2 \left( \frac{1}{3} + 2\varepsilon(1 - 2\alpha_3) \right) \quad (\text{B.9})$$

$$\varphi_\parallel(\alpha_i) = 120\delta^2\varepsilon(\alpha_1 - \alpha_2)\alpha_1\alpha_2\alpha_3 \quad (\text{B.10})$$

$$\tilde{\varphi}_\perp(\alpha_i) = 30\delta^2(1 - \alpha_3)\alpha_3^2 \left( \frac{1}{3} + 2\varepsilon(1 - 2\alpha_3) \right) \quad (\text{B.11})$$

$$\tilde{\varphi}_\parallel(\alpha_i) = -120\delta^2\alpha_1\alpha_2\alpha_3 \left( \frac{1}{3} + \varepsilon(1 - 3\alpha_3) \right) \quad (\text{B.12})$$

$$\begin{aligned} g_1(u) = & \frac{5}{2}\delta^2(1 - u)^2u^2 + \frac{1}{2}\varepsilon\delta^2 \left( u(1 - u)(2 + 13u(1 - u)) + 10u^3 \log u(2 - 3u + \frac{6}{5}u^2) \right. \\ & \left. + 10(1 - u)^3 \log(1 - u)(3u - 1 + \frac{6}{5}(1 - u)^2) \right) \end{aligned} \quad (\text{B.13})$$

$$g_2(u) = \frac{10}{3}\delta^2u(1 - u)(2u - 1). \quad (\text{B.14})$$

And at the scale  $\mu_b$ , we have:

$$\delta^2 = 0.17 \text{ GeV}^2, \quad \varepsilon = 0.36 \quad (\text{B.15})$$

## B.2 Contributions to the semi-leptonic Form Factor

The surface term in (4.2) is given by (at  $q^2 = 0$ ):

$$\begin{aligned} A^+(s_0, M^2)e^{\frac{s_0}{M^2}} = & \frac{\mu_\pi}{6m_b}\varphi_\sigma\left(\frac{m_b^2}{s_0}\right) - \frac{4}{m_b^2}\left(1 + \frac{s_0}{M^2}\right)g_1\left(\frac{m_b^2}{s_0}\right) + \frac{4}{s_0}\frac{dg_1\left(\frac{m_b^2}{s_0}\right)}{du} \\ & + \frac{2}{m_b^2}\left(1 + \frac{s_0}{M^2}\right)\int_0^{\frac{m_b^2}{s_0}} dt g_2(t) - \frac{2}{s_0}g_2\left(\frac{m_b^2}{s_0}\right) \end{aligned} \quad (\text{B.16})$$

The three-particle contributions are:

$$\begin{aligned}
f_{3P}^+(s_0, M^2) = & - \int_0^1 u du \int_0^1 d\alpha_i \delta\left(1 - \sum_i \alpha_i\right) \frac{\Theta(\alpha_1 + u\alpha_3 - \frac{m^2}{s_0})}{(\alpha_1 + u\alpha_3)^2} e^{-\frac{m_b^2}{(\alpha_1 + u\alpha_3)M^2}} \times \\
& \left[ \frac{2f_{3\pi}}{f_\pi m_b} \varphi_{3\pi}(\alpha_i) \left(1 - \frac{m_b^2}{(\alpha_1 + u\alpha_3)M^2}\right) \right. \\
& \left. - \frac{1}{uM^2} [2\varphi_\perp(\alpha_i) - \varphi_\parallel(\alpha_i) + 2\tilde{\varphi}_\perp(\alpha_i) - \tilde{\varphi}_\parallel(\alpha_i)] \right] \quad (\text{B.17})
\end{aligned}$$

While these two contributions were taken from Khodjamirian [8], we will use the first order corrections to the twist 2 wave function from [22]. These are easier to handle numerically and one can also see explicitly the soft and hard contributions to the heavy-light decay in the heavy quark limit  $m_b \rightarrow \infty$ :

$$\frac{f_B m_B^2}{f_\pi m_b^2} f^{+(1)}(0) e^{-\frac{m_B^2}{M^2}} = -\frac{\alpha_s}{3\pi} T^{(1)}(s_0, M^2), \quad (\text{B.18})$$

where

$$\begin{aligned}
T^{(1)}(s_0, M^2) = & \int_0^1 du \frac{\varphi_\pi(u)}{(1-u)} \int_{\frac{m_b^2}{m_b^2}}^{s_0} dt \frac{m_b^2 - t}{t} \left(\frac{2}{t} + L_1\right) e^{-\frac{t}{M^2}} \\
& + \int_0^{\frac{m_b^2}{s_0}} du \frac{\varphi_\pi(u)}{(1-u)} e^{-\frac{m_b^2}{uM^2}} \int_{\frac{m_b^2}{m_b^2}}^{s_0} dt \frac{m_b^2 - t}{m_b^2 - ut} e^{-\frac{ut - m_b^2}{uM^2}} L_2 \\
& + \int_{\frac{m_b^2}{s_0}}^1 du \frac{\varphi_\pi(u)}{(1-u)} e^{-\frac{m_b^2}{uM^2}} \times \\
& \left[ \int_{\frac{m_b^2}{m_b^2}}^{s_0} dt \frac{m_b^2 - t}{m_b^2 - ut} e^{-\frac{ut - m_b^2}{uM^2}} L_2 + \int_{\frac{m_b^2}{m_b^2}}^{s_0} dt L_2 - \int_{\frac{m_b^2}{m_b^2}}^{us_0} dt \frac{m_b^2}{t} \left(\frac{m_b^2 - t}{tm_b^2} + L_1\right) e^{-\frac{t - m_b^2}{uM^2}} \right] \\
& + \int_{\frac{m_b^2}{s_0}}^1 du \frac{\varphi_\pi(u)}{u} e^{-\frac{m_b^2}{uM^2}} \times \\
& \left[ \frac{5}{2} - \frac{\gamma_E}{2} + 2 \log \frac{uM^2}{m_b^2} - \frac{3}{2} \log \frac{uM^2}{\mu^2} + \frac{1}{2} Ei \left(\frac{m_b^2 - us_0}{uM^2}\right) + \int_{\frac{m_b^2}{m_b^2}}^{s_0} dt L_2 \right. \\
& + \int_{s_0}^{\infty} dt \frac{m_b^2}{m_b^2 - ut} L_2 + \int_{\frac{m_b^2}{m_b^2}}^{us_0} dt \left(\frac{1}{2} - \frac{(t - m_b^2)^2}{2t^2} + m_b^2(L_1 + L_2)\right) \frac{e^{-\frac{t - m_b^2}{uM^2}} - 1}{m_b^2 - t} \\
& \left. + \int_{\frac{m_b^2}{m_b^2}}^{us_0} dt \left(\frac{1}{t} - L_2\right) e^{-\frac{t - m_b^2}{uM^2}} - \int_{us_0}^{\infty} \frac{dt}{m_b^2 - t} \left(\frac{1}{2} - \frac{(t - m_b^2)^2}{2t^2} + m_b^2(L_1 + L_2)\right) \right] \quad (\text{B.19})
\end{aligned}$$

and

$$Ei(x) = - \int_{-x}^{\infty} \frac{e^{-t}}{t} dt, \quad (\text{B.20})$$

$$L_1 = \frac{1}{t} \left( -1 + \log \frac{(t - m_b^2)^2}{t\mu^2} \right), \quad (\text{B.21})$$

$$L_2 = \frac{1}{t} \left( -\frac{m_b^2}{t} + \log \frac{(t - m_b^2)^2}{t\mu^2} \right). \quad (\text{B.22})$$

# Bibliography

- [1] M. A. Shifman, A. I. Vainshtein, and V. I. Zakharov, “QCD AND RESONANCE PHYSICS. SUM RULES,” *Nucl. Phys.* **B147** (1979) 385–447.
- [2] M. A. Shifman, A. I. Vainshtein, and V. I. Zakharov, “QCD and resonance physics: Applications,” *Nucl. Phys.* **B147** (1979) 448–518.
- [3] A. V. Radyushkin, “Introduction into QCD sum rule approach,” [hep-ph/0101227](#).
- [4] P. Colangelo and A. Khodjamirian, “QCD sum rules: A modern perspective,” [hep-ph/0010175](#).
- [5] M. Jamin and B. O. Lange, “ $f(B)$  and  $f(B/s)$  from QCD sum rules,” *Phys. Rev.* **D65** (2002) 056005, [hep-ph/0108135](#).
- [6] V. A. Nesterenko and A. V. Radyushkin, “SUM RULES AND PION FORM-FACTOR IN QCD,” *Phys. Lett.* **B115** (1982) 410.
- [7] A. Szczepaniak, A. Radyushkin, and C.-R. Ji, “Consistent analysis of  $O(\alpha(s))$  corrections to pion elastic form factor,” *Phys. Rev.* **D57** (1998) 2813–2822, [hep-ph/9708237](#).
- [8] A. Khodjamirian and R. Ruckl, “QCD sum rules for exclusive decays of heavy mesons,” *Adv. Ser. Direct. High Energy Phys.* **15** (1998) 345–401, [hep-ph/9801443](#).
- [9] K. G. Chetyrkin and M. Steinhauser, “Heavy-light current correlators at order  $\alpha(s)^2$  in QCD and HQET,” *Eur. Phys. J.* **C21** (2001) 319–338, [hep-ph/0108017](#).
- [10] M. A. Shifman, “Snapshots of hadrons or the story of how the vacuum medium determines the properties of the classical mesons which are produced, live and die in the QCD vacuum,” *Prog. Theor. Phys. Suppl.* **131** (1998) 1–71, [hep-ph/9802214](#).
- [11] K. G. Wilson, “Nonlagrangian models of current algebra,” *Phys. Rev.* **179** (1969) 1499–1512.
- [12] L. J. Reinders, H. Rubinstein, and S. Yazaki, “HADRON PROPERTIES FROM QCD SUM RULES,” *Phys. Rept.* **127** (1985) 1.
- [13] M. Jamin and M. Munz, “Current correlators to all orders in the quark masses,” *Z. Phys.* **C60** (1993) 569–578, [hep-ph/9208201](#).
- [14] T. M. Aliev and V. L. Eletsky, “ON LEPTONIC DECAY CONSTANTS OF PSEUDOSCALAR D AND B MESONS,” *Sov. J. Nucl. Phys.* **38** (1983) 936.
- [15] M. Jamin, “Flavour-symmetry breaking of the quark condensate and chiral corrections to the Gell-Mann-Oakes-Renner relation,” *Phys. Lett.* **B538** (2002) 71–76, [hep-ph/0201174](#).

- [16] V. M. Belyaev and B. L. Ioffe, “DETERMINATION OF BARYON AND BARYONIC RESONANCE MASSES FROM QCD SUM RULES. 1. NONSTRANGE BARYONS,” *Sov. Phys. JETP* **56** (1982) 493–501.
- [17] S. Narison, “DECAY CONSTANTS OF THE B AND D MESONS FROM QCD DUALITY SUM RULES,” *Phys. Lett.* **B198** (1987) 104.
- [18] V. M. Braun, “Light-cone sum rules,” [hep-ph/9801222](#).
- [19] V. M. Braun and I. E. Filyanov, “QCD SUM RULES IN EXCLUSIVE KINEMATICS AND PION WAVE FUNCTION,” *Z. Phys.* **C44** (1989) 157.
- [20] P. Ball, V. M. Braun, and H. G. Dosch, “Form-factors of semileptonic D decays from QCD sum rules,” *Phys. Rev.* **D44** (1991) 3567–3581.
- [21] P. Ball, V. M. Braun, and H. G. Dosch, “On vector dominance in the decay  $B \rightarrow \pi e \bar{\nu}$ ,” *Phys. Lett.* **B273** (1991) 316–318.
- [22] E. Bagan, P. Ball, and V. M. Braun, “Radiative corrections to the decay  $B \rightarrow \pi e \bar{\nu}$  and the heavy quark limit,” *Phys. Lett.* **B417** (1998) 154–162, [hep-ph/9709243](#).
- [23] M. Beneke, “Renormalons,” *Phys. Rept.* **317** (1999) 1–142, [hep-ph/9807443](#).
- [24] S. Narison, “Extracting  $m_{\bar{c}}(M(c))$  and  $f(D/s, B)$  from the pseudoscalar sum rules,” *Nucl. Phys. Proc. Suppl.* **74** (1999) 304–308, [hep-ph/9811208](#).
- [25] S. Narison, “c, b quark masses and  $f(D/s)$ ,  $f(B/s)$  decay constants from pseudoscalar sum rules in full QCD to order  $\alpha_s^2$ ,” *Phys. Lett.* **B520** (2001) 115–123, [hep-ph/0108242](#).
- [26] C. A. Dominguez and N. Paver, “Leptonic decay constants of D(s) and B(s) mesons from QCD sum rules,” *Phys. Lett.* **B318** (1993) 629–634.
- [27] A. X. El-Khadra and M. Luke, “The mass of the b quark,” *Ann. Rev. Nucl. Part. Sci.* **52** (2002) 201–251, [hep-ph/0208114](#).
- [28] A. Abada *et al.*, “Decays of heavy mesons,” *Nucl. Phys. Proc. Suppl.* **83** (2000) 268–270, [hep-lat/9910021](#).
- [29] UKQCD Collaboration, K. C. Bowler *et al.*, “Decay constants of B and D mesons from non-perturbatively improved lattice QCD,” *Nucl. Phys.* **B619** (2001) 507–537, [hep-lat/0007020](#).
- [30] H. Wittig, “Status of lattice calculations of B-meson decays and mixing,” [hep-ph/0310329](#).
- [31] C. A. Dominguez and N. Paver, “LEPTONIC DECAY CONSTANTS OF HEAVY FLAVOR MESONS OF ARBITRARY MASS,” *Phys. Lett.* **B246** (1990) 493–497.
- [32] A. Khodjamirian, R. Ruckl, S. Weinzierl, and O. I. Yakovlev, “Perturbative QCD correction to the light-cone sum rule for the  $B^* \rightarrow B \pi$  and  $D^* \rightarrow D \pi$  couplings,” *Phys. Lett.* **B457** (1999) 245–252, [hep-ph/9903421](#).
- [33] V. M. Braun and I. E. Filyanov, “CONFORMAL INVARIANCE AND PION WAVE FUNCTIONS OF NONLEADING TWIST,” *Z. Phys.* **C48** (1990) 239–248.

- [34] A. Khodjamirian, R. Ruckl, S. Weinzierl, and O. I. Yakovlev, “Perturbative QCD correction to the  $B \rightarrow \pi$  transition form factor,” *Phys. Lett.* **B410** (1997) 275–284, [hep-ph/9706303](#).
- [35] P. Ball and R. Zwicky, “Improved analysis of  $B \rightarrow \pi e \nu$  from QCD sum rules on the light-cone,” *JHEP* **10** (2001) 019, [hep-ph/0110115](#).
- [36] V. M. Belyaev, V. M. Braun, A. Khodjamirian, and R. Ruckl, “ $D^* \rightarrow D \pi$  and  $B^* \rightarrow B \pi$  couplings in QCD,” *Phys. Rev.* **D51** (1995) 6177–6195, [hep-ph/9410280](#).
- [37] P. Colangelo *et al.*, “On the coupling of heavy mesons to pions in QCD,” *Phys. Lett.* **B339** (1994) 151–159, [hep-ph/9406295](#).
- [38] H. G. Dosch and S. Narison, “ $B^* \rightarrow B \pi(\gamma)$  couplings and  $D^* \rightarrow D \pi(\gamma)$  - decays within a  $1/M$ -expansion in full QCD,” *Phys. Lett.* **B368** (1996) 163–170, [hep-ph/9510212](#).
- [39] F. S. Navarra, M. Nielsen, M. E. Bracco, M. Chiapparini, and C. L. Schat, “ $D^* \rightarrow D \pi$  and  $B^* \rightarrow B \pi$  form factors from QCD sum rules,” *Phys. Lett.* **B489** (2000) 319–328, [hep-ph/0005026](#).
- [40] D. Melikhov, “Dispersion approach to quark-binding effects in weak decays of heavy mesons,” *Eur. Phys. J. direct* **C4** (2002) 2, [hep-ph/0110087](#).
- [41] A. Abada *et al.*, “Lattice measurement of the couplings  $g(\infty)$  and  $g(B^* \rightarrow B \pi)$ ,” *JHEP* **02** (2004) 016, [hep-lat/0310050](#).
- [42] **CLEO** Collaboration, S. Ahmed *et al.*, “First measurement of  $\Gamma(D^{*+})$ ,” *Phys. Rev. Lett.* **87** (2001) 251801, [hep-ex/0108013](#).
- [43] D. Becirevic *et al.*, “Possible explanation of the discrepancy of the light-cone QCD sum rule calculation of  $g(D^* \rightarrow D \pi)$  coupling with experiment,” *JHEP* **01** (2003) 009, [hep-ph/0212177](#).
- [44] H.-c. Kim, “Re-analysis of the  $D^* \rightarrow D \pi$  coupling in the light-cone QCD sum rules,” *J. Korean Phys. Soc.* **42** (2003) 475–478, [hep-ph/0206170](#).
- [45] D. Asner, “The CLEO-c research program,” [hep-ex/0405009](#).
- [46] G. Rodrigo and A. Santamaria, “QCD matching conditions at thresholds,” *Phys. Lett.* **B313** (1993) 441–446, [hep-ph/9305305](#).
- [47] K. G. Chetyrkin, B. A. Kniehl, and M. Steinhauser, “Strong coupling constant with flavour thresholds at four loops in the  $\overline{MS}$  scheme,” *Phys. Rev. Lett.* **79** (1997) 2184–2187, [hep-ph/9706430](#).
- [48] S. C. Generalis, “QCD sum rules. 1: Perturbative results for current correlators,” *J. Phys.* **G16** (1990) 785–793.
- [49] R. Tarrach, “THE POLE MASS IN PERTURBATIVE QCD,” *Nucl. Phys.* **B183** (1981) 384.
- [50] N. Gray, D. J. Broadhurst, W. Grafe, and K. Schilcher, “THREE LOOP RELATION OF QUARK (modified)  $\overline{MS}$  AND POLE MASSES,” *Z. Phys.* **C48** (1990) 673–680.
- [51] V. L. Chernyak and A. R. Zhitnitsky, “Asymptotic behavior of exclusive processes in QCD,” *Phys. Rept.* **112** (1984) 173.